

Theoretical and Experimental Studies of Dendritic Metacommunities

THÈSE N° 5955 (2013)

PRÉSENTÉE LE 3 DÉCEMBRE 2013

À LA FACULTÉ DE L'ENVIRONNEMENT NATUREL, ARCHITECTURAL ET CONSTRUIT
LABORATOIRE D'ÉCOHYDROLOGIE
PROGRAMME DOCTORAL EN GÉNIE CIVIL ET ENVIRONNEMENT

ÉCOLE POLYTECHNIQUE FÉDÉRALE DE LAUSANNE

POUR L'OBTENTION DU GRADE DE DOCTEUR ÈS SCIENCES

PAR

Francesco CARRARA

acceptée sur proposition du jury:

Prof. R. Bernier-Latmani, présidente du jury
Prof. A. Rinaldo, Dr F. Altermatt, directeurs de thèse
Prof. J. G. Hering, rapporteur
Prof. M. Holyoak, rapporteur
Prof. A. Maritan, rapporteur



ÉCOLE POLYTECHNIQUE
FÉDÉRALE DE LAUSANNE

Suisse
2013

*Essentially, all models are wrong,
but some are useful.*
— Robert E. P. Box

To my beloved family

Acknowledgements

First, I would like to deeply thank my supervisor, Professor Andrea Rinaldo, for his generosity and the true engagement and passion for my research. He has been for me a model during these years at EPFL.

A special thank to my co-supervisor Dr. Florian Altermatt, for his constant support, for his precious advice, and for a sincere friendship that goes beyond the academic life since our first meeting in Bodega Bay, Summer 2010.

A big thank goes to the two “Paladins” of Echo lab, Enrico Bertuzzo and Lorenzo Mari, also for their decisive help and motivation during the last days of this work.

I’m also grateful to Amos Maritan and Marino Gatto for the intense and always enlightening scientific discussions.

I would like to thank my dear colleagues and friends Andrea Giometto, Pierre Queloz, Allyn Knox, and Flavio Finger. Thanks also to my colleagues Bettina Schaepli, Anna Rothenbühler, and Bernard Sperandio. Thanks to Felipe de Alencastro for his generous laboratory support.

I also thank my colleagues from Eawag, namely Mat Seymour, Elvira Mächler, Kristy Deiner, Emanuel Fronhofer and Regula Illi, as well as the Department of Aquatic Ecology at Eawag for hosting and giving me access to use the lab.

I remember and thank the glorious members of Echo lab, Ludovico Nicotina, Samir Suweis, Lorenzo Righetto, and Serena Ceola for the precious moments spent together during these years at EPFL.

Then, I thank my parents Lucia and Paolo, my brother Matteo, and all my family.

Lausanne, 5 Août 2013

Francesco Carrara

Preface

The present thesis is submitted in fulfillment of the requirements of the degree of Docteur ès Sciences at the École Doctorale in Civil and Environmental Engineering (EDCE) of the École Polytechnique Fédérale de Lausanne (EPFL). It contains the result of the outstanding scientific work carried out by the candidate Francesco Carrara. The candidate conducted the work both at the Laboratory of Ecohydrology (ECHO) within the School of Architecture, Civil and Environmental Engineering (ENAC), EPF Lausanne under the supervision of Prof. Andrea Rinaldo and at the Department of Aquatic Ecology at Eawag under the co-supervision of Dr. Florian Altermatt. The thesis work spans a period of about three and a half years (spring 2010 to summer 2013). The thesis contains extensive theoretical and experimental results and scientific advancements. The theoretical work was supervised by Prof. Andrea Rinaldo, while the experimental work was supervised by Dr. Florian Altermatt. Initial experimental work was carried out at the Bodega Marine Laboratory at University of California, Davis. The main studies, on which all results of the present thesis are based, have been carried out either at EPFL in Lausanne or at Eawag in Dübendorf under the joint supervision of the thesis director and co-director. The successful collaboration is underlined by the track record of joint publications.

The thesis contains scientific findings of theoretical, experimental and empirical nature that are organized in six independent chapters. Chapter 1 is a general introduction, while chapters 2 to 6 will each stand as independent peer-reviewed publications. Chapters 4 and 5 are already published or accepted respectively in the *Proceedings of the National Academy of Sciences of the United States of America* and *The American Naturalist*. The thesis provides the first direct experimental evidence that spatially constrained dendritic connectivity is a key factor for community composition and population persistence in riverine landscapes. As such, the thesis assesses a longstanding issue in spatial community ecology. The chapters are ordered in a sequential order, which starts with a local, method-focused perspective (chapters 2 and 3), extends to the two core chapters on diversity patterns in dendritic networks (chapters 4 and 5) and is concluded by a synthetic chapter applying the previous results to comparative data from a natural ecosystem (chapter 6). The five chapters 2 to 6 are framed by an introduction (chapter 1) and a separate conclusion section. The general introduction outlines the conceptual framework that embeds the various issues studied. Specifically, the conceptual thread linking all research questions addressed deals with how community composition and diversity patterns are shaped by species interactions, dispersal and landscape structure. The chapters are tailored from the published material or from material in preparation for submission. The candidate managed to conduct three large experiments, which resulted in four different chapters and publications

Preface

respectively. In combination with the extensive theoretical modeling pursued along all experiment design and implementation, this, in the thesis directors' opinion, is deemed an exceptionally productive dissertation which reflects the skills of the candidate to design and conduct model-guided experiments and analyze data. Each chapter contains independent sets of conclusions, putting forth perspectives and further possible developments. Although the contents of each chapter relies on published or submitted material, they are thoughtfully revisited, blended and edited for consistence, and at time expanded as appropriate for a doctoral thesis. The original references for the independent chapters 2 to 6, unambiguously attributable to a leading role of the candidate, are:

chapter 2 : F. Carrara, A. Giometto, M. Seymour, A. Rinaldo and F. Altermatt, Experimental evidence for strong stabilizing forces at high functional diversity in microbial communities, manuscript ready for submission to *Methods in Ecology & Evolution*;

chapter 3 : F. Carrara, A. Giometto, M. Seymour, A. Rinaldo and F. Altermatt, Predicting microbial community properties from pairwise experiments at different resolution of interaction strength, manuscript ready for submission to *Journal of Animal Ecology*;

chapter 4 : F. Carrara, F. Altermatt, I. Rodriguez-Iturbe and A. Rinaldo (2012) Dendritic connectivity controls biodiversity patterns in experimental metacommunities, *Proceedings of the National Academy of Sciences of the United States of America*, 109: 5761–5766.

chapter 5 : F. Carrara, A. Giometto, A. Rinaldo and F. Altermatt (2013) Complex interaction of dendritic connectivity and hierarchical patch size on biodiversity in river-like landscapes, *The American Naturalist*, in press, October 2013;

chapter 6 : F. Carrara, E. Bertuzzo, F. Altermatt and A. Rinaldo. The mid-altitude effect in river landscapes: patterns and processes, manuscript in preparation.

The topics addressed in the thesis are always referred to the current frontiers of research in ecohydrology, community ecology and biodiversity research. The results obtained by the candidate are noteworthy. The first publication (Carrara et al. PNAS 2012) received a *must read* evaluation by the Faculty of 1000, and has already been cited over ten times. It is a rare case that one doctoral candidate manages to combine excellent experimental work, brilliant modeling and theoretical insight and frame it in the most current understanding of community ecology. The candidate has shown a broad command of the ecological literature and managed to blend theoretical and conceptual findings with empirical data in a truly noteworthy manner. With the submission of this thesis, the writers are confident that the candidate Francesco Carrara will receive proper academic recognition.

Originality

The present thesis complies with the requirements of originality and relevance required by the standards of EPFL and of the Doctoral School EDCE. The depth and breadth of the methods employed, the clear linkage of the various issues under the framework of the study of dendritic

metacommunities, and the quality of the work completed – both in quantity and quality – concerts a very special thesis work that we recommend for acceptance with confidence¹.

Lausanne and Dübendorf, 2 August 2013

Prof. Andrea RINALDO
Thesis Director

and

Dr. Florian ALTERMATT
Thesis Co-Director

¹The research and the doctoral position of the candidate at EPFL have been founded by the SNF/FNS project 200021_124930/1 and the ERC Advanced Grant Program through the project RINEC-227612.

Abstract

The present thesis deals with the understanding of the origins and the mechanisms of maintenance of biodiversity in natural landscapes, in particular by identifying key processes that define large-scale patterns of abundance and diversity. Biological communities often occur in spatially structured habitats where connectivity directly affects dispersal and metacommunity processes. Recent theoretical work suggests that dispersal constrained by the connectivity of specific habitat structures affects diversity patterns and species interactions. This is particularly relevant in dendritic networks epitomized by fluvial ecological corridors. This thesis addresses whether connectivity alone can explain observed features of biodiversity and selectively promote different components of community composition in river-like landscapes, such as local species richness or the among-community similarity. The relevance of this thesis lies in the major ecological challenges posed by the topic, and its fundamental importance to conservation biology. The studies pursued herein are also deemed relevant because of the influence of the spatial connectivity and dispersal on population dynamics and of the relevance of biodiversity to ecosystem functioning. Mechanisms of species coexistence were investigated with a blend of theoretical tools (broadly related to statistical mechanics and the theory of stochastic processes) and experimental work using laboratory microbial communities. The research tools ranged from aspects of modern coexistence theory in a local perspective to the recent concept of the metacommunity in spatial ecology, within a unified framework. The study of biodiversity in riverine ecosystems guided by observational data has been addressed by combining theoretical metacommunity models with laboratory experiments.

The results are diverse. First, they show experimentally that connectivity *per se* shapes key components of biodiversity in metacommunities. Local dispersal in isotropic lattice landscapes homogenizes local species richness and leads to pronounced spatial persistence. By contrast, dispersal along dendritic landscapes leads to higher variability in local diversity and among-community composition. Although headwaters exhibit relatively lower species richness, they are crucial for the maintenance of regional biodiversity. By suitably arranging patch sizes within river-like networks the effect of local habitat capacity (i.e., the patch size) and dendritic connectivity on biodiversity can be experimentally disentangled in aquatic microcosm metacommunities. It is shown in this thesis that species coexistence and community assembly depend on intricate, non-trivial interactions of local community capacity and network positioning. Furthermore, an interaction of spatial arrangement of habitat capacity and dispersal along river-like networks also affects a key ecosystem descriptor, namely regional evenness. High regional evenness in community composition is found only in landscapes preserving geomorphological scaling

Abstract

properties of patch sizes. In riverine environments some of the rarer species sustained regionally more abundant populations and were better able to track their own niche requirements compared to landscapes with homogeneous patch size or landscapes with spatially uncorrelated patch size. All the experimental results were supported and extended by a theoretical analysis where the above mechanisms have been generalized. This thesis provides the first direct experimental evidence that spatially constrained dendritic connectivity is a key factor for community composition and population persistence in riverine landscapes. As such, this thesis assesses a longstanding issue in spatial community ecology. It offers unique insights into the ecological forces structuring natural communities in a key ecosystem, and demonstrates principles that can be further tested in theoretical metacommunity models possibly to be extended to real riverine ecosystems. Taken together, the analyses show how the structure of ecological networks interacts with the spatial environmental matrix in determining biodiversity patterns and the functioning of biological communities. The analyses also suggest that altering the natural linkage between dendritic connectivity and patch size strongly affects community properties at multiple scales.

The first part of this thesis (chapters 2 and 3) addresses key aspects of biodiversity-ecosystem functioning research where the combination of theory-guided experiments and theoretical investigations shows how a stochastic implementation of population dynamics proves fundamental for key community properties such as species persistence and community stability. The diversity-productivity and diversity-stability relationships are explored. Both experimental findings and the results of a stochastic model fitted to the experimental interaction matrix, suggest the emergence of strong stabilizing forces when species from different functional groups interact in the same environment, increasing species coexistence and community biomass production.

The last part (chapter 6) provides a synthesis of this thesis work, in that it aims at unifying aspects from niche-theory, usually adopted in spatially implicit models, with those characteristic of a spatially explicit context from a typical real-life mountainous regions. It is dedicated to the possible explanation for a macroecological pattern routinely observed from organisms in different domains of life, that is, the mid-elevational peak in local species richness. Guided by empirical observations on diversity of macroinvertebrates in Swiss river basins, a theoretical ansatz is provided which is deemed to capture the essential geomorphological drivers and controls relating species-fitness to altitude.

A set of overarching conclusions and perspectives for future research are discussed in the concluding chapter.

Keywords: dendritic ecological networks, riverine ecosystems, metacommunity, community assembly, directional dispersal, functional diversity, species-interactions, experimental microcosms, optimal channel networks, stability, stochastic noise, voter model, zero-sum game.

Sommario

Il presente lavoro di tesi studia l'origine della biodiversità negli ecosistemi naturali ed i meccanismi che la mantengono, con particolare attenzione volta all'identificazione dei processi chiave che definiscono le strutture di biodiversità a grande scala. Le comunità ecologiche abitano un ambiente spazialmente strutturato, dove la connettività del territorio gioca un ruolo diretto nei meccanismi di dispersione e sopravvivenza degli individui. Recenti speculazioni teoriche suggeriscono che la struttura intrinseca di connettività di taluni ambienti naturali possa avere un ruolo predominante nello sviluppo e nella caratterizzazione delle comunità ecologiche. Tali processi sono particolarmente lampanti nei sistemi dendritici incarnati dai sistemi fluviali intesi come corridoi ecologici. Questa tesi indaga se e che ruolo abbia la struttura di connettività dei sistemi fluviali nell'organizzare tali comunità misurandone adeguate proprietà, come il numero di specie che coesistono in una località (α -diversity) ed il grado di correlazione spaziale tra specie (β -diversity). La quantificazione dei possibili effetti introdotti dalla connettività nello sviluppo delle comunità ecologiche è una materia appena agli esordi nel settore della conservazione della biodiversità. La rilevanza della tesi emerge dunque per la sua novità e per l'importanza di uno studio volto alla comprensione degli ecosistemi fluviali, le cui comunità biologiche sono attualmente esposte ad un grave rischio di estinzione.

Le interazioni che si instaurano tra gli individui delle diverse specie sono state studiate con una combinazione di aspetti teorici importati dal settore della meccanica statistica e dalla teoria dei processi stocastici, e di lavoro sperimentale con comunità microbiche. Gli strumenti utilizzati hanno coperto le moderne teorie di coesistenza a scala locale e, nell'estendere l'analisi spazialmente, hanno sfruttato l'impianto concettuale di metacomunità, riassumibile in maniera triviale come comunità di comunità. Lo studio della biodiversità in ecosistemi fluviali ha perseguito un unico filo conduttore in cui i modelli teorici, guidati dai risultati sperimentali e dalle osservazioni empiriche, estendono i risultati e forniscono maggiore generalità.

I risultati sono molteplici. Primo, mostrano che la connettività di per sè controlla le componenti della biodiversità che abbiamo sopra introdotto. Sotto dispersione locale degli individui in due dimensioni, la struttura spaziale ordinata del lattice porta ad una omogeneità della diversità biologica, in combinazione con una maggiore persistenza spaziale. La dispersione locale lungo strutture dendritiche comporta una maggiore variabilità in ambedue le componenti delle quali si compone la biodiversità, ovvero il numero di specie che persistono in una località ed il grado di decorrelazione spaziale delle comunità biologiche. Sebbene le località più isolate della rete idrologica, tipiche degli ambienti montani, abbiano una minore componente di biodiversità in termini assoluti di numero di specie, esse ricoprono un ruolo cruciale in quanto mantengono la

diversità a livello regionale, offrendo rifugio alle specie meno competitive. Si è poi indagato sull'interazione della struttura gerarchica in cui sono organizzate le località nelle reti fluviali, con la connettività dendritica. Nei ecosistemi fluviali, l'area disponibile per la crescita e la dispersione degli individui segue precise leggi di scala imposte dalla geomorfologia del territorio. Si è sperimentato come rompere questo legame tra superficie di territorio disponibile e posizione nel bacino fluviale influisca negativamente su una proprietà della metacomunità fortemente connessa con il rischio di estinzione delle specie più rare. Infatti, l'interconnessione intrinseca del territorio disponibile per le specie con la connettività della rete tipica dei bacini fluviali favorisce lo sviluppo della nicchia ecologica e quindi della persistenza spaziale delle specie più rare. È stato effettuato uno studio dei meccanismi di coesistenza tra specie in cui la struttura specifica di connettività, interagendo con le proprietà locali del territorio, abbia effetti che si estendano su scale regionale. Lo studio presente rappresenta la frontiera nel settore dell'ecologia spaziale, ed è particolarmente efficace nel presentare risultati sperimentali ed un'analisi teorica, suggerendo strategie di intervento per la preservazione degli ecosistemi fluviali, la cui biodiversità è altamente minacciata.

Nei primi due capitoli viene studiata la relazione tra biodiversità, produttività, e stabilità di comunità microbiche. Qui l'intricata connessione delle interazioni ecologiche tra diverse specie di protisti è stata indagata a fondo. Si è rivelato come il concetto di diversità funzionale sia utile nel mantenere stabilmente nel tempo la biodiversità. Questa analisi identifica precise regolarità nella comunità ecologiche, che non risultano essere banalmente determinate dalla somma delle singole componenti in gioco, bensì una proprietà emergente dall'architettura delle interazioni. L'ultima parte (capitolo 6) sintetizza gli approcci sperimentati nei primi capitoli, calando aspetti di coesistenza locale nella complessità spaziale offerta dai bacini montani. Tale analisi offre una possibile spiegazione ad una macrostruttura di biodiversità diffusa in natura – recentemente rilevata anche in comunità di insetti del bacino fluviale svizzero – in cui la diversità locale mostra un picco per altitudini intermedie. Nella modellizzazione del processo, la nicchia ecologica di una specie viene determinata dall'altitudine. Pertanto l'analisi, ancorata ad ipotesi essenziali, è ispirata al principio einsteiniano: “Cerca di trovare la soluzione più semplice di un problema, ma non ricadere su quella banale”.

Conclusioni di questo lavoro e prospettive per sviluppi futuri sono quindi discusse.

Parole chiave: reti ecologiche dendritiche, microcosmi sperimentali, ecosistemi fluviali, metacomunità, dispersione direzionale, assemblaggio di comunità, diversità funzionale, interazioni tra specie, reti fluviali ottime, stabilità, rumore stocastico, modello dell'opinione di voto, gioco a somma nulla.

Contents

Acknowledgements	v
Preface	vii
Abstract	xi
List of figures	xvii
List of tables	xx
1 Introduction	1
1.1 Thesis outline	6
2 Inferring species interactions: a comparison of methods	9
2.1 Introduction	9
2.2 Materials and Methods	11
2.2.1 Aquatic communities	11
2.2.2 The interaction experiments	16
2.2.3 Data analysis	16
2.2.4 Stability analysis	20
2.2.5 Community model	20
2.3 Results	24
2.4 Discussion	28
3 Stabilizing effect of functional diversity on microbial communities	35
3.1 Introduction	35
3.2 Materials and Methods	37
3.2.1 Aquatic communities	37
3.2.2 The interaction experiments	39
3.2.3 Community model	42
3.3 Results	43
3.4 Discussion	49

4	Connectivity rules	57
4.1	Materials and Methods	58
4.1.1	Aquatic communities	58
4.1.2	The landscapes	60
4.1.3	Disturbance-dispersal events	61
4.1.4	Biodiversity patterns	63
4.1.5	Species' traits: size distribution	63
4.1.6	Species' traits: population growth	63
4.1.7	Disentangling processes: 'birth and death' dynamics	65
4.1.8	Stochastic metacommunity model	65
4.1.9	Statistical analysis	66
4.2	Results and Discussion	68
4.2.1	Temporal dynamics	72
4.2.2	Headwaters vs. confluences	72
4.2.3	Competitive exclusion dynamics	74
5	Disentangling habitat patch-size from hierarchical habitat capacity	77
5.1	Introduction	77
5.2	Material and Methods	80
5.2.1	The Riverine landscapes	80
5.2.2	Aquatic communities	83
5.2.3	Patch-size effects	83
5.2.4	The dispersal events	83
5.2.5	Biodiversity patterns	85
5.2.6	Local and regional evenness	86
5.2.7	Modeling metcommunities in dendritic environments	86
5.2.8	Statistical analysis	88
5.3	Results	89
5.3.1	α -diversity patterns	95
5.3.2	Evenness patterns	95
5.3.3	β -diversity patterns	95
5.4	Discussion	97
5.4.1	α -diversity patterns	97
5.4.2	Community composition	100
5.4.3	β -diversity patterns	103
5.4.4	Broader implications for aquatic organisms in streams	105
5.5	Conclusions	106
6	The mid-altitude effect in river landscapes: patterns and processes	109
6.1	Introduction	109
6.2	Methods	113
6.3	Results and Discussion	116

7	Conclusions and perspectives	121
A	Modeling riverine ecosystem connectivity	127
A.1	Synchronization in river networks	128
	Bibliography	131
	Curriculum Vitae	147

List of Figures

1.1	Theoretical frameworks analyzing biological communities in spatially structured landscapes	2
1.2	Connectivity rules key biodiversity measures structuring ecological communities	5
1.3	The dendritic connectivity experiment	7
2.1	Possible pairwise interactions between species	12
2.2	Image analysis for counting efficiency	13
2.3	Species traits: intrinsic growth and diffusion coefficient	14
2.4	Functional dendrogram for protists species defines functional groups	15
2.5	Two-species interaction dynamics	18
2.6	Species-interaction matrices	23
2.7	Distribution of interaction coefficients	25
2.8	Species interactions in protist communities	26
2.9	Predicted species performance	27
2.10	Comparison among the four different methods	28
2.11	Comparison between species ranks with and without <i>Spirostomum</i> species	29
2.12	Competition-colonization trade-off between 9 protist species	30
2.13	Species' temporal dynamics adopting the stochastic community model	31
2.14	Asymptotic stability analysis	32
3.1	Relationship between body size and species carrying capacity in protist species	38
3.2	Pairwise interaction experiments in 11-protist species communities	40
3.3	Interaction strength distribution	43
3.4	Interactions resulting in competitive loops	44
3.5	Interactions resulting in mutualistic loops	45
3.6	Experimental community biomass production	46
3.7	Relationship between functional distance and biomass production in the two-species communities	47
3.8	Community productivity in the six experimental replicates	48
3.9	Temporal dynamics of protists' density from the interaction experiments	50
3.10	Theoretical functional diversity-community biomass production relationship	51
3.11	Species coexistence, community productivity and stability in a gradient of functional diversity	52

List of Figures

4.1	Design of the connectivity experiment	59
4.2	α -diversity for the three replicates of the aquatic microcosm communities in ‘Isolation’ treatment	61
4.3	Dispersal protocol	62
4.4	Cumulative density function (CDF) of α -diversity	67
4.5	Ecological diameter of the river networks	68
4.6	Experimental and theoretical local species richness in river network	69
4.7	Probability density function of α -diversity for RN and 2D landscapes	70
4.8	Time behavior of biodiversity patterns’ in ‘RN’ and ‘2D’ landscapes	71
4.9	α -diversity as a function of connectivity degree	73
4.10	Impact of disturbance events on species persistence	73
5.1	Spatial configuration of dendritic networks and corresponding patch-sizes in the microcosm experiment	79
5.2	Spatial distribution of ecological diameter in river networks	81
5.3	‘Isolation’ treatment	82
5.4	Final volume: non reacting particle scheme	85
5.5	Probability density function for α -diversity, local evenness, and β -diversity	89
5.6	α -diversity and evenness patterns	93
5.7	Community composition at metacommunity scale	94
5.8	Species’ density depending on patch-size	96
5.9	β -diversity patterns	97
5.10	β_J -diversity dependence on topological and environmental distances	98
5.11	Diffusive particles: a control	101
5.12	Metacommunity models for neutral and non-neutral species	102
5.13	Temporal dynamics of regional evenness for neutral and non-neutral communities	104
6.1	Macroinvertebrates α -diversity patterns	110
6.2	Comparison between real-life and conceptualized landscapes	112
6.3	Connectivity of patches with similar altitude	114
6.4	Altitude niche	115
6.5	Conceptual landscape preserving the hypsographic curve of the river basin	116
6.6	α -diversity patterns resulting in the mid-altitude peak	117
6.7	Relative abundance of a subset of species	119
A.1	Synchronization properties in contrasting trees topologies.	130

List of Tables

2.1	Comparing methods to detect species interactions	19
4.1	Experimentally measured species' traits	64
5.1	Correlations among network descriptors.	80
5.2	Effects of network descriptors on α -diversity.	90
5.3	Effects of network descriptors on local community-evenness.	90
5.4	α -diversity patterns.	91
5.5	Local community-evenness patterns.	92
5.6	Mantel tests on β -diversity.	98

1 Introduction

The search for the mechanisms determining the distribution of life on Earth has long been a challenge for ecologists and biogeographers (MacArthur and Wilson, 1963; Sheldon, 1968; Brown, 1995; Gaston, 2000; Hubbell, 2001; Ricklefs, 2004). Researchers aim to draw the link between ecological and evolutionary processes, such as selection, drift, speciation and dispersal, and patterns of diversity and species composition in natural communities (Hubbell, 2001; de Aguiar et al., 2009; Vellend, 2010). Strikingly consistent patterns of biodiversity have been routinely observed over space and time, indicating the presence of regularities in the organization of biological communities (Volkov et al., 2003; Pigolotti et al., 2005; Volkov et al., 2005; Azale et al., 2006; Houchmandzadeh, 2008; Muneeppeerakul et al., 2008a; Bertuzzo et al., 2011). Undoubtedly, both abiotic components and species-interactions drive the spatial and temporal organization of an ecosystem as well as the emergence of characteristic patterns. The complexity of ecosystems stems from the entanglement of species' interaction networks with the spatio-temporal heterogeneity dictated by the environmental conditions (Pillai et al., 2011). Processes operating at a different range of spatiotemporal scales contribute to shape the assembly of natural communities and macroecological patterns of diversity. At regional scales, the species pool is constrained by environmental drivers and evolutionary history (Ricklefs, 2004; Mayfield and Levine, 2010), whereas at local and intermediate scales community compositions are dictated by species interactions in a small neighborhood and dispersal, which determine species coexistence (Chesson, 2000b; Holyoak et al., 2005).

Biological communities often occur in spatially structured habitats. The environmental matrix has been recognized to play a key role in shaping and regulating community dynamics, which are reflected in peculiar diversity patterns, captured by measures of α -, β - and γ -diversities (Muneeppeerakul et al., 2008a; Brown and Swan, 2010; Finn et al., 2011). Until recently, however, studies have either ignored the specific structure of landscapes (the so-called mean-field context, McKane et al. (2000); Vallade and Houchmandzadeh (2003); Houchmandzadeh and Vallade (2003); McKane and Newman (2004)), or employed simplified spatial structures (linear or lattice landscapes, Condit et al. (2000, 2002); Vallade and Houchmandzadeh (2006)). This is surprising

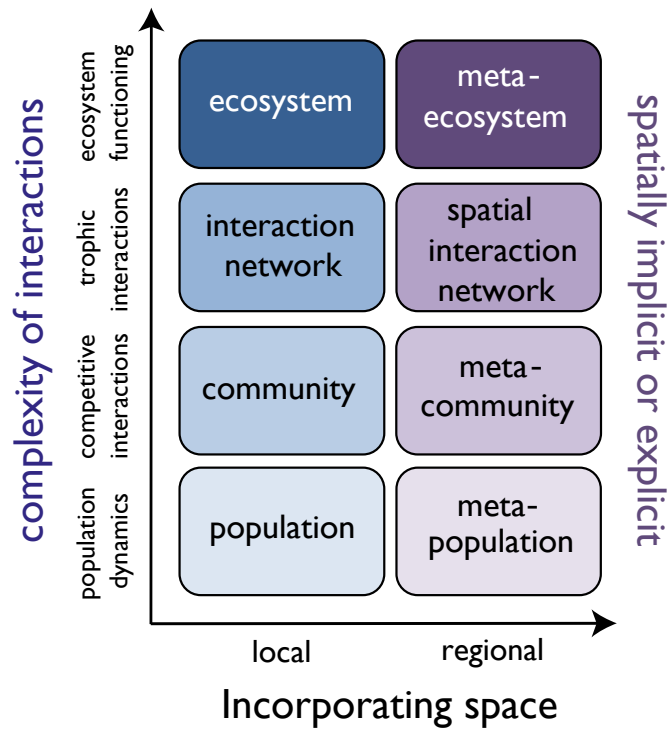


Figure 1.1: Conceptual scheme for biological communities in natural environments. The scheme depicts two important drivers of biodiversity patterns: ecological interactions (vertical axis) and spatial components (horizontal axis). Theoretical frameworks useful to analyze the complexity of natural communities are shown in colored boxes, from local single-species dynamics (population level) to meta-ecosystems at increasing complexity of ecological interaction and incorporation of spatial structure. Freely redrawn from a presentation of François Massol at Winter School on Ecological Theory, at Monte Verità, Ascona, 2013.

because many highly diverse landscapes, such as riverine or mountainous landscapes, exhibit specific hierarchical spatial structures that are shaped by well understood and characterized geomorphological processes (Rodriguez-Iturbe and Rinaldo, 1997; Clarke et al., 2008; Brown and Swan, 2010). Metapopulation and metacommunity theories (Hanski, 1998; Holyoak et al., 2005), whether neutral or species-specific regarding per capita vital rates, have greatly improved our understanding of patterns in population demography and community composition by focusing on the dynamics of dispersal linking local communities together (Figure 1.1). Specifically, theoretical work suggests that dispersal alone constrained by habitat structure shapes community composition, as observed in natural river systems. Riverine landscapes are among the most diverse habitats on earth and their ecosystem functioning is essential for human well-being (Vörösmarty et al., 2010). Currently, diversity and ecosystem functioning of riverine systems are highly threatened due to a combination of habitat modification, invasive species and changes in river connectivity (Gassner, 2006; Urban et al., 2006; Poff et al., 2007; Mari et al., 2011; Ziv

et al., 2012). To mitigate these negative effects, an understanding of factors driving riverine diversity patterns is of the highest priority (Vörösmarty et al., 2010; Grant et al., 2012; Perkin and Gido, 2012; Ziv et al., 2012).

The common traits existing among all types of river basins and their drainage networks (Rinaldo et al., 1992; Rodriguez-Iturbe and Rinaldo, 1997; Rinaldo et al., 2006) suggest the possible existence of general rules according to which the river network structure plays a key role in shaping ecological patterns. Indeed, branching river networks are striking examples of natural fractal patterns which self-organize, despite great diversities in forcing geologic, lithologic, vegetational, climatic and hydrologic factors, into forms showing deep similarities of the parts and the whole across several orders of magnitude. One therefore wonders whether recurrent geometrical and topological patterns bear general ecological implications. Specifically, the ecological corridors provided by river networks induce anisotropy in the spreading of species, populations or pathogens or other agents along the waterways (Rodriguez-Iturbe et al., 2009). In the past, most empirical studies aimed at explaining riverine diversity patterns by using local environmental conditions. Recently, the effect of dispersal along riverine networks on diversity has received more interest. However, empirical studies made two simplifying assumptions that are not completely justified. First, habitat quality and connectivity were generally treated as independent quantities. While this simplification may be appropriate for ecosystems such as islands archipelagos (MacArthur and Wilson, 1963) or forests (Hubbell, 2001), it does not represent many natural landscapes, especially riverine systems. In river basins, hierarchical dendritic structures command related scaling on habitat capacity, and local environmental conditions are intrinsically linked with the specific dendritic connectivity (Lake et al., 2007). Specifically, local community volumes and habitat size scale with the contributing drainage area, and suggest a spatial correlation between local properties and regional network descriptors (Leopold et al., 1964; Rodriguez-Iturbe and Rinaldo, 1997; Benda et al., 2004). Second, mostly constant dispersal rates and symmetric dispersal kernels were used in simplified landscapes. The hierarchical structure of riverine systems and directional dispersal therein have thereby been ignored. Moreover, river streamflow variations at different spatiotemporal scales are reflected in alterations of stream ecosystems (Ceola et al., 2013).

Only recently, theoretical models have investigated effects of connectivity in shaping macroecological patterns in riverine environments. Theoretical work suggests a contrasting effect of dispersal rate on diversity pattern in dendritic systems compared to 2-D systems (Muneepeerakul et al., 2007), such that increased dispersal reduces α -diversity, but does not affect β -diversity, predicting also that regional coexistence of species could be promoted by asymmetric dispersal (Muneepeerakul et al., 2008b; Salomon et al., 2010). Connectivity rules key biodiversity measures structuring ecological communities (Figure 1.2). Species richness geography depends on the configuration of the spatial domain and the directionality of the dispersal imposed by the landscape.

For example, a neutral metacommunity model was used to explain fish biodiversity patterns in the Mississippi-Missouri basin (Muneepeerakul et al., 2008a). It was found that directional

Chapter 1. Introduction

dispersal constrained by specific habitat structures is consistent with the naturally observed diversity pattern, and is consistent with diversity patterns observed in other large river systems, such as the Amazon or Rhine. Connectivity patterns of river networks differ strongly from linear and 2-D landscapes (Fagan, 2002; Fagan et al., 2002), and these differences in connectivity can either enhance or reduce metapopulation persistence compared to the other ones, depending on the details of dispersal (Muneepeerakul et al., 2007, 2008b). Habitat fragmentation in dendritic landscapes has different (and arguably more severe) consequences for fragment size than in linear or 2-D systems, resulting in both smaller fragments and higher variance in fragment size. A deeper understanding of the coupling of disturbance-dispersal events on a river network system is required (Benda et al., 2004). Given the lack of experimental studies covering a comprehensive sampling of headwaters, intermediate branches and the main stem in natural dendritic systems, whether low α -diversity in headwaters are always complemented with a high β -diversity (Finn et al., 2011) is a standing problem. Furthermore, it is unclear whether asymmetric dispersal from the headwaters may increase diversity at the confluence, and if headwater branches are refuges for competitively inferior species (Lowe and Likens, 2005).

The analysis of dendritic habitat structure and diversity was always comparative, and although this approach is certainly interesting, it does not allow a causal understanding of the effects of dendritic habitat structure *per se*. Experiments are thus needed to disentangle the causality between different factors such as the dendritic structure, directionally-biased dispersals and species interactions. Experimental evidence supporting the direct effect of habitat network structure on biodiversity patterns was completely lacking to date, though a simplified analysis has been conducted in 1-D systems (Altermatt et al., 2011a). Aquatic microcosms were adopted as model systems (Holyoak et al., 2000; Cadotte, 2007; Houchmandzadeh, 2008; Altermatt et al., 2011b) to investigate the combined effect of connectivity, and the spatial organization of patch sizes on the biodiversity patterns of dendritic metacommunities. The use of protists as model systems, representing a useful bridge between theory and nature, has contributed to several breakthroughs in ecological understanding of population, metapopulation and metacommunity dynamics (Holyoak and Lawler, 2005). This opened up the possibility to use laboratory experiments to test theory, develop new models to explain experimental results, in an iterative manner. Protist species cover a wide range of body sizes (from 10^{-6} to 10^{-3} gr) (Giometto et al., 2013), have rapid generation times (intrinsic growth rates can vary between (from 10^{-1} to 10^1 day $^{-1}$), covering substantial biological complexity in terms of movement ability, trophic levels and species interactions. By manipulating the connectivity of the landscape, patch sizes and the species pool it is possible to resemble different stress conditions that species might face in natural situations, like extensive human landuse, habitat fragmentation, biological invasions, and climate change.

Dispersal, which refers to species' pathways constrained by the particular habitat connectivity, can also be manipulated, opening the possibility to test directly predictions provided by spatially explicit theory at different spatial and temporal scales. The timescales involved in these experiments rarely exceed one month, as system relaxation to stationary conditions after perturbations happens in few days (Altermatt et al., 2011a). This allows to investigate over meaningful ecological scales through experiments that spans over few weeks. Thus, this combination of theory

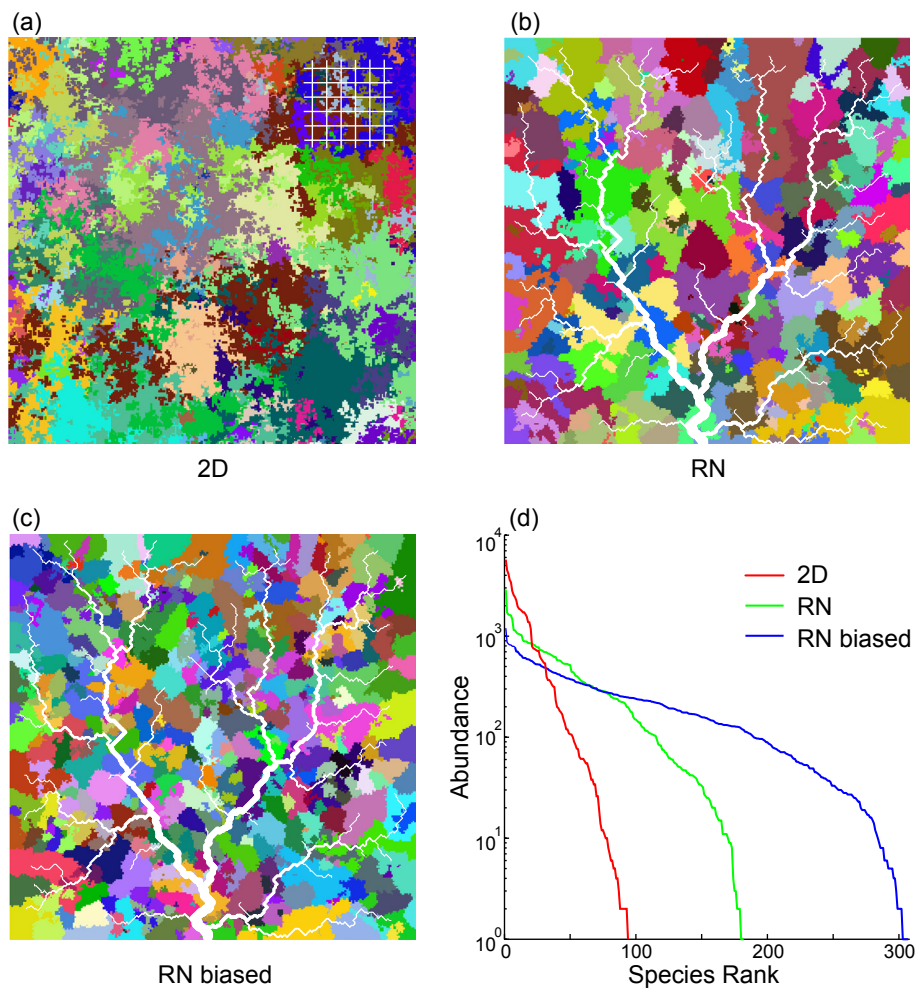


Figure 1.2: Biodiversity patterns in contrasting landscape topologies. (a, b) illustrate the spatial biodiversity configurations obtained theoretically for two landscapes (respectively a 2-D square lattice (2D) and a river network (RN)). An individual-based voter-like model obeying neutral dynamics has been adopted in the simulations. The results are qualitatively reproduced regardless of modeling details (e.g., individual-based vs. metapopulation models) and regardless of the structure of dispersal kernels, or migration rates (Muneepeerakul et al., 2008b). Direction of dispersal are highlighted in white: in the 2-D lattice each site has four nearest-neighbors according to von Neumann definition, whereas in the river network individuals move constrained to the dispersal pathways imposed by the dendritic connectivity. The configuration of the space and the directionality of the dispersal imposed by the landscape determine a different species richness geography. Pixels of the same colors represent individuals of the same species, and highlight visually the substantial effect that connectivity and directional dispersal bear on species diversity at the community level. (c) Adding other factors typical of the dispersal in network landscape such as biased transport (e.g., offsprings preferably colonizing downstream) would only enhance the observed differences. (d) Rank-abundance curves are different because of directional dispersal imposed by different connectivity (results from own unpublished simulations).

Chapter 1. Introduction

and realistic model systems is needed to understand ecological processes in depth and infer general ecological principles that act in natural systems at larger spatiotemporal scales. Moreover, microbial communities composed by bacteria, protists and unicellular algae are intrinsically of key ecological significance (Quince et al., 2008). In fact, they are the basic food source of almost all aquatic food webs (Finlay et al., 1996). Unicellular algae are responsible for nearly 50% of the worldwide biomass production. As shifts in these communities can have major global consequences, it is of fundamental importance to understand the mechanisms that regulate their abundance, size distribution and robustness to biotic and abiotic forcing (Finlay and Esteban, 1998).

1.1 Thesis outline

Chapter 2 deals with more methodological aspects: it provides the theoretical and experimental tools to describe community dynamics that will be applied in chapter 3 in local environments, and chapters 4 and 5 to dendritic landscapes. The counting process developed in this thesis work is here presented. An easier estimation of species' ecological traits, such as the intrinsic growth rate, the carrying capacity and the diffusion coefficient was made possible. It is also shown how a stochastic implementation of population dynamics is deemed as a fundamental tool for the derivation of key community properties, such as species persistence and community stability.

Key aspects of biodiversity-ecosystem functioning research are addressed in chapter 3. All pairwise interactions in a pool of 11 species of eukaryotes (10 protists and one rotifer), belonging to three functional groups, were measured. This approach builds upon more traditional experimental investigations, which generally focused on one trophic level. The diversity-productivity and diversity-stability relationships were explored in a local perspective, showing the crucial role played by functional diversity in the maintenance of species coexistence and productivity in trophically structured microbial communities.

Chapter 4 provides the first direct experimental evidence to a longstanding issue in spatial community ecology. It experimentally shows that connectivity *per se* shapes key components of biodiversity in microcosm metacommunities. By conducting a replicated multi-generation experiment with protozoans and rotifers in aquatic microcosm landscapes, the effects of directional dispersal imposed by the habitat-network structure on the biodiversity of metacommunities have been investigated. Experiments were conducted in culture plates connected by dispersal (Figure 1.3), thus imposing by construction a metacommunity structure (Warren, 1996; Haddad et al., 2008): each well hosted a local community within the whole landscape and dispersal occurred by periodic transfer of culture medium among connected LCs (Altermatt et al., 2011b), arranged in two different geometries. Spatially heterogeneous metacommunities arranged in a river network geometry are compared with spatially homogeneous metacommunities, in which every local community has 2D lattice four nearest neighbors.

The coarse-grained river-network landscape was derived from a scheme Rodriguez-Iturbe and

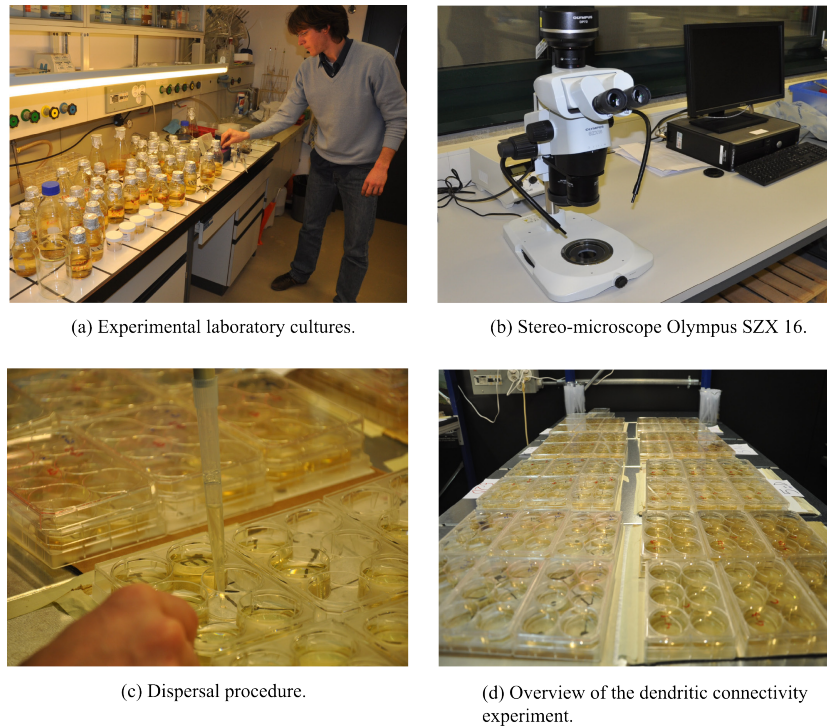


Figure 1.3: Overview of the experimental setup for the connectivity experiment.

Rinaldo (1997) known to reproduce the scaling properties observed in real river systems. Experimental findings were reproduced and extended with a stochastic metacommunity model. Again, this two-fold approach combining ad-hoc-designed experiments with modelling highlights the generality of the findings. Chapter 5 disentangles experimentally the effects of local habitat capacity (i.e., the patch size) and dendritic connectivity on biodiversity in aquatic microcosm metacommunities by suitably arranging patch sizes within river-like networks. The same model system implemented in chapter 4 was adopted to demonstrate that biodiversity patterns strongly depend on the spatial covariance between connectivity, position along the network and habitat quality. Their individual influence were disentangled by using three different configurations of local community volumes, connected following a river-network geometry. These treatments are i) a *riverine* landscape maintaining the intrinsic link of position and patch size, ii) a *random* landscape, with spatial random permutation of the patch volumes in above riverine configuration, and iii) a *homogeneous* landscape, with equal distribution of volumes (total volume is conserved in all cases). The microcosms were set in five independent realizations of river-network geometries.

In chapter 6, the investigation of the causes for the mid-altitude effect is carried out. This macroecological-pattern has been observed, among other datasets, in macroinvertebrates collected for a biodiversity monitoring project in Swiss river basins (BDM Coordination Office, 2009). A zero-sum metacommunity model was adopted to describe the community dynamics occurring

Chapter 1. Introduction

in river basins, where the landscape is sculpted by well-known geomorphological signatures. Specifically, species were assigned a fitness-dependence on altitude and dispersed to the nearest-neighbors (isotropic dispersal). The well-known mid-domain effect (Colwell et al., 2004) is revisited under the light of the appropriate consideration of the spatial environmental matrix. The amplification to multiple spatial scales of the boundary effects induced by the fractal organization of the river landscape was not detected in a null model, that is a regular hillslope-like landscape preserving the same hypsographic curve (the relative distribution of area at the various elevations) of a river landscape for a consistent comparison.

The present thesis, by combining theoretical models with experimental and empirical evidence, provides a unified approach for the understanding the origins and maintenance of diversity within riverine networks, with a focus on both local and regional scales. It is of direct relevance to ecology, conservation biology and environmental sciences, with important implications for a management oriented to the maintenance of ecosystem processes and preservation of endangered species in ecosystems exposed to habitat fragmentation and environmental change. Species are being endangered by a combination of climate warming (Araujo and Rahbek, 2006; Parmesan, 2006; IPCC, 2007) and habitat fragmentation (Fahrig, 2003; Gonzalez et al., 2011) caused by human activity, and there is an urgency in providing insights on the ecosystems' responses to these environmental forcing. Global environmental change, by shrinking and shifting the natural habitat of many taxa, is increasing the extinction risk of many species (Lenoir et al., 2008), with consequences predicted to be even stronger in ecosystems endowed with an intrinsic patchiness (Hanski and Ovaskainen, 2000; Altermatt et al., 2008). The consequences of species losses on ecosystems processes and services may have been drastically underestimated as recent assessments have provided mounting evidence for the key role of biodiversity in the assurance of public goods for societies (Cardinale et al., 2012; Hooper et al., 2012).

The experimental and theoretical findings of the present thesis for a model ecosystem, shaped like fluvial environments, suggest that the understanding of riverine diversity patterns must include a combination of local environmental conditions and their specific arrangement following river-network geometries. Thus, future comparative studies and theoretical models should be seen in this perspective. This thesis work may have implications for a management oriented to the maintenance of ecosystem processes and services.

2 Inferring species interactions: a comparison of methods

2.1 Introduction

Identifying the mechanisms that maintain species coexistence and stability in natural communities is a longstanding issue in ecology (Gause, 1934; MacArthur and Levins, 1967; May, 1972), and still an open problem in conservation biology. Since pioneering theoretical and experimental works (Volterra, 1926; Gause, 1934), researchers have been proposing several explanations for the high biodiversity that is observed in natural communities (MacArthur and Levins, 1967; Chesson, 2000b; Williams and Martinez, 2000; Hubbell, 2001; Allesina et al., 2008). The high biodiversity sustained in natural communities is even more surprising under the light of the phylogenetic limiting similarity hypothesis, recently tested in laboratory experiments using microbial communities with a simple trophic structure (Jiang et al., 2010; Violle et al., 2011; Tan et al., 2012). The limiting similarity hypothesis states that the struggle for coexistence is greater between closely related species than between distantly related species. It dates back to Darwin (1859), and has been thereafter expressed in theoretical formulations such as the competitive exclusion principle (Hardin, 1960; MacArthur and Levins, 1967; Tilman, 1980).

Stability of species coexistence is at the core of community ecology because it is directly related to the persistence of a system over time (McCann, 2000; Ives and Carpenter, 2007; Donohue et al., 2013). The characterization of the interaction matrix unravels the complexity observed in multispecies communities in terms of pairwise species interactions, and allows to systematically study the dynamic response of populations to a perturbation, that is, the asymptotic stability. Community ecologists have long been wondering whether asymptotic stability theory may be applied to ecological communities, where the response of a system to a small perturbation from the equilibrium state is fully described by the eigenvalues of the community matrix (May, 1972). Community matrix theory predicts that species in randomly assembled communities experience higher competitive strength (Bastolla et al., 2005), and that such systems have higher probability to be unstable, suggesting the presence of non-random assembling rules in natural ecosystems (May, 1972; Sole and Montoya, 2001). Theoretical work showed that important properties of the interaction matrix, such as the variance and the mean of the interaction terms, are dictating

Chapter 2. Inferring species interactions: a comparison of methods

the maximum number of species in a community, as well as its stability (Berlow et al., 1999; Kokkoris et al., 2002). Specifically, a recent study (Allesina and Tang, 2012) proved that both the architecture of the ecological networks, and the distribution of interaction strengths are impacting on ecosystem stability.

Measuring interactions among species in natural communities is a formidable task (Laska and Wootton, 1998; Berlow et al., 2004). To test theoretical predictions on the relationship between diversity and stability, scientists have performed experiments on interacting species in controlled environments. However, representative experiments on plants (Roxburgh and Wilson, 2000), or insects (Ayala et al., 1973; Paine, 1992), hydra species (Case and Bender, 1981), or in microbial communities (Gause, 1934; Vandermeer, 1969; McGradySteed et al., 1997; Foster and Bell, 2012), have been given contrasting results on the relationship between diversity and stability in biological communities (Ives and Carpenter, 2007). Experimental and theoretical investigations, however, were generally limited by focusing on one trophic level only (Loreau et al., 2001), and by a lack of a common methodological and conceptual approach to measure species interactions. Furthermore, most studies only focus on one type of interaction (e.g., competition, predation, amensalism, commensalism, or mutualism) at a time, while natural food webs commonly include multiple or all of them simultaneously.

The local coexistence of trophically-structured protist communities was studied in laboratory microcosm experiments, where species are competing for the same resources in homogeneous (in principle no spatial component is involved), and steady physical environments (no temporal environmental fluctuations). Laboratory experiments represent a useful tool to test theoretical predictions in ecology and evolution (McGradySteed et al., 1997; Fox and McGrady-Steed, 2002; Fukami and Morin, 2003; Cadotte, 2006a; Haddad et al., 2008; Carrara et al., 2012; Livingston et al., 2012), providing inferences about causality and bridging the gap between the complexity of natural systems and the level of abstraction inherent to all theoretical models (Holyoak and Lawler, 2005). In this model system, different forms of species interactions, such as competition for the same resources, interference competition, predator/prey dynamics, and in principle even cooperation (mutualistic or win-win relationship, (Bulleri et al., 2008; Gross, 2008; Freilich et al., 2011)) can be expected and have been indirectly observed in our previous work (Altermatt et al., 2011a; Carrara et al., 2012). Attention is focused here on: i) a comparison of the four different methods to measure species interactions and to predict species performance in multispecies communities from pairwise interactions; ii) a systematic discussion of methods and tools, useful for the ecological literature oriented to the study of population and community dynamics; and iii) an analysis of asymptotic stability.

In a set of 11 protists species, the interaction matrix of all possible 55 pairwise species combinations and the individual monocultures were characterized with the following methods: the first, called 'Extinction' method (*EX*), ranks the species balancing the number of extinctions of a species against all the other species (Cadotte, 2006a). The second method ('Relative Yield' method *RY*) weights the population performance of a species in the presence of a competitor, compared to isolation treatment. This method is often used in Biodiversity Ecosystem Functioning

(BEF) literature (Loreau and Hector, 2001). The third ('Lotka-Volterra Equilibrium' = EQ) and the fourth methods ('Lotka-Volterra Dynamics' = LVD) are based on generalized Lotka-Volterra (LV) models (see, e.g., Kokkoris et al. (2002)). EQ is assuming equilibrium (Paine, 1992), whereas LVD is also taking the temporal dynamics into account (see *Materials and Methods*). Table 2.1 gives an overview of the precise definitions, assumptions and data needed for the specific methods. All four methods are individually widely used in both diversity-functioning and predator-prey research (Ives et al., 2005), but to our knowledge have not yet been compared under a consistent framework and on the same empirical data.

2.2 Materials and Methods

2.2.1 Aquatic communities

A pool of 10 protists and one rotifer species were used in our experiments (henceforth called protists). The species were: *Chilomonas* sp., *Colpidium* sp., *Cyclidium* sp., *Dexiostoma* sp., *Euglena gracilis*, *Euplotes aediculatus*, *Paramecium aurelia*, *P. bursaria*, *Spirostomum* sp. and *Tetrahymena* sp. and the rotifer *Cephalodella* sp. *Chilomonas* sp. and *Tetrahymena* sp. were supplied by Carolina Biological Supply Co., whereas all other species were originally isolated from a natural pond (McGradySteed et al., 1997). The species were grown in sterilized culture medium made of local spring water, and 0.45 g l⁻¹ of Protozoan Pellets (Carolina Biological Supply, NC USA). Protozoan Pellets provide nutrients for added bacteria (*Bacillus cereus*, *B. subtilis* and *Serratia marcescens*). The protist species are naturally co-occurring in freshwater habitats and cover a wide range of body sizes, intrinsic growth rates and other important biological traits, such as swimming ability, nutrient uptake and photosynthetic capabilities (Altermatt et al., 2011a; Carrara et al., 2012). The experiment was conducted in a climatized room at 21°C under constant fluorescent light. Local communities were kept in culture well-plates containing 10 ml of culture medium.

Species' traits: population growth

Population growth curves are usually well described by the Malthus-Verhulst differential equation. In such a framework, the population density of species s , $\phi_s(t) = \langle N(t) \rangle / V$, starting at ϕ_s^0 individuals per ml of medium, grows in time following the logistic curve

$$\frac{d\phi_s}{dt} = r_s \phi_s \left(1 - \frac{\phi_s}{K_s} \right), \quad (2.1)$$

where r_s is the intrinsic growth rate, and K_s is the carrying capacity of species s . The complete results for intrinsic growth rates and carrying capacities of our study species are shown in Table 4.1 of chapter 4, where protists have been cultivated in single-species cultures at identical conditions as used for the interaction experiment in the current study.

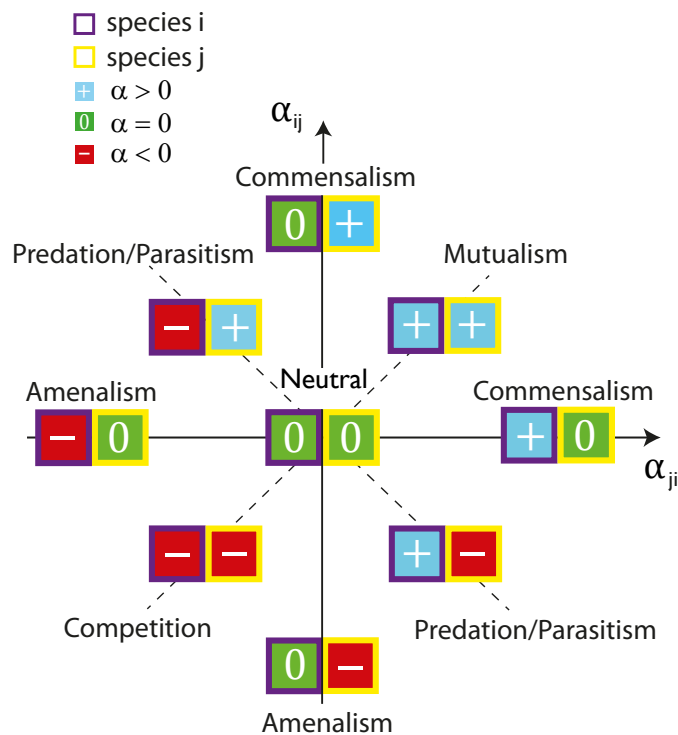


Figure 2.1: Schematic illustration of all possible pairwise interactions between species i and j . The constants α_{ij} and α_{ji} describe the effect of species j on species i and the effect of species i on species j respectively. The y - and x - axes are directly comparable to all subsequent interaction strengths α_{ij} and α_{ji} (see Figure 2.7). For competitive interactions both α -values are negative (red squares, loss-loss relationship), whereas in mutualistic interactions both α values are positive (cyan squares, win-win relationship). Predation/parasitism occurs where the two interactions have opposite signs ($\alpha_{ij}\alpha_{ji} < 0$). Non-interacting species fall on the origin of the graph.

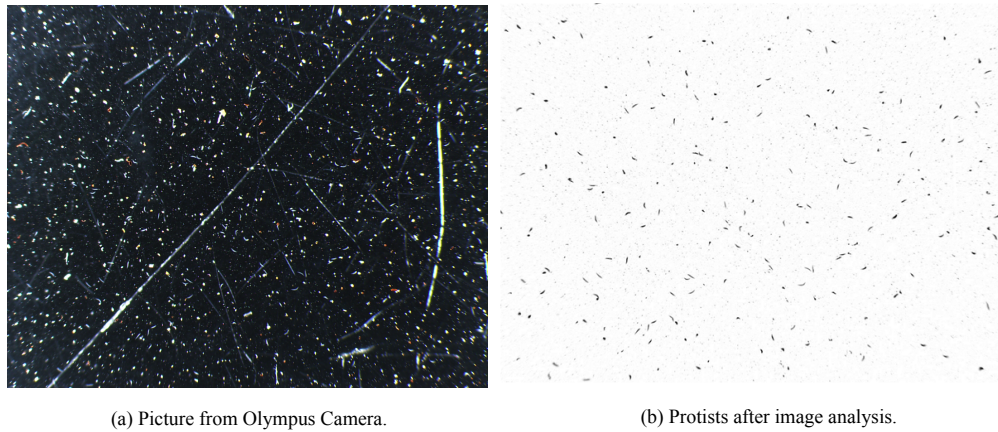


Figure 2.2: Semi-automatic counting procedure.

The protists were measured with a stereo-microscope (*Olympus SZX16*), on which a camera was mounted (*DP72*), and analyzed photographs via software (*cell 3.2*, Figure 2.2). Exposure time and the magnification were optimized for each species. The length of 50 individuals of each species (longest body-axis) were measured to get size distributions (Table 4.1, chapter 4). To get density estimates of the population (Figure 2.3a), three drops of 0.1 ml were taken, and all individuals present in the drops were counted. A way to count easily the protozoan in a drop has been developed: two photographs of the same drop are taken, and by subtracting the two images after conversion in gray-scale (the negative numbers are set to zero not to count twice the individuals), what it is marked it has been moving during the time interval in between the two photographs. To be sure to count only the individuals and not dust particle or very big objects, a threshold was put: from $0.25 \cdot \langle L_s \rangle$ to $4.0 \cdot \langle L_s \rangle$, where $\langle L_s \rangle$ is the mean individuals size.

Species' traits: spreading in space

Two independent ways to get an estimate of the species diffusion coefficients D_s has been developed¹. The diffusion hypothesis holds:

- every individual movement is completely random,
- every individual moves independently of the others.

In the first method, pictures for different exposure times are taken and the linear displacement of all the recognizable traces left on the screen by each individual are recorded, obtaining for every exposure time t^* the ensemble mean $\langle x^2 \rangle_{ens}$. In Figure 2.3b, the fit of the curve is $\langle x^2 \rangle = 4Dt + A(1 - e^{-t/\tau_c})$. Actually, for $t < \tau_c$, the process is not diffusive but it is in the

¹The experimental conditions are the same for the interaction experiment.

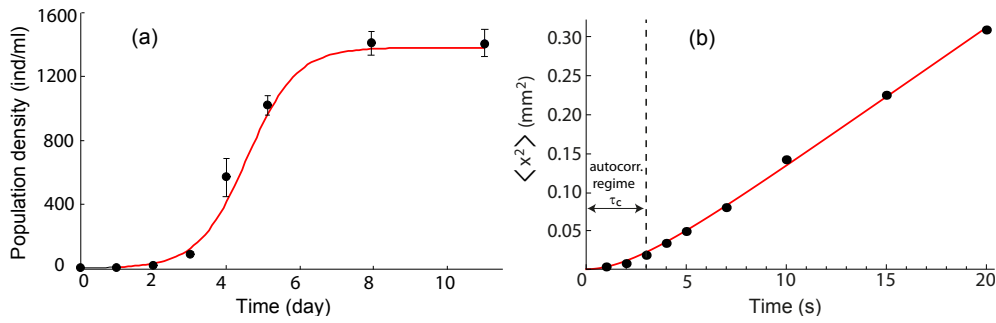


Figure 2.3: (a) Population growth curve for a population of *Colpidium* sp., starting at a density of 10 ind ml^{-1} obtained in the same conditions of the metacommunity experiment. Average \pm s.d. of six experimental replicates (black points) and logistic fit (red line). (b) Mean square linear displacement for *Euglena gracilis*. Two regimes can be recognized: for $t < \tau_c$, the autocorrelation time $\langle x^2 \rangle \propto t^2$, for $t > \tau_c$ we find the diffusion regime $\langle x^2 \rangle = 4Dt$. $\tau_c = 2.6 \text{ s}$, $D = 0.0049 \text{ mm}^2\text{s}^{-1}$.

autocorrelated (Taylor) regime. In the second method, the diffusive regime was explored for longer time, by following one single individual in time (till the individual can be followed under the microscope view), taking pictures for time interval longer than autocorrelation time τ_c recovered by the first method, to assure the position in every pictures is uncorrelated with the previous one. By taking auto-averages in time it is possible to compare the estimate of two diffusion coefficients. If the process was ergodic, the two estimates would coincide. However, the second methods is affected by the fact that individuals are not all equal as it would have been for pollen particles in pure Brownian motion (Uhlenbeck and Ornstein, 1930). There is a dependence on the state of the single individual (i.e., age, size, feeding state). Moreover, in the first method a crowding phenomenon could be also present, weakening the second assumption postulated above.

The estimates of the species diffusion coefficients and the average species-velocity were useful to analyze the experimental results in Altermatt et al. (2011a). The effects of connectivity coupled with recurrent disturbances were studied on a very simple system of two patches connected by tubing, in which one randomly chosen patch was disturbed. Part of the analysis focused on the relationship between species abundance and species traits, provided by our experiments. A weak relationship was found between the wave speed obtained theoretically via relationship $v_{min} = 2\sqrt{D_s r_s}$ and the post-disturbance recovery.

Species' traits: functional groups

All species can feed on bacteria, but may prefer different bacteria species, depending on morphology or phylogeny of both protists and bacteria (Glücksman et al., 2010). Specifically, an individual's diet is directly linked to body size, which reflects important predator-prey relationship from allometric scaling theory (Allesina et al., 2008). Functional groups were defined by

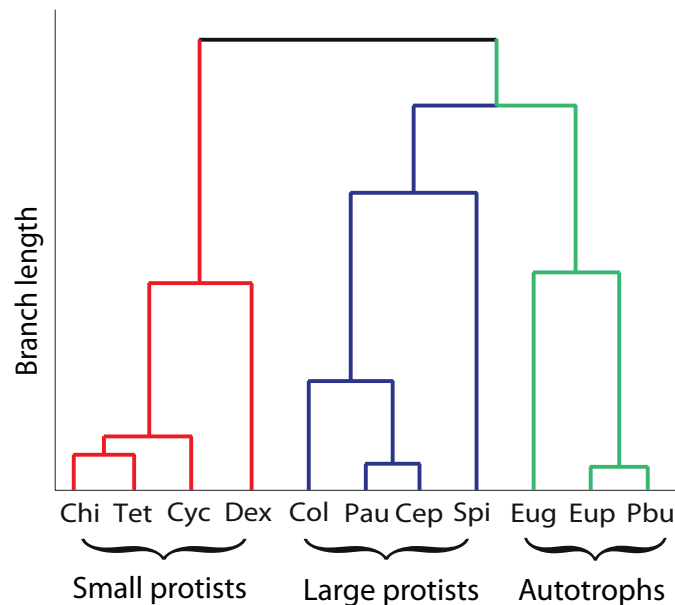


Figure 2.4: Community dendrogram based on intrinsic growth rate, body size, and ability to photosynthesize as species traits. The 11 species are: *Chilomonas* sp. (*Chi*), *Cyclidium* sp. (*Cyc*), *Tetrahymena* sp. (*Tet*), *Dexiostoma* sp. (*Dex*), *Colpidium* sp. (*Col*), *Paramecium aurelia* (*Pau*), *Cephalodella* sp. (*Cep*), *Spirostomum* sp. (*Spi*), *Euglena gracilis* (*Eug*), *Euplotes aed.* (*Eup*), and *Paramecium bursaria* (*Pbu*). Different colors are associated to different functional groups (red: small bacterivorous, *Chi*, *Cyc*, *Tet*, *Dex*; blue, large bacterivorous, *Col*, *Pau*, *Cep*, *Spi*; green, autotrophs, *Eug*, *Eup*, and *Pbu*).

grouping species that share similar ecological traits, reflecting fitness (intrinsic growth rate), and niche difference (body size, and photosynthetic ability). Functional distance was measured as the euclidean distance in trait space (Walker et al., 1999). These three ecological traits were used to build a trait dendrogram (Petchey and Gaston, 2002), where species are assigned to the tips of the dendrogram (Figure 2.4). At the highest hierarchical level of the community dendrogram, functional groups were defined by grouping species belonging to the same branch. *Chilomonas* sp., *Cyclidium* sp., *Tetrahymena* sp., and *Dexiostoma* sp. are small bacterivorous species ($0.6\text{--}4.5 \cdot 10^{-6}$ g, body size values from Giometto et al. (2013) with high growth rates ($r > 1.5 \text{ day}^{-1}$). *Colpidium* sp., *P. aurelia*, *Cephalodella* sp., and *Spirostomum* sp. are large bacterivorous species ($20\text{--}1000 \cdot 10^{-6}$ g) with small growth rate ($r < 1.5 \text{ day}^{-1}$). Furthermore, *Cephalodella* sp., *Paramecium aurelia*, and *Spirostomum* sp. may not only feed on bacteria, but may also predate on smaller flagellates, which are always present in cultures and remain unidentified. These species may also feed directly on smaller protist species, such as *Chilomonas* sp., *Cyclidium* sp., *Tetrahymena* sp., and *Dexiostoma* sp. Finally, *Euglena grac.*, *Euplotes aed.*, and *P. bursaria* are autotrophic species, but can also feed on bacteria (i.e., they are mixotrophic).

2.2.2 The interaction experiments

The outcome of all 55 pairwise species-combinations was measured in microcosm experiments. All 11 species were initially grown in pure cultures to carrying capacity. Then, 5 ml of medium of species i at carrying capacity was mixed to 5 ml of species j at carrying capacity (total volume, $V = 10$ ml). Initial densities (ϕ_i^0, ϕ_j^0) were measured and are thus known. In this manner, individuals of different species started immediately to strongly compete for resources, as the communities were initially saturated with individuals. Furthermore, species coexistence was tested in communities composed of all 11 protists, initializing the microcosms by taking $V/11$ volume medium volume from each species' pure culture. The 11-species, the 55 two-species, and the 11 single-species communities were replicated six times each. After three weeks, at $t^* = 21$ days, the density of each species was measured in all microcosms. A variable quantity of medium was sampled (for method details, see Altermatt et al. (2011a)), and counted densities under a stereo-microscope. The density of *Spirostomum* sp. was directly counted in the well-plates, as it naturally occurs at very low densities.

2.2.3 Data analysis

Four different methods were used to analyze the interaction experiment ('Extinction' = EX , 'Relative Yield' = RY , 'LV Equilibrium' = EQ , 'LV Dynamics' = LVD ; see also Table 2.1). These methods are widely used in both diversity-functioning literature and predator-prey research (Ives et al., 2005), but are hardly ever compared under a consistent framework. In all the four methods, the parameter α_{ij} reveals the strength of interaction of species j on i . Table 2.1 summarizes the characteristics of the four methods, as well as the type of information needed to calculate them.

Measures for species-interaction strengths

Extinction. The EX method balances the number of extinctions caused by a species in all the 10 different pairwise trials with the number of extinctions faced by the same species, across all the six replicates: $\alpha_{ij}^{EX} = \sum_{rep=1}^6 (\phi_{i|j}^* = 0)$, where $\phi_{i|j}^*$ is the number of individuals of species i per ml interacting with individuals of species j , at the sampling time $t^* = 21$ days, and index rep sums over the six experimental replicates.

Relative Yield. The RY method compares the reduction (or increase) in population density of species i caused by species j relative to the single-species performance of i (Paine 1992), $\alpha_{ij}^{RY} = \phi_{i|j}^* / K_i - 1$. With this method, $\alpha_{ij}^{RY} \geq -1$ by definition, with $\alpha_{ij}^{RY} = -1$ when species j has competitively excluded species i .

Lotka-Volterra Equilibrium. Both methods EQ and LVD are based on a Lotka-Volterra (LV) model, where EQ assumes equilibrium conditions at sampling time, while the LVD does not. In this framework, the change in the population density of species i over time due to the presence of

species 1..., S is written as

$$\frac{d\phi_i}{dt} = \phi_i f_i(\phi_1, \dots, \phi_S), \quad (2.2)$$

where f_i is the per capita growth rate of species i . The interaction coefficients are mathematically described as the change in the per capita growth rate of species i under a small change in density of species j :

$$\alpha_{ij} = \frac{\partial f_i(\phi_1, \dots, \phi_S)}{\partial \phi_j}. \quad (2.3)$$

In LV models, the dynamics of species i and species j are characterized by the following phenomenological equation:

$$\frac{d\phi_i}{dt} = r_i \phi_i \left(1 + \frac{\alpha_{ii}\phi_i + \alpha_{ij}\phi_j}{K_i} \right), \quad (2.4)$$

where α_{ij} measures the strength of inter-specific competition and α_{ii} that of intra-specific competition, which is equal to -1 for all species. The values α_{ij} for all pairwise i and j constitute the interaction matrix \mathbf{A} . After rescaling the density of species i by its carrying capacity K_i , $n_i = \phi_i/K_i$, $\alpha'_{ij} = \alpha_{ij}K_j/K_i$, the LV model becomes

$$\frac{dn_i}{dt} = r_i n_i \left(1 - n_i + \alpha'_{ij} n_j \right). \quad (2.5)$$

Method *EQ* makes the assumption that after 3 weeks all the communities have reached their equilibrium point. This assumption is based on previous experiments made in similar setups (Cadotte, 2006a; Haddad et al., 2008), where this method was used to quantify interaction strengths. The inter-specific interaction strengths is measured by setting the temporal derivative in Eq. (2.5) equal to zero (equilibrium condition), and solving for the interaction term $\alpha_{ij}^{EQ} = (n_i^* - 1)/n_j^*$, where n_i^* and n_j^* represent rescaled densities for species i and j at time $t^* = 21$ days. For this method, species' intrinsic growth rates and initial conditions play no role in the characterization of species interactions. The only important component is the imbalance of the species' density in isolation compared to its density in the presence of another species (Mouquet et al., 2004).

Lotka-Volterra Dynamics. For the *LVD* method, interactions α_{ij}^{LVD} were derived without assuming equilibrium. This can be done by fitting the time series of the two-species interaction through a LV dynamical model, constrained to the initial conditions adopted in the experiment, n_i^0, n_j^0 , and the final (rescaled) densities n_i^*, n_j^* at t^* . This estimate of the interaction terms is integrating the information of growth rate r_i (measured in Carrara et al. (2012) in the same environmental conditions, see Table 4.1 in chapter 4) and the carrying capacity K_i . r_i and K_i are obtained from the single species experiments, and one does not need to make assumptions about the equilibrium of the community at the final time point t^* .

For the *EQ* and *LVD* methods, the range of interaction coefficients was constrained to the highest

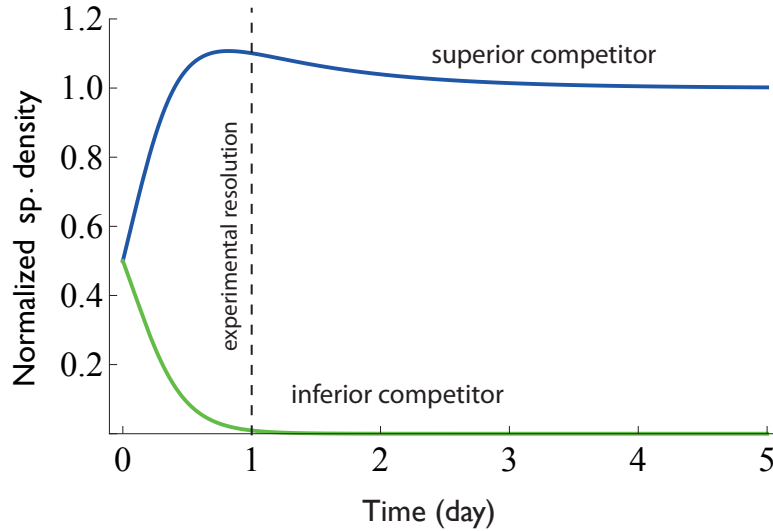


Figure 2.5: Simulated two species interaction dynamics adopting a Lotka-Volterra model, for (antisymmetric) values of $|\alpha_{ij}| = |\alpha_{ji}| = \alpha_{max} = 5$ and intrinsic growth rates $r_i = r_j = 1/\text{day}$ (the average growth rate for the species in our communities). Species interactions with coefficients higher than α_{max} lead to competitive exclusion on timescales faster than the daily experimental resolution (vertical black dashed line at $t = 1$ day).

precision possible with our experiment. As the experimental sampling resolution is of the order of one day, the daily timescale t_{exp} was the finest scale for dynamics in our coexistence experiments. Any interaction term that could lead to extinction of a species on shorter timescales than one day would not be experimentally detectable. This is operatively translating to bound the interaction terms between a certain symmetric range around zero. The dynamics of two competing species was simulated in a LV model: a superior species, i , and an inferior, j , with initial condition equal to our experiments (rescaled density $n_i^0 = n_j^0 \approx 0.5$) and with intrinsic growth rate $r_i = r_j = 1 \text{ day}^{-1}$. The inferior species' density gets to $n_j^* \approx 0$ for (antisymmetric) values of $|\alpha_{ij}| = |\alpha_{ji}| = 5$ (Figure 2.5).

Species interaction types

The methods *RY*, *EQ* and *LVD* in principle include the complete range of possible ecological interactions (Figure 2.1). Species with competitive interactions have negative α -values ($-/-$). The sign of α is positive when a predator-prey ($+/-$) or mutualistic interaction ($+/+$) is occurring between two species (although not in *EX*). A predator-prey interaction $i - j$ has $\alpha_{ij}\alpha_{ji} < 0$. In mutualistic interactions, both α_{ij} and α_{ji} are positive ($\phi_i > K_i, \phi_j > K_j$). Amensalism/commensalism arises when one value of α is equal to zero and the other is negative/positive, respectively. Non-interacting (neutral) species have both α values equal to zero (Figure 2.1). The interaction type and α values were assigned for each species-pair using the above-described categories, by considering the experimental uncertainty associated to each α value as the confidence interval.

Table 2.1: Comparison of four methods describing species interactions (*EX*= Extinction, *RY*= Relative Yield, *EQ*= Lotka-Volterra Equilibrium, *LVD*= Lotka-Volterra Dynamics). The table describes the methods, gives the mathematical formula to derive them, and lists the type of data needed to calculate them (*r* = intrinsic growth rate, *K* = carrying capacity, time series, long term experiment).

Method	Description	Formula	r	K	Time Series	Long Term
'EX'	balancing the number of extinctions in competition trials.	$\alpha_{ij}^{EX} = \sum_{rep=1}^6 (\phi_{ij}^* = 0)$	-	-	-	✓
'RY'	reduction of population density relative to carrying capacity.	$\alpha_{ij}^{RY} = \phi_{ij}^*/K_i - 1$	-	✓	-	✓
'EQ'	fitting two-species interaction terms (by Lotka-Volterra equations at equilibrium) using single species parameters.	$\alpha_{ij}^{EQ} = (\phi_i^* - K_i)/\phi_j^*$	-	✓	-	✓
'LVD'	fitting two-species interaction terms time series data (by Lotka-Volterra equations), using single species parameters.	α_{ij}^{LVD} : best fit numerical solution	✓	✓	✓	-

Uncertainties on α values were obtained by propagating errors from equations in Table 2.1 (for method *EX* by bootstrapping over 10000 runs), thus taking into account the natural variation associated to the value of K_s , measured in the isolation experiment from six replicates. Differences in intra- vs. inter-group distributions of species interaction strength were tested by a Kolmogorov-Smirnov test on the cumulative distributions.

Species ranking

Species were ranked by their competitive ability, which was derived by subtracting the competitive effects from the responses of a species to all other species in the community in the pairwise interaction rounds (Mouquet et al., 2004; Haddad et al., 2008). A species ranking measure R was obtained from the interaction matrix \mathbf{A} , by summing the values of the columns (responses) and subtracting the values of the rows (effects). For species i this is $R_i = \sum_j (\alpha_{ij} - \alpha_{ji})$. Rescaling the rank measure R_i between one and 11 allowed to make statistical comparisons between the four methods. In every method, each value of α is the average over the six different replicates. As a precise relationship is not expected, statistical significance between species rank R_i and normalized species density n_i was tested with power-laws, varying the exponents between one and five, and exponential relationships (weighted least square method with experimental errors). With that measure, each species performance in the 11-species experiments in terms of density (rescaled to each species' carrying capacity) was predicted from the pairwise experiments.

2.2.4 Stability analysis

The community matrix for the LV model coincides with the Jacobian matrix system, linearized at equilibrium $\mathbf{n}^* = (n_1^*, \dots, n_S^*)$, where interaction coefficients are constant:

$$J = [\partial(dn_i/dt)\partial n_j]_{\mathbf{n}^*}. \quad (2.6)$$

Generalizing Eq. (2.5) to a community with $S = 11$ species, a system of coupled differential equations is derived, where density changes of species i are described by:

$$\frac{d\phi_i}{dt} = r_i\phi_i \left(1 - \frac{\phi_i - \sum_{j \neq i} \alpha_{ij}\phi_j}{K_i}\right), \quad (2.7)$$

which after rescaling becomes

$$\frac{d\mathbf{n}}{dt} = \mathbf{r} \cdot \mathbf{n} (1 + \mathbf{A}'\mathbf{n}), \quad (2.8)$$

where \mathbf{A}' is the experimental interaction matrix (rescaled to each species carrying capacity). Thus, Eq. (2.6) becomes

$$J = \text{diag}(r_1 n_1^*, \dots, r_S n_S^*) \mathbf{A}', \quad (2.9)$$

where $\text{diag}(\dots)$ represents a diagonal matrix by listing its diagonal elements $\mathbf{r} \cdot \mathbf{n}^*$ at equilibrium. The community matrix predicts if the community will sustain the current biodiversity level, or if instead the system is in an unstable configuration, and will be more prone to rearrangements under environmental fluctuations. An equilibrium is stable if the real part of the dominant eigenvalue of J is negative, $\text{Re}(\lambda(J)) < 0$. The asymptotic stability analysis of our 11-species community was conducted by applying the above procedure, for both initial and final communities, by adopting the interaction matrix \mathbf{A} derived from the *LVD* method. To test the significance of the deterministic stability analysis, we performed a stability analysis by considering the experimental variation on the intrinsic growth rate r , the carrying capacities K and the α -values of the interaction matrix. In assessing the asymptotic stability of a community for the derivation of the eigenvalue $\lambda(J)$, the experimental uncertainty over the parameters r_s , and α'_{ij} in Eq. (2.9) was taken into account. 20000 simulations were conducted, randomly extracting values from the interval $[\bar{x} \pm \sigma_x]$, where \bar{x} is the mean value for the quantity x (r and α') and σ_x quantifies experimental uncertainty for x .

2.2.5 Community model

Community dynamics was investigated through simulations by using the experimental interaction matrix \mathbf{A}' derived through the *LVD* method. The system in Eq. (2.9) is solved using an implicit Runge-Kutta scheme. All species are present with a known initial density of $\phi_s^0/11$, as in the main experiment. Deterministic solutions are good approximations for high density species and for large volume V of medium. Due to the limited community volume $V = 10$ ml and the fact

that the species' carrying capacity in some cases is small (less than hundred individuals per ml of medium, see e.g., Table 4.1), fluctuations around the macroscopic solutions may not be negligible. playing instead a significant role in the dynamics of the process (Melbourne and Hastings, 2008). A stochastic description of the growth process is therefore required to obtain more reliable results.

The deterministic solution provided in Eq. (2.1) is a good approximation for high density species (Figure 2.3 shows the *Colpidium* sp. growth curve) and for large volume V of medium. V denotes the available space that can be occupied by protists and bacteria. The following facts hold:

- bacteria species are at least one order of magnitude smaller in length than the smallest protozoan species in our experiment;
- bacteria carrying capacities are of the order of millions per ml;
- bacteria growth rates are at least ten folds higher than protozoan growth rates.

Thus, the decision not to include bacteria dynamics in our model was made, assuming that their abundance may be considered constant at the time scale of protists dynamics.

Single species: 'birth and death process'

The stochastic formulation of the logistic process (the one-step 'birth and death process' with space/food limitation, van Kampen 2007) is necessary when the volume of the community or the number of individuals considered are small. Each individual has a natural death rate d and a probability b per unit time to divide. To insure that the Markov property holds, d and b are assumed to be fixed and independent of the age or size of the individual (for a modeling approach which took explicitly into account size see Giometto et al. (2013)). Moreover, competition gives rise to an additional death rate $\gamma(N-1)/V$, proportional to the number of other individuals present. For a population of N individuals, the transition probabilities read

$$T(N-1|N) = dN + \frac{\gamma}{V}N(N-1) \quad (2.10)$$

$$T(N+1|N) = bN. \quad (2.11)$$

The master equation is

$$\begin{aligned} \frac{dp_N(t)}{dt} &= \left[d(N+1) + \frac{\gamma}{V}(N+1)N \right] p_{N+1}(t) + b(N-1)p_{N-1}(t) - \\ &- \left[bN + dN + \frac{\gamma}{V}N(N-1) \right] p_N(t). \end{aligned} \quad (2.12)$$

Chapter 2. Inferring species interactions: a comparison of methods

Expansion in V (van Kampen 2007) gives the macroscopic equation for concentration ϕ

$$\frac{d\phi}{dt} = (b - d)\phi - \gamma\phi^2, \quad (2.13)$$

in which the logistic equation of Eq. (2.1) is derived, by identifying the macroscopic carrying capacity K with $(b - d)/\gamma$, which is the metastable stationary solution for $\phi(t) = \langle N(t) \rangle / V$.

Multispecies

Generalizing the above arguments, the case of multiple species living in a homogeneous environment and competing for the same resources is considered. The competition term $\gamma_i(N_i - 1)/V \approx r_i(N_i - 1)/(K_i V)$, valid for species i in pure cultures, changes when taking into account also the inter-specific interactions. The transition probabilities for the birth and the death of an individual of the i th species, within a community with $\vec{N} = (N_1, N_2, \dots, N_i, \dots, N_S)$ individuals in species pool $P = (1, 2, \dots, i, \dots, S)$ respectively, read:

$$T(\vec{N} + \vec{e}_i | \vec{N}) = b_i N_i \quad (2.14)$$

$$T(\vec{N} - \vec{e}_i | \vec{N}) = d_i N_i + \frac{(b_i - d_i) N_i (N_i - 1)}{K_i V} \left(1 + \sum_{j \neq i} \alpha_{ij} N_j \right), \quad (2.15)$$

where b_i , d_i , are the birth and death rates of species i , and α_{ij} are the interaction terms experimentally derived by the *LVD* method in the pairwise interaction experiments. The multivariate master equation for the community is given by (Volkov et al., 2009)

$$\begin{aligned} \frac{d}{dt} p(\vec{N}, t) &= \sum_i \left\{ T(\vec{N} | \vec{N} + \vec{e}_i) p(\vec{N} + \vec{e}_i, t) + \right. \\ &+ T(\vec{N} | \vec{N} - \vec{e}_i) p(\vec{N} - \vec{e}_i, t) - \\ &\left. \left[T(\vec{N} + \vec{e}_i | \vec{N}) + T(\vec{N} - \vec{e}_i | \vec{N}) \right] p(\vec{N}, t) \right\}. \end{aligned} \quad (2.16)$$

The resulting equations for the first moments are:

$$\frac{d\langle N_i \rangle}{dt} = r_i \left(\langle N_i \rangle - \sum_{j=1}^{S=10} \frac{\langle N_i N_j \rangle}{K_j V} \right). \quad (2.17)$$

Numerical simulations were performed employing the Gillespie algorithm (Gillespie 1977), which directly solves the master equation associated to the deterministic system of Eq. (2.9), thereby employing demographic stochasticity (van Kampen 2007).

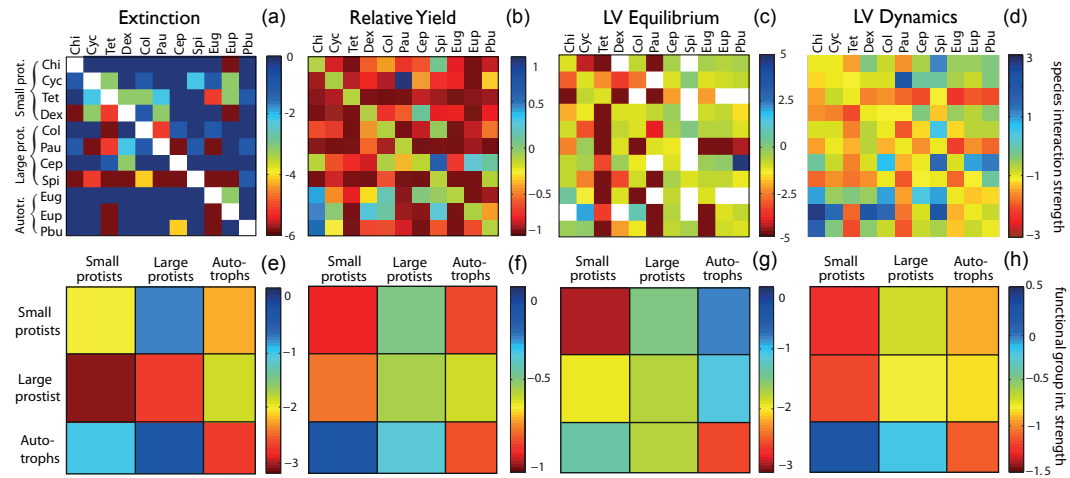


Figure 2.6: Interaction matrices describing all experimentally measured pairwise interaction strengths (α) between the 11 species (upper panels), and between functional groups (lower panels), obtained by four methods: (a,e) Extinction method (*EX*), indicates the number of extinctions over the six experimental replicates; (b,f) Relative Yield method (*RY*), based on population reduction/increase, scaled to carrying capacity obtained in isolation; (c,g) Lotka-Volterra Equilibrium method (*EQ*), and (d,h) Lotka-Volterra Dynamics method. The color of the square at position (i, j) indicates the effect of species j on species i . The color gradient gives the strength and the sign of the interaction. A blank square indicates a species' combination for which the inference of the interaction term α was not applicable. The 11 species are: *Chilomonas* sp. (*Chi*), *Cyclidium* sp. (*Cyc*), *Tetrahymena* sp. (*Tet*), *Dexiostoma* sp. (*Dex*), *Colpidium* sp. (*Col*), *Paramecium aurelia* (*Pau*), *Cephalodella* sp. (*Cep*), *Spirostomum* sp. (*Spi*), *Euglena gracilis* (*Eug*), *Euplotes aed.* (*Eup*), and *Paramecium bursaria* (*Pbu*). Species are ordered according to the three functional groups (small protists, large protists, autotrophs), and with increasing body size within each group. Lower panels show the average interaction strength within each functional group (red versus blue gradient, see Figure 2.1). Many extinctions and high competitive strengths are clustered along the diagonal, confirming the limiting similarity hypothesis.

2.3 Results

An interaction experiment in a pool of 11 protist species over all the 55 pairwise species combinations was performed, six times replicated. All pairwise interaction-strengths were characterized with four different methods, implementing an increasing degree of model complexity (Figs. 2.6–2.8, Table 2.1): ‘Extinction’ = *EX*, ‘Relative Yield’ = *RY*, ‘LV Equilibrium’ = *EQ*, and ‘LV Dynamics’ = *LVD*. The competitive exclusion principle was observed in many species combinations (207 population extinctions over 660 populations, in the 330 microcosms, Figure 2.6a). Interaction strength distributions of intra- vs. inter-group interactions were significantly different in all but the *EX* method (Kolmogorov-Smirnov test, $P_{RY} = 0.05$; $P_{EQ} = 0.05$; $P_{LVD} = 0.005$, $P_{EX} = 0.39$, Figure 2.7).

The majority of observed interactions were of competitive nature (*RY* 67%, *EQ* 73%, *LVD* 56%). Furthermore, a consistent part were predator-prey interactions (*RY* 22%, *EQ* 11%, *LVD* 26%) and amensalistic interactions (*RY* 16%, *EQ* 16%, *LVD* 18%). No neutral interaction, or commensalistic and mutualistic interactions were instead detected (Figure 2.8a). Interactions of species belonging to different functional groups were distinct for both the nature (i.e., the signs in the α -pair, discriminating between competitive, predator/prey, amensalistic, commensalistic, mutualistic or neutral interaction), and strength of the links (i.e., the absolute values of the α in the interaction matrix **A**). For intra-group interactions, competitive links were the majority (*RY* 80%, *EQ* 89%, *LVD* 80%), with very few predator-prey links (always less than 10%). For inter-group interactions, stronger predator-prey dynamics were detected (*RY* 27.5%, *EQ* 11%, *LVD* 32.5%), balanced by a lower proportion of competitive links (always less than 70%) compared to the intra-group interactions (Figure 2.8b).

Species’ competitive ranking, R_s , was a good predictor of species-performance in terms of final biomass production (Figure 2.9a) in 11-species communities (normalized to each species’ carrying capacity, K_s , initial conditions with all species starting at $K_s/11$). *RY* was the best method in predicting biomass production in the 11-species community from the pairwise interactions (Figure 2.9c). *RY* was superior to the other methods irrespective of the relationship assumed in the fitting procedure (best fit for $n_s^*/K_s = cR_s^4$). The worst predictor was the LV model based on equilibrium assumption ($r_{EX}^2 = 0.81$, $r_{RY}^2 = 0.88$, $r_{EQ}^2 = 0.10$, $r_{LVD}^2 = 0.79$). The fit was only for the *EQ* method not significant ($P_{EQ} = 0.41$). In fact, *EQ* was poorly correlated with *RY* ($R = 0.41$, $p = 0.21$) and *LVD* ($R = 0.46$, $p = 0.16$) and correlated to *EX* ($R = 0.74$, $p = 0.01$). A high degree of correlation was found between *RY* and *LVD* ($R = 0.96$, $p < 10^{-4}$, Figure 2.10). *Spirostomum* sp. was a rather poor competitor in our experimental conditions, but the results on the ranking were not affected by the removal of this species (Figure 2.11).

However, biological communities often occur in spatially structured habitats (Holyoak et al., 2000), where environmental conditions may vary consistently over years. In the evolutionary process, species could differentiate in response to these sources of environmental variability, and mechanisms such as competition-colonization trade offs (Cadotte, 2006b; Livingston et al., 2012) and the storage effect (Chesson, 1994) have been suggested to contribute in maintaining

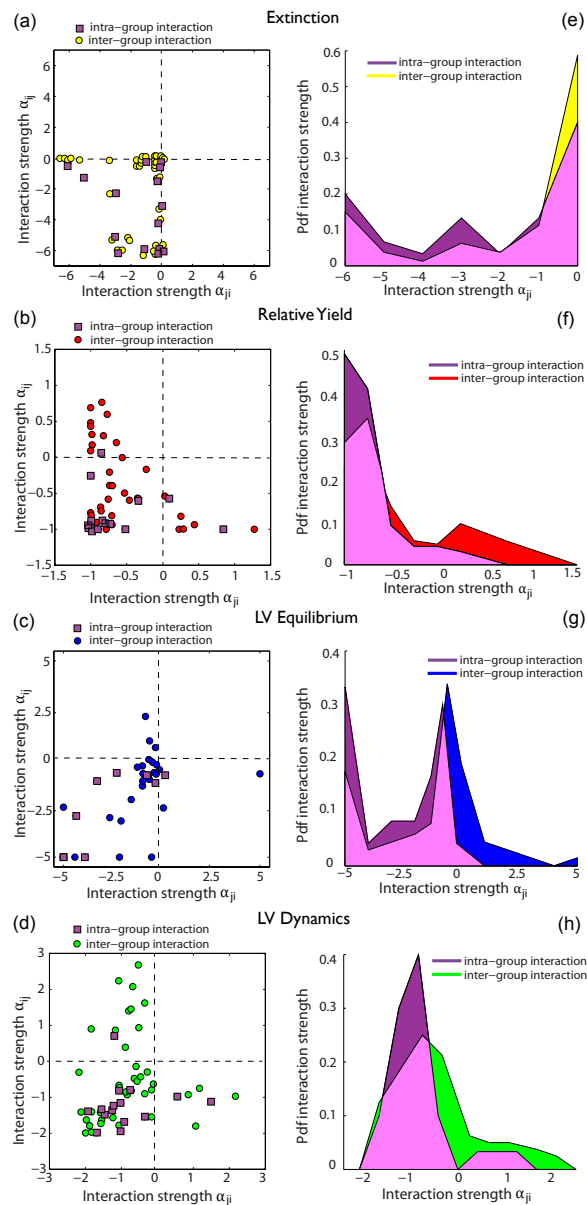


Figure 2.7: (a–d) Distribution of interaction coefficients (α_{ij} vs. α_{ji}) for all species combinations, measured by four different methods. (a) Extinction (*EX*, yellow); (b) Relative Yield (*RY*, red); (c) Lotka-Volterra Equilibrium (*EQ*, blue); (d) Lotka-Volterra Dynamics (*LVD*, green). The *RY* method has an upper boundary at $\alpha = -1$ by definition (competitive exclusion). Mutualistic links (both $\alpha > 0$ in pairwise experiments of 11 protist species are missing in all methods). In magenta, species interactions from inter-functional groups are plotted. (e, h) Probability density function (*pdf*) of intra-group (magenta) and inter-group interaction strengths by the four different methods. Lighter color indicates where distributions overlap. (e) Intra-group interactions cause higher extinction rates, and higher competitive strengths (left side in panels f–h). More similar species, belonging to the same ecological group, compete more strongly on average than species from different groups. Inter-group distributions present higher values in the positive side (predator/prey dynamics).

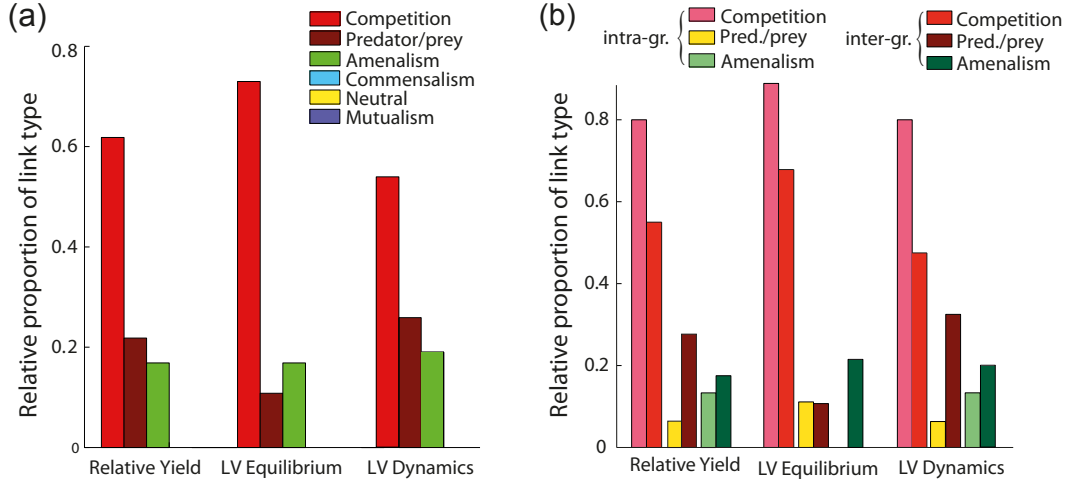


Figure 2.8: (a) Relative proportion of competitive (red), predator/prey (brown), amensalism (green), commensalism (cyan), neutral (yellow), and mutualistic (blue) interactions for all 11 species, by Relative Yield (RY), LV Equilibrium (EQ), and LV Dynamics (LVD) methods. (b) Relative proportion for intra- and inter-group interactions separately. Mutualistic (both α 's > 0), commensalistic (one $\alpha > 0$, the other α equal to zero), and neutral links (both α 's equal to 0) have not been detected in pairwise experiments of 11 protist species.

biodiversity in natural ecosystems. This aspect is documented for our model system in Figure 2.12, by combining the results of the interaction experiment with the dispersal experiment (see *Material and Methods* section).

Experimentally observed average species richness of the 11-species communities was $\langle \alpha_{11} \rangle_{exp} = 7.5 \pm 0.55$ (mean \pm s.d.). Only *Spirostomum* sp. went extinct in all six replicates. Numerical deterministic simulations for the 11-species communities with the same experimental initial conditions, fitted to the pairwise experimental interaction strengths, showed the coexistence of six species (*Tet*, *Dex*, *Col*, *Pau*, *Spi* went extinct in all 11-species simulations rounds, Figure 2.13). Stochastic simulations, implementing demographic stochasticity, showed the stable coexistence with a maximum of eight species. Demographic noise was hampering coexistence: in the stochastic simulations, the average species richness was $\langle \alpha_{11} \rangle_{theo} = 5.2 \pm 1.06$.

Asymptotic stability analysis performed by using the (deterministic) community matrix derived with the LVD method predicted the 11-species to be unstable both at the start and at the end of the experiment: $Re(\lambda(J[n_1^0, \dots, n_S^0])) > 0$, $Re(\lambda(J[n_1^*, \dots, n_S^*])) > 0$ (Figure 2.14a). By considering the experimental uncertainties over the species intrinsic growth rates r_s , carrying capacities K_s , and α -values in the interaction matrix, the instability value detected from the deterministic analysis was not significantly different from the stability-instability boundary, that is the zero value for the real part of the dominant eigenvalue (Figure 2.14b).

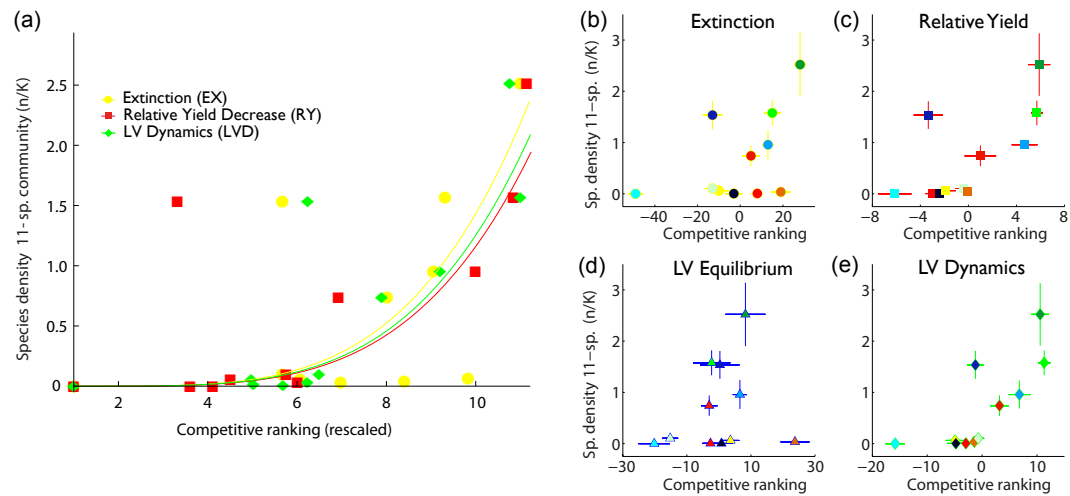


Figure 2.9: (a) Predicted species performance in 11-species community, based on the competitive rank R_i (rescaled between 1 and 11 for statistical comparison) obtained through the four methods from the pairwise interaction experiment (b, Extinction, yellow circles; c, Relative Yield, red squares); d, LV Equilibrium, blue triangles; e, LV Dynamics, green diamonds). The vertical axis gives the average species density, n , normalized to each species' carrying capacity K (y-axis, mean \pm s.e.m over the six replicates). Error bars on x-axis represent uncertainty over the interaction coefficients. Lines represent the best fit ($n_i \propto R_i^\delta$) with $\delta = 4$. RY is the best method in predicting species performances, for values of $\delta \in (1, 5)$ (similar results for fitting with an exponential curve). EQ has never provided significant results (d). Species identity is color coded (*Chilomonas* sp., dark red; *Cyclidium* sp., red; *Tetrahymena* sp., orange; *Dexiostoma* sp., yellow; *Colpidium* sp., dark blue; *Paramecium aurelia*, blue; *Cephalodella* sp., light blue; *Spirostomum* sp., cyan; *Euglena gracilis*, dark green; *Euplotes* sp., green; *Paramecium bursaria*, light green).

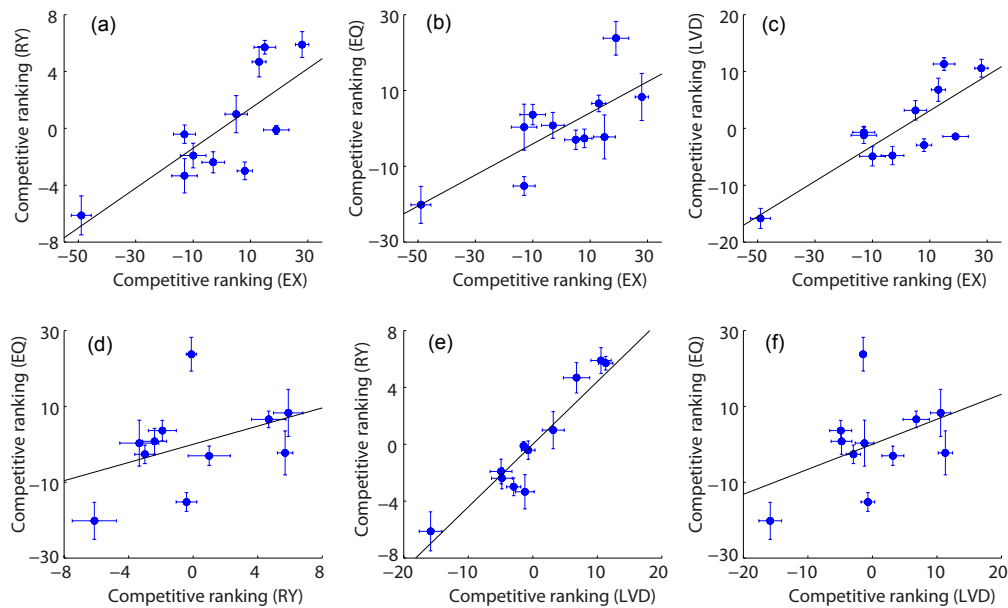


Figure 2.10: Comparison among the four different methods, Extinction (*EX*), Relative Yield (*RY*), LV Equilibrium (*EQ*), LV Dynamics (*LVD*) employed to estimate species rank, based on pairwise species interactions. Error bars represent the s.e.m. over the six experimental replicates.

2.4 Discussion

Recent ecological studies call for analysing multiple trophic levels at a time and stressing on the interconnections between trophic levels in order to determine global properties of the food webs (Berlow et al., 2004; Duffy et al., 2007; Haddad et al., 2011). Experimental and theoretical investigations, however, were generally limited by focusing on one trophic level only (Loreau et al., 2001). Most of previous studies, only focused on one type of interaction (e.g., competition, predation, amensalism, commensalism, or mutualism) at a time, while natural food webs commonly include multiple or all of them simultaneously. For example, in biodiversity ecosystem-functioning (BEF) research the analyses has been mostly on consumer-producers (plants) systems (Loreau et al., 2001; Tilman et al., 2001; Allan et al., 2011; Cadotte, 2013). Also, there is also a lack of a common methodological and conceptual approach to measure species interactions (Berlow et al., 2004).

In this chapter, all pairwise interactions among 11 protists species belonging to three functional groups were measured by four different methods. The 11-species community represents a complex food web with (at least) three trophic levels. A consistent picture is emerging from our analysis that ranged over different levels of resolution, focusing on extinction rates, biomass production, or per-capita interaction rates (Figs. 2.6–2.8). The main proportion of the pairwise links obtained in the different analyses were competitive links (Foster and Bell, 2012). The proportion of

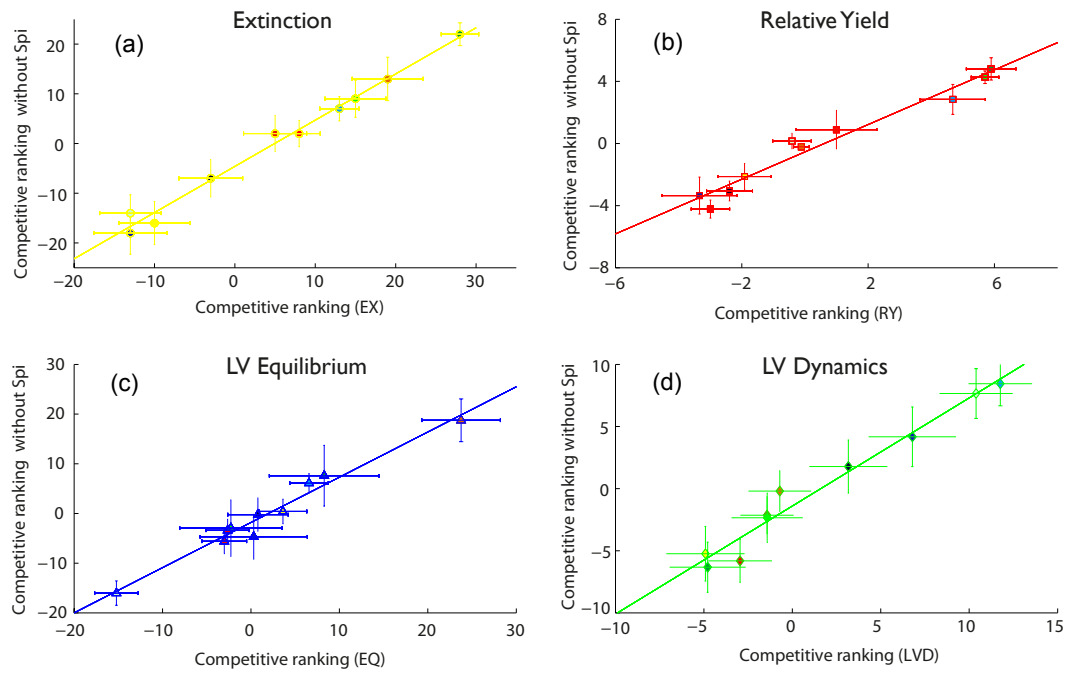


Figure 2.11: Comparison between species ranks with and without *Spirostomum* sp., for (a) Extinction; (b) Relative Yield; (c) LV Equilibrium; (d) LV Dynamics. Species ranking is not sensitive to species removal. Species identity is color coded (*Chilomonas* sp., dark red; *Cyclidium* sp., red; *Tetrahymena* sp., orange; *Dexiostoma* sp. yellow; *Colpidium* sp., dark blue; *Paramecium aurelia*, blue; *Cephalodella* sp., light blue; *Spirostomum* sp., cyan; *Euglena gracilis*, dark green; *Euplotes* sp., green; *Paramecium bursaria*, light green). The correlation between the two ranks is highly significant for all the four different methods ($P < 10^{-4}$).

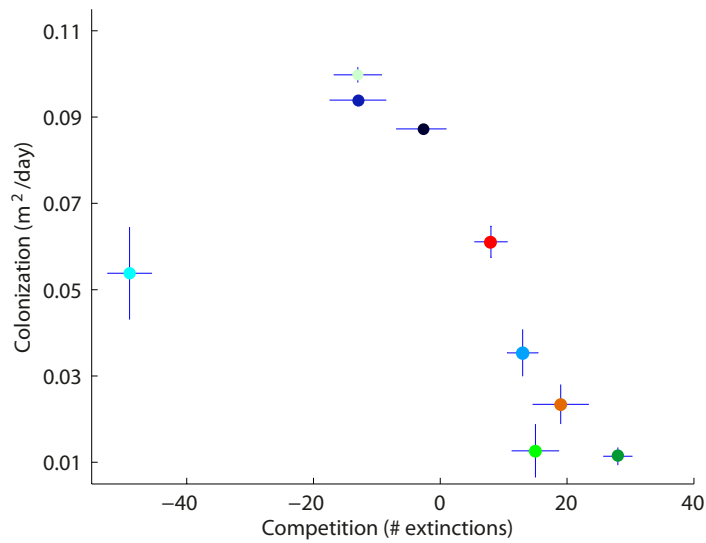


Figure 2.12: Colonization ability (calculated as $v = 2\sqrt{rD}$) as a function of competition ranking. Species identity is color coded (*Chilomonas* sp., dark red, *Tetrahymena* sp., orange; *Colpidium* sp., dark blue; *Paramecium aurelia*, blue; *Cephalodella* sp., light blue; *Spirostomum* sp., cyan; *Euglena gracilis*, dark green; *Euplotes* sp., green; *Paramecium bursaria*, light green. For *Cyclidium* sp. and *Dexiostoma* sp. the colonization ability was not measured. Clearly, a pattern relating species dispersal ability and competitive ranking is present in the protist species adopted in our experiments. *Spirostomum* species (cyan dot on the left hand of the graph) was a poor competitor.

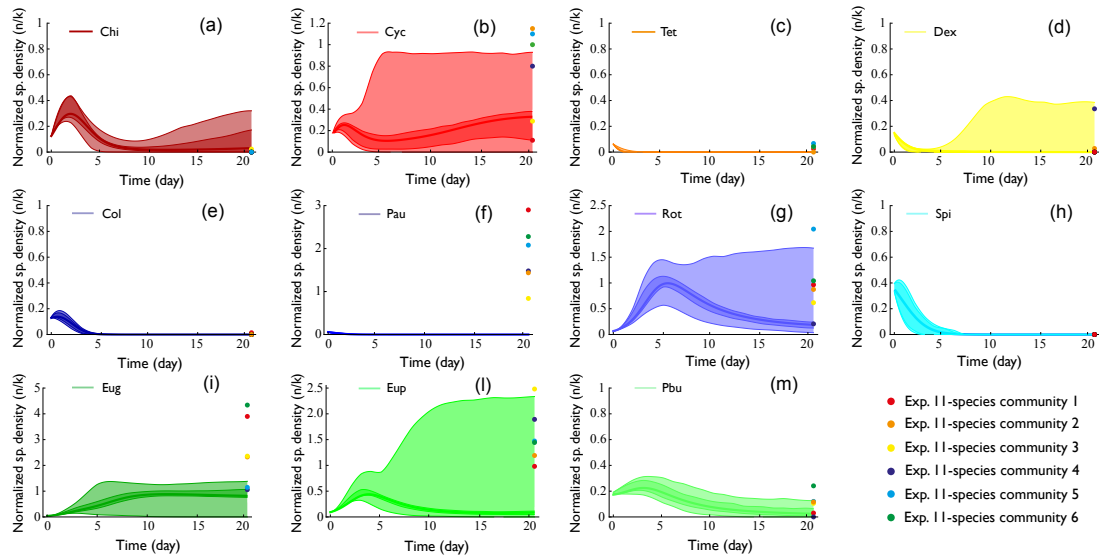


Figure 2.13: Species temporal dynamics based on simulations adopting the community model fitted to the experimental pairwise-interactions (*LVD* method, data rescaled to each species carrying capacity). (a–d) Species from the first functional group (small bacterivorous); (e–h) species from the second functional group (large bacterivorous and predators); and (i–m) species from the third functional group (autotrophs). Thick colored lines are obtained by (deterministic) integration of the community model; darker colored area (5th–95th percentile) refer to stochastic simulations of the same model in Eq. (2.9), employing demographic stochasticity; lighter colored area (5th–95th percentile) refers to stochastic simulations, adding to demographic noise the experimental uncertainties on the α -values of the derived interaction matrix. Colored dots at $t = 21$ day refer to experimental species yields in the 11-species communities (each color represent a different replicate). The stochastic model generally captures the mean and the observed variability in species performances. However, the systematic underestimation of the density for *Euglena gracilis* and *Paramecium aurelia* by an additive Lotka-Volterra model suggests the emergence of positive non-additive effects in trophically-structured (and functionally diverse) microbial communities. These mechanisms may include the production of dissolved organic matter (DOM) and inorganic nutrients via sloppy feeding, and excretion by larger protists, available to *Euglena gracilis* (Janet Hering, personal communication).

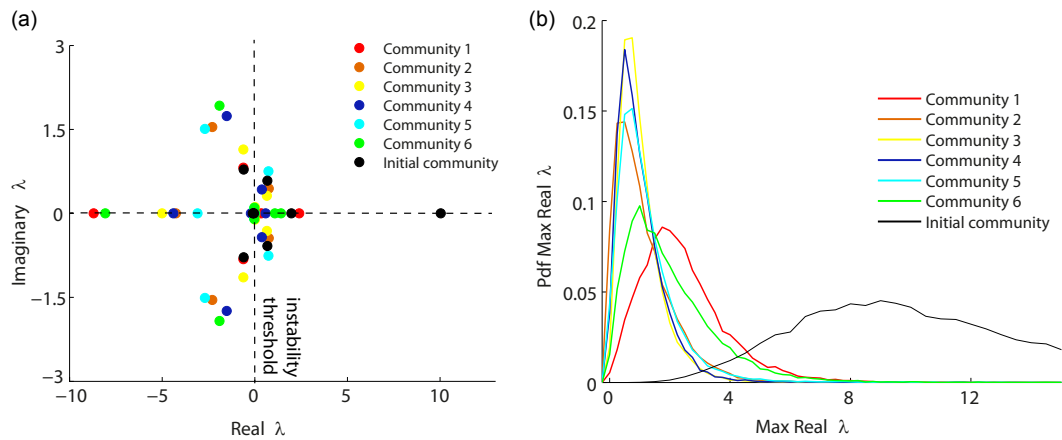


Figure 2.14: (a) Asymptotic stability analysis of the Jacobian community matrix for the final configuration of all the six experimental replicates (colored dots) of 11-species protist community (different colors for different experimental replicates), and for the initial community (black dots). On xy -axis real/imaginary parts of the eigenvalues are plotted. The deterministic analysis predicted the final configuration of the system to be in an unstable equilibrium, as highlighted by the positive real part of maximum eigenvalues in all the six community matrices. The initial configuration with each species s at its $K_s/11$ was highly unstable (black dot on the right side). (b) Probability density function of the maximum real part of community matrices eigenvalues, by considering experimental uncertainties on intrinsic growth rates r_s , carrying capacities K_s , and interaction matrix, \mathbf{A} . In four over six replicates, the distribution of eigenvalues is compatible ($P > 0.05$) with the zero value. Only the first (red line) and the sixth community (green line) were predicted to be unstable. The stochastic stability analysis confirmed the instability for the initial community configuration (black line).

competitive interactions for species from the same functional groups was higher compared to inter-group interactions, whereas the relative proportion of predator-prey links increased when considering species from two distinct functional group. This resulted in significantly different interaction strength distributions between intra- and inter-group interaction, with a right skewed distribution for the latter (Figure 2.7, see also chapter 3, where a detailed discussion for these differences in the interaction-strength distributions is provided).

A competitive hierarchy was derived from the interaction matrices (Mouquet et al., 2004; Haddad et al., 2008) for each of the methods and used it to predict species performance in the 11-species communities (Figure 2.9). The observed relationship between the rank and species performance is highly non-linear (Figure 2.9a). Comparing the different methods employed in the analysis of the pairwise interaction experiment, they provide a good match in the species ranks measurements (Figure 2.10), with higher correlation between RY and LVD (Figure 2.10e). Generally, the rank extracted from the population-based method (RY) was the best in predicting from pairwise interactions the biomass production in 11-species community (Figure 2.9a, c), and it was superior

to the other methods irrespective of the relationship assumed in the fitting procedure. The worst predictor was the LV model based on the equilibrium assumption (Figure 2.9d). In fact, two main issues arose when adopting the *EQ* method, assuming equilibrium: i) when species j went extinct when in combination with species i ($\phi_j^* = 0$), then it is not possible to reconstruct α_{ij} , because of zeros in the denominator (see Table 1, *EQ* method); ii) the equilibrium assumption may not be truly satisfied. Paradoxically, when few individuals of species j were still surviving in combination with species i , but were likely on a path towards extinction, this may lead to overestimate α_{ij}^{EQ} because it is a per-capita based model. This is making the method strongly dependent on experimental sampling times. Despite all these limitations, the LV modeling assuming equilibrium is widely adopted to infer species interactions (e.g., (Mouquet et al., 2004; Haddad et al., 2008)). Simpler methods, like balancing extinctions (Cadotte, 2006a) or looking at population reduction/increase in competition compared to the single-species case (Paine, 1992; Roxburgh and Wilson, 2000), are however better capturing each species' biomass production in multispecies communities at the final term of the experiment (Figure 2.9b, c).

Methods *EX* and *RY* (especially *RY*) are well-suited for analysing simple dynamics, and they better apply to transitive communities (see discussion in chapter 3). However, they do suffer a lack of predictive power for out of equilibrium or transient dynamics. Furthermore, making predictions from pairwise to multispecies community with *EX* and *RY* methods presents strong limitations when transferring on larger organisms with longer generation times, because such methods depend on the effective observation of an extinction event, or on longer relaxation time to equilibrium state. On the other side, a dynamical LV model may capture the interaction coefficients from earlier dynamics, without the requirement of reaching an equilibrium state, which is instead a firm assumption in the other three methods investigated here. Moreover, a more mechanistic based approach, such as the *LVD*, can capture not only the average species performances in multispecies communities, but also the variability around the average, providing richer information on important community properties, such as its stability. By looking at the community matrix built on the interaction matrix derived from the *LVD* method, both a deterministic and a stochastic stability analysis were conducted. In predicting the composition and the stability properties of multispecies communities from pairwise competitive experiments, a strong recommendation is to complement deterministic analyses with a stochastic approach, that is taking into account the possible sources of variability (Ives et al., 1999; de Mazancourt et al., 2013). In fact, population and community dynamics incorporate non-linear processes with inherent sources of stochasticity (McKane and Newman, 2005). Thereby, a stochastic-based analysis results in a more accurate inference of population dynamics and community stability. This has important implications for ecosystem management, in the selection of species combinations that are not only more productive, but also present higher stability.

3 Stabilizing effect of functional diversity on microbial communities

3.1 Introduction

Investigating the mechanisms that promote species coexistence and maintain stability in biological communities is deemed as a fundamental area of community ecology (May, 1972; Chesson, 2000b; Ives et al., 2005; Mayfield and Levine, 2010; Loreau and de Mazancourt, 2013). Several recent theories have advanced our understanding of the high levels of biodiversity observed in certain natural communities (e.g., Hubbell (2001); Holyoak et al. (2005); Allesina et al. (2008)). Field observations, showing the stable coexistence of species-rich and diverse communities (Kier et al., 2005), are often in contrast with predictions from theoretical models, which generally suggest competitive exclusion of species feeding on the same resources (MacArthur and Levins, 1967; Tilman, 1980). Specifically, the theory of limiting similarity predicts that closely related species (e.g., functionally related) tend to exclude each other, that is, the competitive exclusion principle (Hardin, 1960). A synthetic view states that stabilizing effects jointly act with equalizing effects, enabling species coexistence (Chesson, 2000b). Stabilizing effects refer to the niche concept, whereas equalizing effects reflect fitness inequalities between species. In such a framework, two closely related species tend to have weak equalizing and stabilizing forces, manifesting similar fitness and high niche overlap.

Stability of species-coexistence is at the core of community ecology because it is directly related to the persistence of a system over time (Ives and Carpenter, 2007). Community matrix theory predicts that species in randomly assembled communities experience strong competition (Kokkoris et al., 2002; Bastolla et al., 2005), increasing the likelihood for community instability (May, 1972). Experimental findings suggest instead that communities with higher number of species are more stable (McGradySteed et al., 1997; Haddad et al., 2011), and more productive (Allan et al., 2011), providing evidence for a positive diversity-function relationship. Many mechanisms have been suggested to explain the diversity-functioning and diversity-stability relationships (Ives et al., 2005). These include portfolio (Tilman et al., 1998) and sampling effects (Loreau, 1998), niche partitioning (Finke and Snyder, 2008), apparent mutualism induced by predation (Saleem et al., 2012), and phylogenetic diversity (Cadotte, 2013). Theoretical work has

Chapter 3. Stabilizing effect of functional diversity on microbial communities

shown that both properties of the interaction matrix and species' ecological traits are influencing community stability and the maximum number of species within a trophic level (Kokkoris et al., 2002; Bastolla et al., 2005) or a food web (Gross et al., 2009). Thereby, both the architecture of the ecological networks, and the distribution of interaction strengths impact ecosystem stability (Allesina and Tang, 2012). Specific properties of the food web topology, e.g., nestedness (Bastolla et al., 2009) or compartmentalization (Stouffer and Bascompte, 2011), may promote ecosystem stability, suggesting the presence of non-random assembling rules in natural ecosystems (May, 1972; Sole and Montoya, 2001).

To test theoretical predictions on the relationship between diversity, stability, and productivity of biological communities, scientists have performed experiments on interacting species in controlled environments. Experiments included a variety of study organisms, such as plants (Roxburgh and Wilson, 2000), insects (Paine, 1992), hydra species (Case and Bender, 1981), microbial communities (McGradySteed et al., 1997; Foster and Bell, 2012), with contrasting results (Ives and Carpenter, 2007). However, the majority of experiments in the Biodiversity Ecosystem Functioning (BEF) research focused on one trophic level (but see McGradySteed et al. (1997)). By focusing on one trophic level, competition for the same resources gained the most attention (Ives et al., 2005). In natural communities many other kinds of species interactions exist like, for example interference competition (Amarasekare, 2002), predator-prey and host-parasite interactions, resulting in win-loss relationships, or positive relationships, like mutualism or cooperation, where both species profit – a win-win relationship (Freilich et al., 2011). Also, theoretical work suggests that competition and predation, jointly structuring biological communities, may be envisioned in a unified symmetric framework (Chesson and Kuang, 2008).

Investigating the mechanisms promoting stability and productivity in trophically structured communities is needed (Ives et al., 2005; Duffy et al., 2007; Haddad et al., 2011). Microbial organisms, such as bacteria and protists, drive the bulk of ecosystem processes, and cover substantial biological complexity in terms of ecological traits, species interactions, and trophic levels (Holyoak and Lawler, 2005), and thereby offer ideal study systems. A microbial study organisms was used, including ten protist and one rotifer species. These species are competing for the same resources (bacteria) in a homogeneous environment (*Materials and Methods*), but some of them can also photosynthesize or consume smaller protists. As such, they belong to three functional groups (small bacterivorous, large bacterivorous that also consume smaller protists, mixotrophs). Interaction experiments for species monocultures and for all possible 55 pairwise species combinations were conducted. Furthermore, communities with all 11 species interacting present were composed. The interaction matrix in a generalized Lotka-Volterra (LV) framework was then characterized from the pairwise experiments. Numerical simulations using a stochastic LV 11-species community model were generated, fitted to the pairwise experimental interaction strengths collected in the interaction matrix, and experimental results were quantitatively reproduced. The experimental methods employed in this chapter are largely those described in chapter 2. However, while the latter was dedicated to the study and the comparison of species interactions, attention is focused here on the role of functional diversity

in trophic structured microbial communities. How species' trait-relatedness and properties of the interaction matrix affect coexistence and community productivity? As the communities were composed of different levels of species richness and functional diversity, functional diversity was identified as a crucial driver of productivity and stability in trophically structured microbial communities.

3.2 Materials and Methods

The first methods sections describing the experimental set-up are overlapping with the first method sections of chapter 2, but are repeated here for clarity and convenience.

3.2.1 Aquatic communities

A pool of 10 protists and one rotifer species were used in the experiments (henceforth called protists). The experiment was conducted in a climatized room at 21°C under constant fluorescent light. Local communities were kept in culture well-plates containing 10 ml of culture medium. The species were: *Chilomonas* sp. (*Chi*), *Colpidium* sp. (*Col*), *Cyclidium* sp. (*Cyc*), *Dexiostoma* sp. (*Dex*), *Euglena gracilis* (*Eug*), *Euplotes aediculatus* (*Eup*), *Paramecium aurelia* (*Pau*), *P. bursaria* (*Pbu*), *Spirostomum* sp. (*Spi*), and *Tetrahymena* sp. (*Tet*) and the rotifer (*Cephalodella* sp. (*Cyc*). *Chi* sp. and *Tet* sp. were supplied by Carolina Biological Supply Co., whereas all other species were originally isolated from a natural pond (McGradySteed et al., 1997). The species were grown in sterilized culture medium made of local spring water, and 0.45 g l⁻¹ of Protozoan Pellets (Carolina Biological Supply, NC USA). Protozoan Pellets provide nutrients for bacteria (*Bacillus cereus*, *B. subtilis* and *Serratia marcescens*), which were added one day before the beginning of the experiment. In such way, bacteria were supposed to have reached the carrying capacity. The protist species are naturally co-occurring in freshwater habitats and cover a wide range of body sizes, intrinsic growth rates and other important biological traits, such as swimming ability, nutrient uptake and photosynthetic capabilities (Altermatt et al., 2011a; Carrara et al., 2012).

Species' traits: functional diversity

Population growth curves are usually well described by the Malthus-Verhulst differential equation (Dublin and Lotka, 1925). In such a framework, the population density of species *s*, $\phi_s(t) = \langle N(t) \rangle / V$, starting at ϕ_s^0 individuals per ml of medium, grows in time following the logistic curve

$$\frac{d\phi_s}{dt} = r_s \phi_s \left(1 - \frac{\phi_s}{K_s} \right), \quad (3.1)$$

where r_s is the intrinsic growth rate, and K_s is the carrying capacity of species *s*. The complete results for species intrinsic growth rates and body sizes of this study are shown in Table 4.1 of

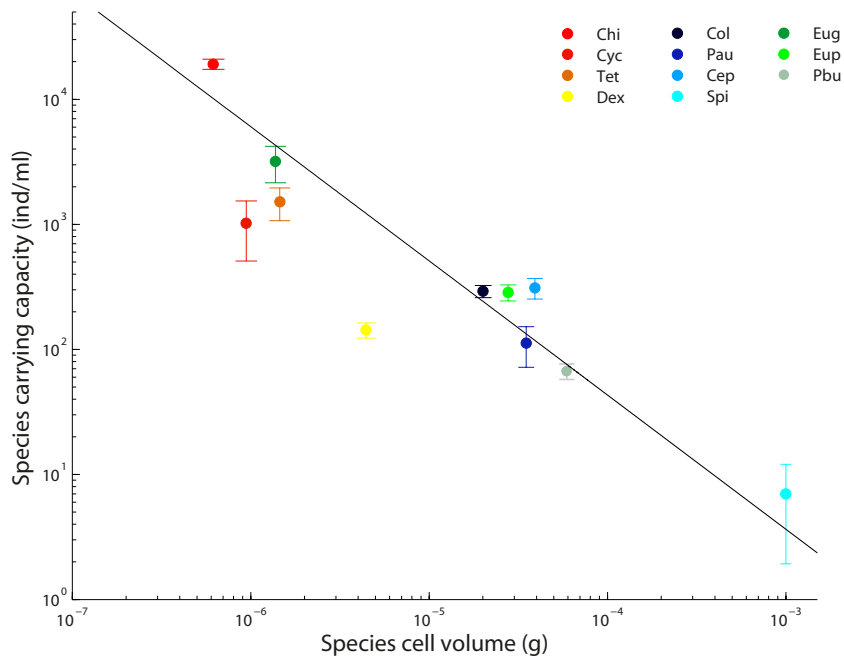


Figure 3.1: Relationship between body size and density (carrying capacity) for 11 protist species used in the interaction experiment. Body size values (v , mean of the distribution) are taken from Giometto et al. (2013), which measured body size in identical environmental conditions of the experiment. Carrying capacities, K_s , are obtained from the single species experiment. The line, representing the Cross-Community Scaling Relationship (CCSR; White et al. (2007)), is the best fit for $K = av^b$, with best fit exponent $\bar{b} = -1.07$, considering the variation associated to the experimental carrying capacities. Damuth's rule would have a value $b = -0.75$.

chapter 4 and in Giometto et al. (2013) respectively, where protists have been cultivated in single-species cultures at identical conditions as used for the interaction experiment in the current study. K_s scales with body size (White et al. (2007), Figure 3.1). Intrinsic growth rate is reflecting fitness differences (equalizing forces), while body size and ability to photosynthesize are impacting the resource use overlap between species (stabilizing forces). These three ecological traits were used to build a functional dendrogram, where species are assigned to the tips of the dendrogram (Figure 3.2b). Functional diversity for a given community was calculated summing the paths length along the branches, from the occupied tips to the top of the dendrogram (Petchey and Gaston, 2002). All species can feed on bacteria, but may prefer different bacteria species, depending on morphology or phylogeny (Glücksman et al., 2010). At the highest hierarchical level of the community dendrogram, functional groups were defined by grouping species belonging to the same branch (Figure 3.2b). *Chi*, *Cyc*, *Tet* and *Dex* are small bacterivorous species (from 0.6 to 4.5 10^{-6} g) with high growth rates ($r > 1.5 \text{ day}^{-1}$), *Col*, *Pau*, *Cep*, and *Spi* are large bacterivorous species (from 20 to 1000 10^{-6} g). Furthermore, *Cep*, *Pau*, and *Spi* may not only feed on bacteria, but may also predate on microflagellates, which are always present in cultures and remain unidentified. These species may also feed directly on smaller protist species, such as *Chi*, *Cyc*, *Tet*, and *Dex*. *Eug*, *Eup*, and *Pbu* are mixotrophic species.

3.2.2 The interaction experiments

An interaction experiment was performed in trophically structured microbial communities with a pool of 11 protist species, belonging to three different functional groups. All the possible 55 pairwise species-combinations were measured in microcosms experiments, six times replicated (Figure 3.2). All pairwise species interaction strengths were characterized by fitting a generalized Lotka-Volterra model. All 11 species were initially grown to carrying capacity in isolated cultures. Then, 5 ml of medium of species *i* at carrying capacity was mixed to 5 ml of sp. *j* at carrying capacity (total volume, $V = 10 \text{ ml}$). Initial densities (ϕ_i^0 , ϕ_j^0) were measured and are thus known. In this manner, individuals of different species started immediately to strongly compete for resources, as the communities were initially saturated with individuals. Species specific carrying capacities K_s were measured in pure cultures in a control experiment.

Additionally, the species' ability to coexist was tested in communities composed of all 11 protists, initializing the microcosms with $V/11$ volume medium volume of each species. The 11-species, the 55 two-species, and the 11 single-species communities were replicated six times each. After three weeks, at $t^* = 21 \text{ days}$, the density of each species was measured in all microcosms. A variable quantity of medium was sampled (for method details see Altermatt et al. (2011a)), and densities were counted under a stereo-microscope. The density of *Spirostomum* sp. was directly counted in the well-plates, as it naturally occurs at very low densities.

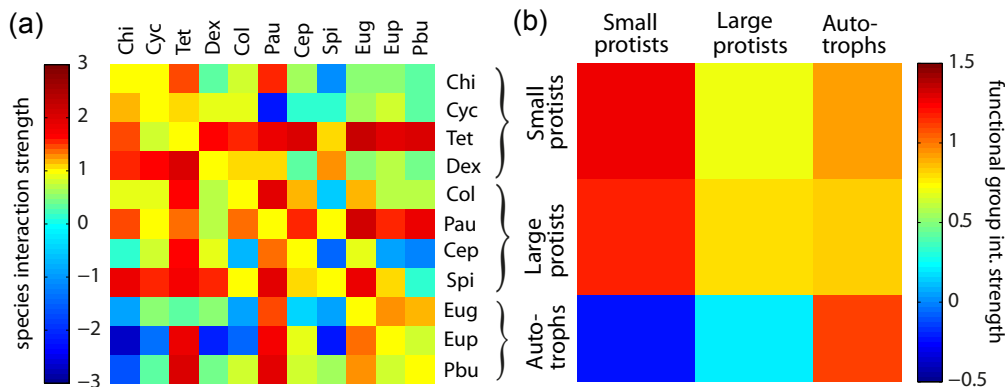


Figure 3.2: (a) Interaction matrix describing all experimentally measured pairwise interaction strengths (α_{ij}) between the 11 species. The color of the square at position (i, j) indicates the effect of species j on species i . Species are ordered according to three functional groups (small protists, large protists, autotrophs, see emphAquatic communities section for species names). (b) Average interaction strength within each functional group. High competitive strengths are clustered along the diagonal, confirming the limiting similarity hypothesis, by which similar species compete more strongly among each other than distantly related species.

Time series

In addition to the above-described interaction experiment with one abundance measurement after three weeks, time-series data on two-, three-, and four-species communities were also measured. A gradient in richness and functional diversity level was implemented (see *Species' traits* section above) on a smaller subset of species at identical experimental conditions. Time series (six times replicated, sampling every day for at least 10 days) were obtained for the following two-species combinations: *Col-Tet*, *Col-Cep*, *Cep-Tet*. Also, time series for the three-species community *Col-Cep-Tet* and for the four species community *Col-Eug-Cep-Tet* were obtained.

Community productivity

Productivity was obtained by multiplying the number of individuals in a community times the average cell size of each species (measured in Giometto et al. (2013)). Biomass is always expressed in g ml^{-1} , directly obtained from body size by assuming a constant density equal to the density of water (Fenchel, 1974), and therefore refer to body size and mass without distinction (Giometto et al., 2013). For single-species communities, B_1 is the average yield obtained in monocultures; for the two-species setup, B_2 is the average yield obtained in all the 330 microcosms of the pairwise interaction experiment; for the 11-species setup, B_{11} is the average over the six replicates yields. The relationship between biomass production and functional distance in the 55 pairwise communities was tested by a linear regression analysis. An additive partitioning analysis was conducted to calculate the total biodiversity effect in terms of complementarity and

selection effects (Loreau and Hector, 2001). Results were compared in terms of biomass relative to each species monoculture, by rescaling to carrying capacity, $n_i^* = \phi_i^*/K_i$. Thus, we could consider the sum of species relative yields in the community rescaled to the number S of species in the community, $A_S = (\sum_{i=1}^S n_i^*)/S$, as a measure of additivity in a S -species community. A complete additive community would give one. A was calculated for the two-species communities (A_2), differentiating for intra- (A^{intra}) and inter-group species (A^{inter}), and for the 11-species community setup (A_{11}).

Species interaction type

In LV models, the dynamics of species i and species j are characterized by the following phenomenological equation:

$$\frac{d\phi_i}{dt} = r_i \phi_i \left(1 - \frac{\alpha_{ii}\phi_i + \alpha_{ij}\phi_j}{K_i} \right), \quad (3.2)$$

where α_{ij} measures the strength of interspecific competition and α_{ii} that of intraspecific competition, which is equal to one for all species. The values α_{ij} for all pairwise i and j constitute the interaction matrix, \mathbf{A} . After rescaling the density of species i by its carrying capacity K_i (Kokkoris et al., 2002), $n_i = \phi_i/K_i$, $\alpha'_{ij} = \alpha_{ij}K_j/K_i$, the LV model becomes

$$\frac{dn_i}{dt} = r_i n_i \left(1 - n_i - \alpha'_{ij} n_j \right). \quad (3.3)$$

Interactions α_{ij} were derived by fitting the time series of the two-species interaction to a LV model, constrained to the initial conditions adopted in the experiment, n_i^0 , n_j^0 , and the final densities n_i^* , n_j^* at t^* .

The generalized LV modelling approach in principle includes predator-prey dynamics and positive interactions. Species with competitive interactions have positive α -values. The sign of α 's is negative when a predator-prey or mutualistic interaction is occurring between two species. A predator-prey interaction $i - j$ has $\alpha_{ij}\alpha_{ji} < 0$. In mutualistic interactions, both α_{ij} and α_{ji} are negative ($\phi_i^* > K_i$, $\phi_j^* > K_j$). Amensalism/commensalism arises when one value of α is equal to zero and the other is positive/negative, respectively. Non-interacting species have both α values equal to zero (neutral interaction). α values and the interaction type were assigned for each species-pair using the above-described categories, considering the experimental errors associated to each α value. Uncertainties on α values were obtained by considering the variation among the six replicates. Differences in intra- vs. inter-group distributions of species interaction strength were tested with a Kolmogorov-Smirnov test on the cumulative distributions.

Adjacency graphs were built, reflecting competitive exclusion dynamics between 11 protist species adopted in the interaction experiments. The arrows in the graphs point from the excluded species to the superior competitor (as convention in the food web literature for prey/predator links). A deterministic extinction of an inferior species caused by the superior species happens for six

extinction events over the six replicates. It was possible to detect the presence of competitive or mutualistic loops within protists interactions, where such loops reflect the degree of intransitivity in competitive interactions (Allesina and Levine, 2011). A set of species defined a mutualistic loop when each species was favouring another species forming a closed chain of positive species interactions.

3.2.3 Community model

Generalizing Eq. (3.1) to a community with $S = 11$ species, a system of coupled differential equations is derived, where density changes of species i are described by:

$$\frac{d\phi_i}{dt} = r_i \phi_i \left(1 - \frac{\phi_i + \sum_{j \neq i} \alpha_{ij} \phi_j}{K_i} \right), \quad (3.4)$$

which after rescaling becomes:

$$\frac{d\mathbf{n}}{dt} = \mathbf{r} \cdot \mathbf{n} (1 - \mathbf{A}' \mathbf{n}), \quad (3.5)$$

where \mathbf{A}' is the experimental interaction matrix (rescaled to each species carrying capacity). The deterministic solution provided in Eq. (3.1) is a good approximation for high density species and for large volume V of medium. Multispecies community-dynamics was investigated through simulations by using the interaction matrix \mathbf{A} fitted to the pairwise experiments. In the simulations, all species are present with a known initial density of $\phi_s^0/11$, as in the main experiment. A Gillespie algorithm was employed (Gillespie, 1977) to directly solve the master equation associated to the deterministic system of Eq. (3.5), thereby also including demographic stochasticity (for a stochastic formulation of this model, see chapter 2). Simulations were run for each initial community composed of species belonging to one functional group only (100 simulations for each functional group separately), two functional groups (three functional groups combinations, 300 simulations in total) and three functional groups (the 11-species experiment, 100 simulations). The relationship between functional diversity and species coexistence, community stability and productivity was also investigated with numerical simulations. 10000 simulations were run over the entire range of species richness (from 2 to 11), preserving the proportion of different combinations (the binomial coefficient) at each richness level. At the same richness level, communities with different functional diversity were randomly initialized. Thereby the relationship between functional diversity and species richness was disentangled, and the assessment of the corresponding impacts on species coexistence, community productivity, and community stability was performed. All simulations were run over 21 days, that is, the experimental duration. Productivity was quantified as total biomass production at the end of one simulation (i.e., yield). Stability was captured by the coefficient of variation of community biomass (CV), measured over day 11–21 of each simulation.

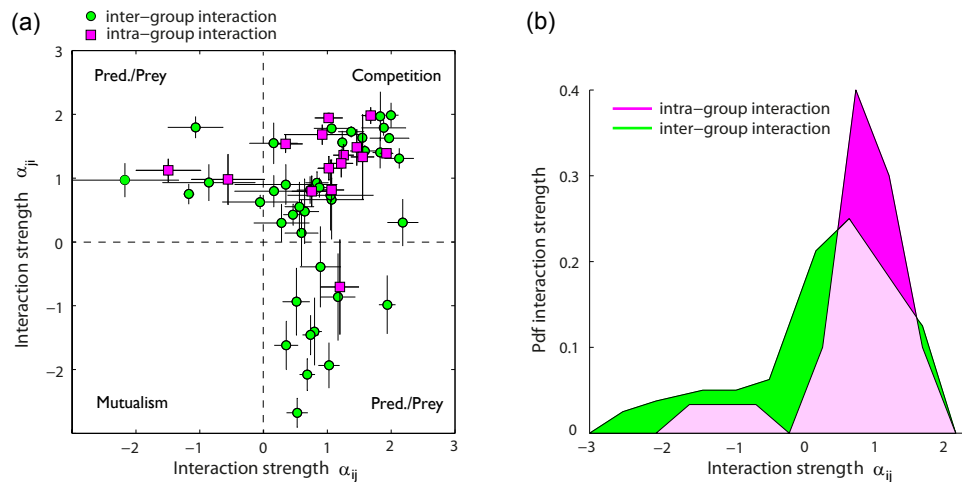


Figure 3.3: (a) Interaction strength distribution for the pairwise experiments between the 11 protist species for all experimentally measured pairwise interactions between 11 protist species, separately given for species belonging to the same functional groups (intra-group, magenta), and to different groups (inter-group, green). In a Lotka-Volterra model, the interaction coefficients are captured by constant values of α , describing the effect of species j on species i (α_{ij}) and the effect of species i on species j (α_{ji}). For competitive interactions both α -values are positive. In mutualistic interactions, both α values are negative. Predation/parasitism occurs where the two interactions have opposite signs ($\alpha_{ij}\alpha_{ji} < 0$). Non-interacting (neutral) species fall on the origin of the graph. Intra-group interactions cause higher competitive strengths (upper right side in the panel). Error bars represent the uncertainty associated to each α value. (b) Probability density function (*pdf*) of intra-group (magenta) and inter-group interaction strengths (lighter color where distributions overlap). More similar species, belonging to the same ecological group, compete more strongly than species from different groups. Inter-group distributions present a more skewed distribution with higher values in the negative side (predator/prey dynamics), which eventually stabilizes the community.

3.3 Results

A total of 207 population species extinctions were observed in the total 330 microcosms, with initially 660 starting populations. The majority of observed interactions were competitive (56%). Furthermore, predator-prey interactions constituted 26% and amensalistic interactions 18%. No neutral interaction, or commensalistic and mutualistic interactions were detected (Figures 3.2a, 3.3a). Interaction-strength distributions of intra- vs. inter-group interactions were significantly different (Kolmogorov-Smirnov test, $P = 0.005$, Figure 3.3b). Intra-group interactions were dominated by competitive type (80%), and showed very few predator-prey links (6%), while inter-group interactions showed a weaker majority of competitive type (less than 50%), with strong predator-prey dynamics (33%). No competitive loops were found among the 11 protists species (3.4), meaning that communities manifested a high degree of transitivity. On the contrary,

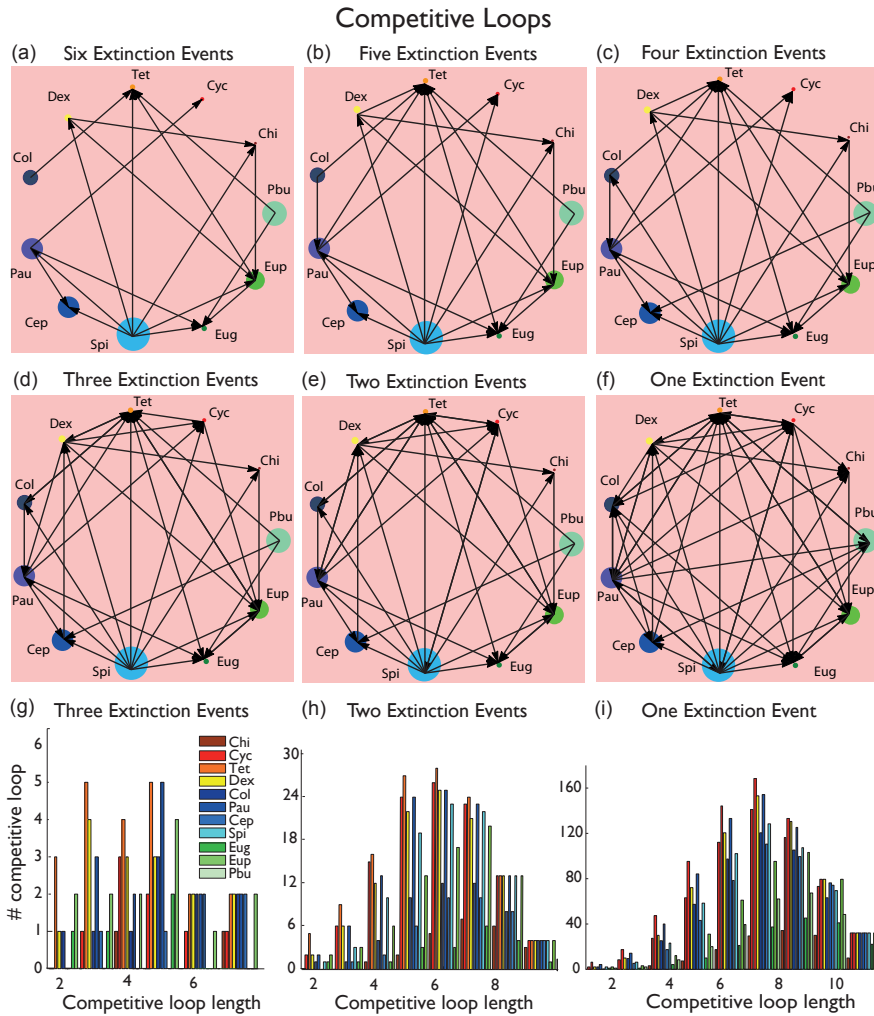


Figure 3.4: (a–f) Interactions resulting in competitive exclusion: Adjacency graphs show competitive exclusion dynamics between 11 protist species adopted in the interaction experiments. Arrows point from the excluded species to the superior competitor, for decreasing extinction events over the six replicates: (a) deterministic extinction (six extinction events over six rounds), (f) one extinction over six rounds. Circle size reflects the species’ body size, and different colors are associated to different functional groups (red to yellow, small bacterivorous, *Chilomonas* sp., *Cyclidium* sp., *Tetrahymena* sp., *Dexiostoma* sp., dark blue to cyan, large bacterivorous, *Colpidium* sp., *Paramecium aurelia*, *Cephalodella* sp., *Spirostomum* sp., and dark to light green, autotrophs, *Euglena gracilis*, *Euplotes aed.*, and *Paramecium bursaria*). Interestingly, no loops due to intransitivity in competitive interactions (e.g., rock, paper, scissor dynamics) were detected, reflecting a high transitivity of the interaction matrix. (g–i) Competitive loops were detected for adjacency matrices that were connecting species with three or less extinctions over six experimental rounds ($N_{loops}(ex \geq 3) = 23$, $N_{loops}(ex \geq 2) = 140$, $N_{loops}(ex \geq 1) = 772$), where ex is the number of extinctions over the six experimental replicates. Panels (g–i) show the distribution of loop lengths for each species considering three, two and one extinction events (from left to right). Small protists (*Cyc*, red, *Tet*, orange, *Dex*, yellow) and *Pau* (dark blue) took part in more numerous and shorter competitive loops (also had the highest connectivity degree, see upper panels) compared to autotrophs (green species), which are instead stabilizing the community.

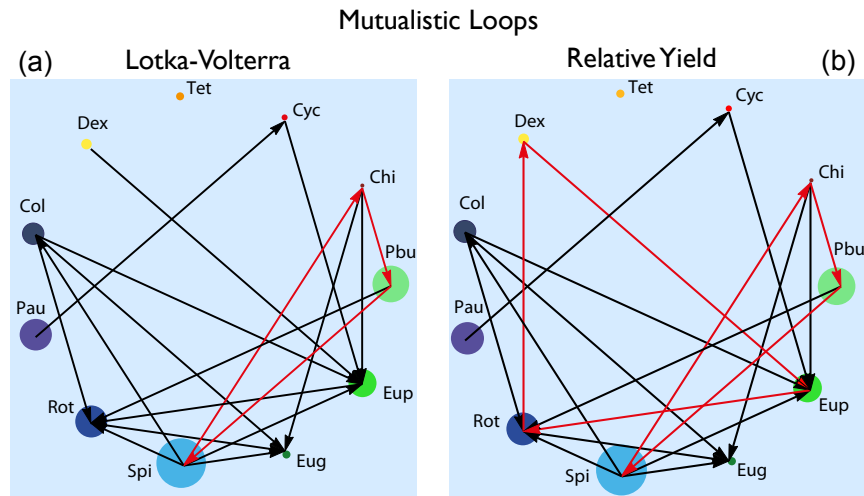


Figure 3.5: Interactions resulting in mutualistic loops between the 11 protist species adopted in the interaction experiments, considering the Lotka–Volterra (*LV*) interaction matrix (a), and the Relative–Yield (*RY*) interaction matrix (b). The *RY* method considers the interaction term $\alpha_{ij} = (K_i - \phi_i)/K_i$. Arrows in the adjacency graphs point from the prey (cooperator) to the predator (defector). Circle size reflects the species’ body size, and different colors are associated with different functional groups (red to yellow, small bacterivorous, *Chilomonas* sp., *Cyclidium* sp., *Tetrahymena* sp., *Dexiostoma* sp., dark blue to cyan, large bacterivorous, *Colpidium* sp., *Paramecium aurelia*, *Cephalodella* sp. (*Cep*), *Spirostomum* sp., and dark to light green, autotrophs, *Euglena gracilis*, *Euplotes aed.*, and *Paramecium bursaria*). A mutualistic loop (red arrows) between *Chi–Pbu–Spi* was detected for the *LV*–adjacency matrix. The *RY* method detected the same links, but showed also a mutualistic loop between *Dex–Eup–Rot*. Each species in mutualistic loops belong to a different functional group.

mutualistic loops (Freilich et al., 2011) of length three were detected between species in the three different functional groups (*Chilomonas–Paramecium bursaria–Spirostomum* sp., *Dexiostoma–Euplotes–Cephalodella* sp. (Figure 3.5).

Community biomass production by single-species were not statistically different from two-species communities ($B_1 = 5.5 \cdot 10^{-3} \text{ g ml}^{-1}$, $B_2 = 5.5 \cdot 10^{-3} \text{ g ml}^{-1}$, t-test, $P = 0.99$, Figure 3.6). By applying additive partitioning to the two-species communities (Loreau and Hector, 2001) a perfect balance between a moderate positive selection (*SE*) forces ($SE_2 = 2 \cdot 10^{-4} \text{ g ml}^{-1}$) and a negative complementarity effect (*CE*), ($CE_2 = -1.7 \cdot 10^{-4}$) was found. A positive significant relationship between functional distance and biomass production was found, considering the final yields of all the possible 55 pairwise combinations of the 11 protist two-species communities ($r^2 = 0.23$, $P = 0.01$, Figure 3.7). Results changed for the 11-species communities, where average community biomass, B_{11} , was significantly higher than both B_1 and B_2 ($B_{11} = 0.0429 \text{ g ml}^{-1}$, Figure 3.6), due to a strong positive complementarity effect ($CE_{11} = 3.74 \cdot 10^{-2} \text{ g ml}^{-1}$) and a moderate selection effect ($SE_{11} = 2.1 \cdot 10^{-3} \text{ g ml}^{-1}$). Inset of Figure 3.6 shows the relative species biomass production

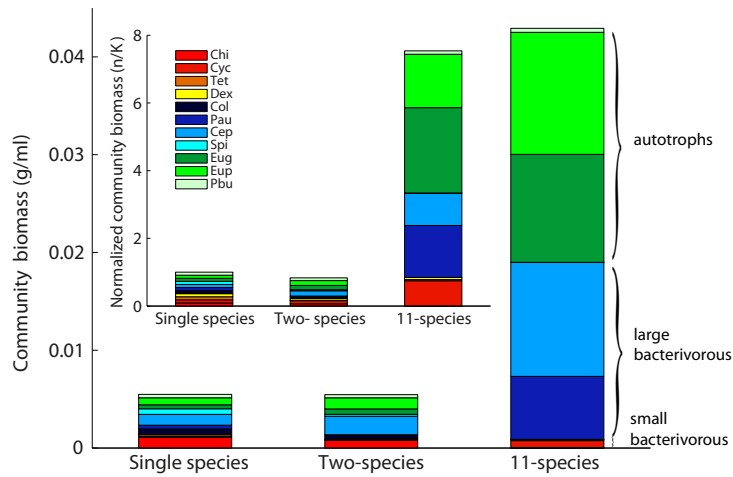


Figure 3.6: Biomass production in single species (average over the 11 one-species yields), two-species (average over the 55 two-species combinations), and 11-species communities. All values represent the average over six experimental replicates. Inset: productivity rescaled to each species' carrying capacity, K_s . A complete additive community would result in a normalized productivity equal to species richness (i.e., values of 1, 2 and 11, all experimentally observed values are lower). Species order is the same as in Figure 3.2a, from bottom (*Chi*) to top (*Pbu*). Species belonging to the same functional group share similar colors (red colors = small bacterivorous, blue colors = large bacterivorous, green colors = autotrophs).

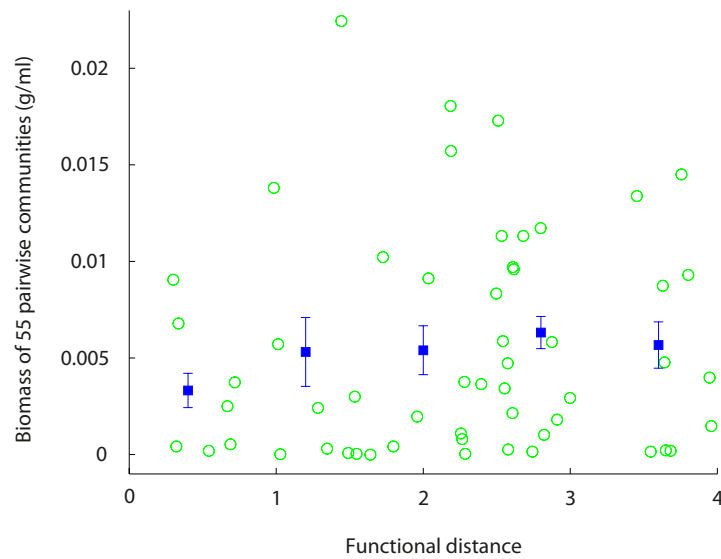


Figure 3.7: Relationship between functional distance and biomass production, considering the final yields of all the possible 55 pairwise two-species combinations of the 11 protist species adopted for the interaction experiment (green circles). Functional distance is calculated as the euclidean distance between two species in the species traits' space. Blue squares represent the average after a binning procedure has been implemented for visualization purposes. The relationship is significant, adopting a correlation analysis over the rough data ($r^2 = 0.23$, $P = 0.01$).

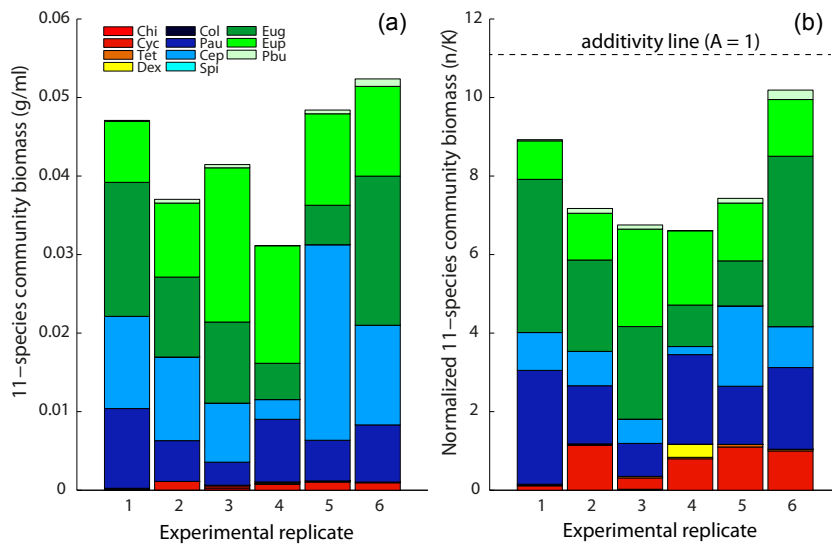


Figure 3.8: (a) Variability in community biomass production between the six experimental replicates of the 11-species setup. (b) Productivity rescaled to each species' carrying capacity, K_s . Species order is the same as in Figure 3.6, from bottom (*Chi*) to top (*Pbu*). Species belonging to the same functional group share similar colors (red colors = small bacterivorous, blue colors = large bacterivorous, green colors = autotrophs). A complete additive community ($A = 1$, dashed line) would result in a normalized productivity equal to species richness (i.e., 11, all experimentally observed values are lower).

in single-, two-, and 11-species communities. An additivity measure for relative yields gives $A_2 = 0.41$, where a pure additive community would give one. Intra-group additivity was higher than inter-group additivity ($A_2^{intra} = 0.27$, $A_2^{inter} = 0.47$). Additivity in 11-species communities was also higher ($A_{11} = 0.69$) compared to two-species communities (Figure 3.8). These patterns were confirmed at lower richness values, where a subset of species was followed (two to four species from the total pool) over time (Figure 3.9). Complementarity and selection effects were comparable in the two-species communities (Figure 3.9a–c), with low level of functional diversity ($CE_2 = 0.028 \text{ g ml}^{-1}$, $SE_2 = 0.013 \text{ g ml}^{-1}$). In the three-species combination CE was four times greater than SE ($CE_3 = 0.0106 \text{ g ml}^{-1}$, $SE_3 = 0.0025 \text{ g ml}^{-1}$, Figure 3.9d) and in the four species combination SE was negative ($CE_4 = 0.004 \text{ g ml}^{-1}$, $SE_4 = -0.007 \text{ g ml}^{-1}$), where four species from three different functional groups were grown together (Figure 3.9e).

Experimentally observed average species richness of the 11-species communities was $\langle \alpha_{11} \rangle_{exp} = 7.5 \pm 0.55$ (mean \pm s.d.), where only *Spirostomum* sp. went extinct in all six replicates. Numerical simulations for the 11-species communities with the same experimental initial conditions, fitted to the pairwise experimental interaction strengths, showed stable coexistence with a maximum of eight species (*Colpidium* sp., *Paramecium aurelia*, and *Spirostomum* sp. went extinct in all 11-species simulations rounds), with an average species richness of $\langle \alpha_{11} \rangle_{theo} = 5.2 \pm 1.06$ in the stochastic simulation models. A positive relationship between functional diversity and total biomass production was found in the stochastic simulations (Figure 3.10a). Communities composed of species from a single or two functional groups were less productive compared to communities where species belonged to the three functional groups (Figure 3.10b–h). Moreover, looking at species coexistence of communities initially composed of the same species richness level across a functional diversity gradient, a higher final species richness was observed for communities with a higher initial functional diversity (Figure 3.11a). This pattern is reflected in higher community productivity (total biomass production, Figure 3.11b), and a generally higher stability (coefficient of variation of community biomass over time, Figure 3.11c) when community composed of more functional diversity were initialized.

3.4 Discussion

Experimental results (Figures 3.6, 3.9) and theoretical investigations (Figures 3.10, 3.11) support the positive relationship between functional diversity and species coexistence, community stability and total biomass production in microbial communities. Results from the pairwise interaction experiment support the limiting similarity hypothesis (Hardin, 1960), which predicts higher competitive strength among more related species (Figures 3.2a, b, 3.3b), as recently found in microbial communities using protists (Violle et al., 2011), and yeast (Peay et al., 2012) and bacteria (Jiang et al., 2010; Tan et al., 2012). Surprisingly, however, this ecological principle was masked when also functionally dissimilar species were present in the community, leading to increased coexistence of the more related species. The presence of species of different functional groups (e.g., autotrophs next to predators) lead to increased coexistence of the more related species within the individual groups (i.e., within autotrophs and predators; Figure 3.9). This

Chapter 3. Stabilizing effect of functional diversity on microbial communities

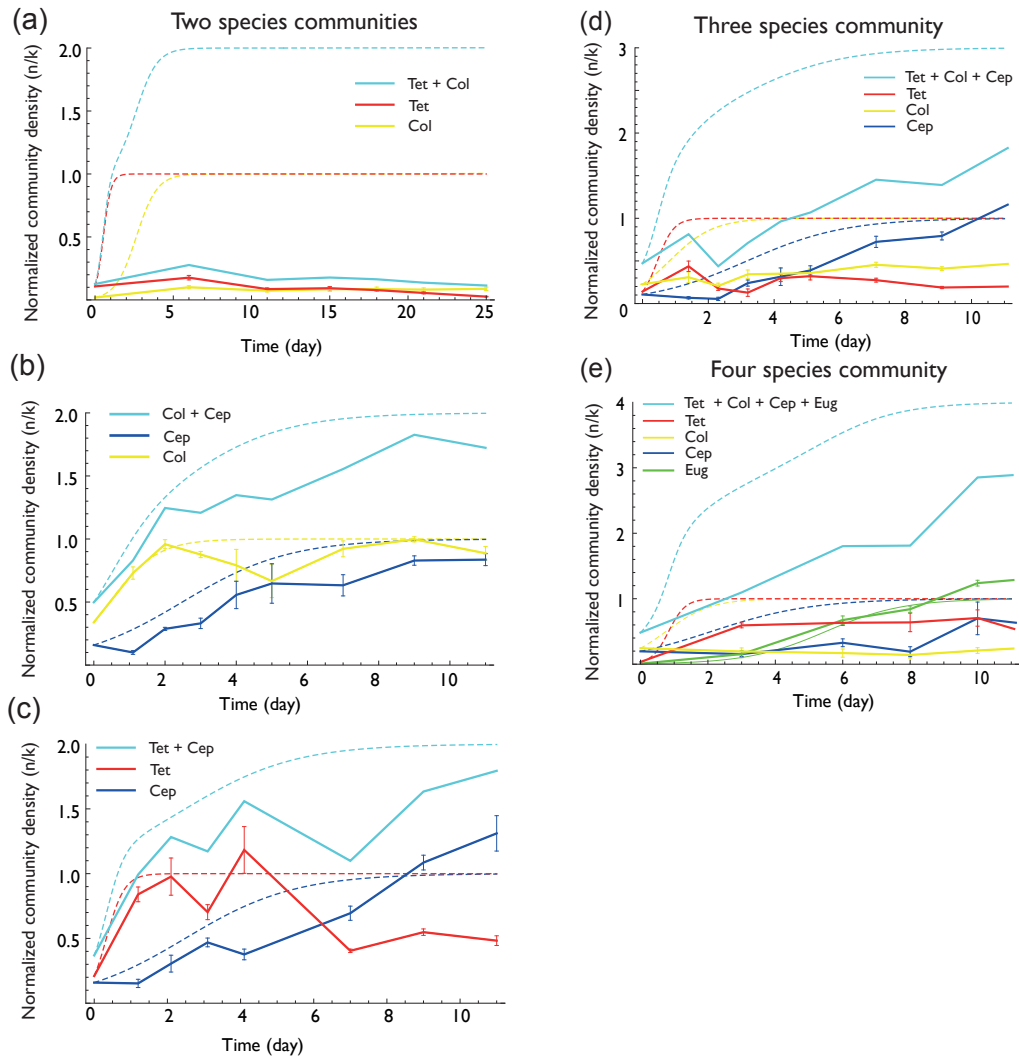


Figure 3.9: Time series of protists' density from the interaction experiments for the two–species combinations: (a) *Colpidium* sp. (yellow) and *Tetrahymena* sp. (red), (b) *Colpidium* sp. and *Cephalodella* sp. (blue), (c) *Cephalodella* sp. and *Tetrahymena* sp., (d) the same three species together, (e) the three species in combination with *Euglena gracilis* (green). In cyan, the sum of the experimental density (solid lines) and of the single species density (dashed lined) without interaction is plotted. Density is normalized to each species' carrying capacity. A complete additive community ($A = 1$) would follow the dashed cyan curve. Solid lines are the average \pm s.e.m. over six experimental replicates, dashed lines of the same color represent the theoretical expectation for single species (logistic equations). Panels are ordered with an increasing gradient of functional diversity. An additive partitioning analysis revealed that the relative importance of complementarity over selection effects was increasing with increasing functional diversity.

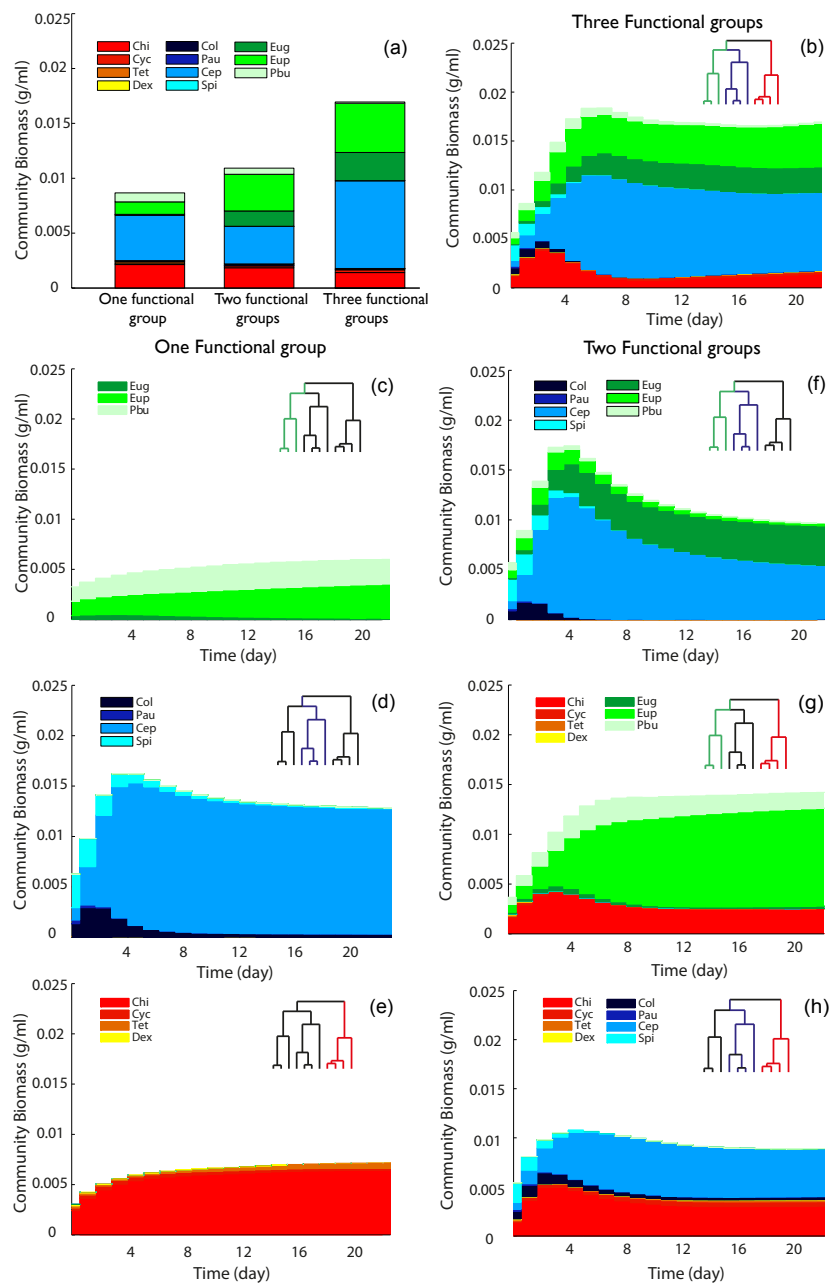


Figure 3.10: Relationship between total biomass production and functional diversity based on simulations adopting a generalized Lotka-Volterra model. The interaction matrix in the model is fitted on the empirical data from the pairwise–interaction experiment (Figure 3.2a). (a) Total biomass production in a gradient of functional diversity (increasing number of functional groups). The left and central bars, corresponding to communities with species from one and two functional groups respectively, are the averages of panels (c–e) and (f–h). (b–h) time series plot, showing a gradient in functional group diversity from one to three. The values are the average community biomass production over 100 simulations of different combinations of species. The inset dendrograms show the community used in each panel. The branch color of the dendrograms give the functional groups (red: small bacterivorous; blue: large bacterivorous; green: autotrophic species).

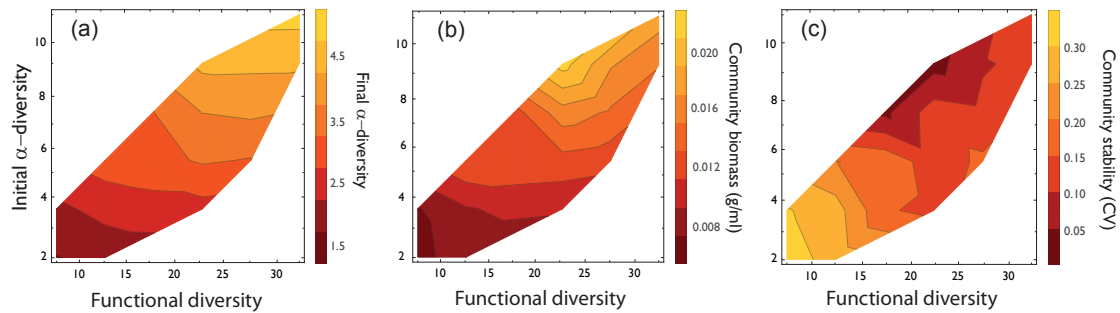


Figure 3.11: Results from simulations adopting a generalized Lotka-Volterra model on the impact of functional diversity on species coexistence (a), total biomass production (b), and community stability (c). Color gradients show realized final α -diversity, total biomass and coefficient of variation (CV), at the end of simulations. The simulations are based on initially identical communities with respect to species richness (2 to 11 species), but at different levels of functional diversity. The interaction matrix in the model is fitted on the pairwise interaction experiments (Figure 3.2c, as for Figure 3.10). The colored domain represents the feasible region with the lowest/highest functional diversity (x-axis), at each level of species richness 2 to 11 species, y-axis). At higher values of initial species richness, there is redundancy in functional diversity and the curves start to saturate.

higher species coexistence then resulted in enhanced productivity in 11-species communities compared to the average single-species and two-species communities (Figures 3.6, 3.9).

This experimental finding was confirmed in the numerical simulations, adopting a generalized LV approach. A stochastic community model, fitted by the experimental interaction matrix, was developed in parallel to the experiments, predicting quantitatively both the composition and the dynamics of protist communities (Figure 3.10a, b), and allowing generalization of the results (Figures 3.10c–h, 3.11). The relative contribution of species richness and functional diversity on community composition was disentangled (Figure 3.11), supporting recent empirical observations from the BEF literature of the positive effect of diversity on community productivity and stability (Allan et al., 2011; Cadotte, 2013), through a more mechanistic-based approach (Loreau and de Mazancourt, 2013).

When studying the effects of diversity on community stability or productivity, researchers have primarily conducted experiments observing the response of plants or grassland systems in competition for resources, using a simple trophic structure (Levine and HilleRisLambers, 2009; Allan et al., 2011; Cadotte, 2013). Recently, experimental evidence of how change in diversity on a particular trophic level is impacting over the whole food web McGradySteed et al. (1997) has motivated calls for analyses that are embracing several trophic levels at the same time (Duffy et al., 2007; Haddad et al., 2011). Additionally, there is a need to provide more mechanistic explanations for experimental evidences (Faust and Raes, 2012; Loreau and de Mazancourt, 2013; Turnbull et al., 2013). The present experiments extended from these

previous studies, and observed dynamics regarding diversity-stability and diversity-productivity in a more complex food web, with (at least) three trophic levels. The food web studied included a blend of competitive, predator-prey and amensalistic interactions (Figure 3.3a). The intra-group interactions for functional groups were mostly competitive, whereas the relative proportion of predator-prey links increased when considering species from distinct functional groups. This resulted in significantly different interaction-strength distributions between intra- and inter-group interactions. The distribution of interactions between species belonging to different functional groups was left skewed (Figure 3.3b), and stabilized the community (Allesina and Tang, 2012).

Based on species traits, reflecting fitness (intrinsic growth rate), and niche differences (body size, and photosynthetic ability), the 11 protist species were divided into three functional groups (see *Materials and Methods*). These groups correspond to the observation that a species's diet is directly linked to phylogeny and body size (Glücksman et al., 2010; Violle et al., 2011), which reflects important predator-prey relationship from allometric scaling theory (Allesina et al., 2008). Direct predation on smaller protists belonging to the first functional group (*Chilomonas* sp., *Cyclidium* sp., *Tetrahymena* sp. and *Dexiostoma* sp.) from large bacterivorous (i.e., *Paramecium aurelia*, *Cephalodella*, and *Spirostomum*) and *Euplotes aed.* happened regularly. In this model system, the interaction between competition for bacteria (the common food resource) and intraguild predation, which happens at similar timescales, may have played a role in determining the experimental outcome in the 11-species community (Chesson and Kuang, 2008), as recently found by experiments on bacteria species (Saleem et al., 2012). Furthermore, many other ecological traits (e.g., protist mouth size and structure, Fenchel (1980); Violle et al. (2011)) that were not taken into account in this analysis may have influenced species dynamics and interactions, but their identification goes beyond the scope of this study.

Using an additive partitioning analysis we detected the presence of strong complementarity forces in multispecies communities. Higher additivity for functionally diverse communities was also found, at different degrees of species richness. These findings, strongly support previous findings of complementarity effects due to niche differences in resources use (niche partitioning, Finke and Snyder (2008); Levine and HilleRisLambers (2009)), generalizing to trophically structured communities and functionally dissimilar species. However, the increase in productivity, when species were grown as communities, was less than the total biomass of all species when grown in isolation (inset Figure 3.6). This echoes recent experimental findings with single trophic level bacterial communities (Foster and Bell, 2012). Specifically, a non-additive effect of the total biomass production in a species richness gradient. A complete additive model, assuming null species' niche-overlaps, would represent an unrealistic assumption for this model system, where the main food source for protists species are bacteria. In fact, precise allometric relationships dictates a species's diet (Allesina et al., 2008), implying overlaps in resource use for protist species.

Moreover, the natural variability in intrinsic growth rates, resulting in high functional diversity, allows species from different functional groups to have differential responses over time (Tilman et al., 1998), eventually favoring coexistence (Allan et al., 2011; Loreau and de Mazan-

Chapter 3. Stabilizing effect of functional diversity on microbial communities

court, 2013), and enhancing ecosystem predictability (McGradySteed et al., 1997). By these mechanisms, species recover in a community when at low numbers, resulting in more effective intraspecific/intra-group interactions compared to interspecific/inter-group interactions (Figures 3.2, 3.3; Chesson (2000b); Levine and HilleRisLambers (2009)). On the contrary, communities composed of species within the same functional group, where stabilizing forces are generally weaker (Chesson, 2000b; Adler et al., 2007), and intrinsic growth rates are similar, tend to be more unpredictable. Stochastic effects may play a stronger role in community assembly for closely related species, determining species coexistence and the productivity level. Neutral theory represents the limit case, where both niche differences and fitness differences are set to zero, and stochastic drift is the only force structuring the community (Hubbell, 2001). Stronger priority effects for phylogenetic related species were experimentally observed in microbial communities (Peay et al., 2012; Tan et al., 2012). This resulted in the system in a decrease of system stability (Figure 3.11c), likely due to the emergence of multiple domains of attraction and alternative stable states (Ives and Carpenter, 2007), where dynamics are strongly dependent on the initial conditions.

In the interaction experiment, only one species (*Spirostomum* sp.) went extinct from the 11-species community in all six replicates. All other remaining 10 species persisted in at least one replicate. From the pairwise experimental results, a high degree of transitivity was found among the 11 species as no competitive loops were detected (Figure 3.4). The transitivity, therefore, explained the general agreement between an additive model fitted on the pairwise interactions and the experimental results of the 11-species community. Even though the additive LV model showed results consistent with the experimental findings, it cannot capture non-additive effects, relative non-linearities in intrinsic growth rate (Chesson, 2000b), or other forms of positive or negative interactions, such as interference competition (Amarasekare, 2002), which likely occurred in experimental communities. The average species richness observed in the 11-species experiment was higher than the species richness that persisted in the stochastic simulations of the generalised LV model. The main difference between the experimental results and theoretical predictions was largely due to the performance of *Paramecium aurelia*, which was detected in the community experiment, but went extinct deterministically in the model. *P. aurelia*, which appeared as a bad competitor in the pairwise rounds, routinely flourished in the 11-species community (Figure 3.6). This result could be linked to the degree of species transitivity (Allesina and Levine, 2011). *P. aurelia* had the highest degree of intransitivity (measured by the number of competitive loops formed by a certain species, Figure 3.4). Another possible explanation for this behavior could be related to the presence of microflagellates, which can deeply affect *P. aurelia* dynamics when this species is cultivated in monocultures or in species-poor communities (Marcel Holyoak, personal communication). In fact, bacteria and microflagellates were not measured and it is likely that competition dynamics at lower trophic levels may have consequences for the protists dynamics, suggesting that more complex mechanisms, like prey switching or interference competition, could have played a role in our microbial communities (Glücksman et al., 2010; DeLong and Vasseur, 2012).

More complex dynamics, such as non-additive effects, may emerge when multiple agents interact

(Case and Bender, 1981). In a grassland experiment, the system was found to be unstable (though near to the stability instability boundary) through a pairwise model, even if the plant species were observed to coexist in the field for several generations (Roxburgh and Wilson, 2000). Through a randomization procedure, the authors showed the particular configuration of species interactions in the community matrix was promoting stability, claiming for a highly non-random architecture in the interaction matrix (May, 1972; Sole and Montoya, 2001; Stouffer and Bascompte, 2011). In such cases, with multiple trophic levels (McGradySteed et al., 1997), the variety of species interactions due to functional diversity is hypothesized to promote stability and biomass production at the community level. Through this approach, the existence of positive non-additive effects was proved for certain species in functionally diverse communities, which were instead not detected in pairwise competition rounds. Interestingly, mutualistic loops between triplets of distantly related species were detected, belonging to three different functional groups (Figure 3.5). The following remarks are noteworthy: i) indirect forms of mutualism emerged only at high degrees of functional diversity in microbial communities; ii) theoretical estimates on the positive effect of functional diversity on community productivity and species coexistence were conservative, as our model was not taking into account positive non-additive effects .

Taken together, these results provide experimental evidence and theoretical explanations for the mechanisms that promote species coexistence, community stability, and productivity in trophically structured microbial communities. It is concluded that looking at species richness only as a proxy of diversity of a community may be misleading. It is thus suggested that complementing information, such as functional traits, is needed and will result in a more powerful approach to predict community properties, namely its stability and productivity. The inclusion of trophic trait structure has important implications for conservation strategies and ecosystems managements, which otherwise might be misguided or oversimplified.

4 Connectivity rules

A major aim of community ecology is to identify processes that define large-scale biodiversity patterns (Sheldon, 1968; Hastings and Higgins, 1994; Urban and Keitt, 2001; Fagan, 2002; Holyoak et al., 2005; Grant et al., 2007; Muneeppeerakul et al., 2008a; Bertuzzo et al., 2011). For simplified landscapes, described geometrically by linear or lattice structures, a variety of local environmental factors have been brought forward as the elements creating and maintaining diversity among habitats (Vallade and Houchmandzadeh, 2003; de Aguiar et al., 2009). Many highly diverse landscapes, however, exhibit hierarchical spatial structures that are shaped by geomorphological processes and neither linear nor two-dimensional environmental matrices may be appropriate to describe biodiversity of species living within dendritic ecosystems (Rodriguez-Iturbe and Rinaldo, 1997; Benda et al., 2004). Furthermore, in many environments intrinsic disturbance events contribute to spatio-temporal heterogeneity (Benda et al., 2004; Madin and Connolly, 2006). Previous microbial experiments found that spatio-temporal heterogeneity among local communities induced by disturbance (Fukami, 2001) and dispersal (Gonzalez et al., 1998; Cadotte, 2006b) events have a strong influence on species coexistence and biodiversity. These factors, directly affecting the history of community assembly (Fukami and Morin, 2003; Fukami et al., 2010), introduce variability in community composition in term of abundances and local species richness. Riverine ecosystems, among the most diverse habitats on earth (Fernandes et al., 2004), represent an outstanding example of such mechanisms (Clarke et al., 2008; Fér and Hroudová, 2008; Muneeppeerakul et al., 2008a).

Here, the effects of directional dispersal imposed by the habitat-network structure on the biodiversity of metacommunities ('MC's) were investigated, by conducting a laboratory experiment using aquatic microcosms. Experiments were conducted in 36-well culture plates (Figure 4.1), thus imposing by construction a metacommunity structure (Warren, 1996; Haddad et al., 2008): each well hosted a local community ('LC') within the whole landscape and dispersal occurred by periodic transfer of culture medium among connected LCs (Altermatt et al., 2011a), following two different geometries [see *Materials and Methods*]. Spatially heterogeneous MCs following a river network geometry ('RN'; Figure 4.1d) were compared with spatially homogeneous MCs, in which every LC has 2D lattice four nearest neighbors ('2D'; Figure 4.1e). The coarse-grained

RN landscape is derived from a scheme (Rodriguez-Iturbe and Rinaldo, 1997) known to reproduce the scaling properties observed in real river systems (Figure 4.1a). To single out the effects of connectivity, other geomorphic features of real river networks were deliberately not reproduced, such as the bias in downstream dispersal, the growing habitat capacity with accumulated contributing area or other environmental conditions connected to topographic elevation. Directional dispersal refers to the pathway constrained by the habitat connectivity and does not imply downstream-biased dispersal kernels, that is, in all treatments dispersal kernels were identical and symmetric. Disturbance consisted of medium replacement and reflects the spatial environmental heterogeneity inherent to many natural systems (*Materials and Methods*). The microcosm communities were composed of nine protozoan and one rotifer species, which are naturally co-occurring in freshwater habitats, with bacteria as common food resource (Haddad et al., 2008). These species cover a wide range of body sizes (Figure 1b), intrinsic growth rates and other important biological traits (Altermatt et al. (2011a), see Table 4.1). Thus, the microcosm communities cover substantial biological complexity in terms of more structured trophic levels and species interactions that can not be entirely captured by any model (Jessup et al., 2004; Holyoak and Lawler, 2005). The experimental design sheds light on connectivity in driving important biodiversity patterns of simplified metacommunities, disentangling complex natural systems' behavior (Holyoak and Lawler, 2005). Basic mechanisms of dispersal and disturbance dynamics were studied in river network geometry as important benchmark. RN and the 2D landscapes were compared focusing on three measures of biodiversity: the number of species present in a local community (α -diversity), among-community diversity (β -diversity) and the number of LCs in which a given species is present (species occupancy) (Muneepeerakul et al., 2008a). In parallel to the experiment a stochastic model was developed, generalizing across spatial and temporal scales (*Materials and Methods*). The model embeds spatio-temporal environmental heterogeneity, and is based on a Lotka-Volterra competition model. The dynamics of species competing for space and food resources on the same trophic level was simulated, subjected to periodic perturbation events consisting of partial habitat destruction. The model, considering only competition for space, is an approximation to the experimental system, and does not contain trophic dynamics that may occur in the protists communities (see chapters 2 and 3). Dispersal to neighboring patches can generate recolonization.

4.1 Materials and Methods

4.1.1 Aquatic communities

Each local community ('LC') within a metacommunity ('MC') was initialized with nine protozoan species, one rotifer species and a set of common freshwater bacteria as a food resource. The nine protozoan species were *Blepharisma sp.*, *Chilomonas sp.*, *Colpidium sp.*, *Euglena gracilis*, *Euplotes aediculatus*, *Paramecium aurelia*, *P. bursaria*, *Spirostomum sp.* and *Tetrahymena sp.*, and the rotifer was *Cephalodella sp.*. *Blepharisma sp.*, *Chilomonas sp.*, and *Tetrahymena sp.* were supplied by Carolina Biological Supply Co., while all other species were originally isolated

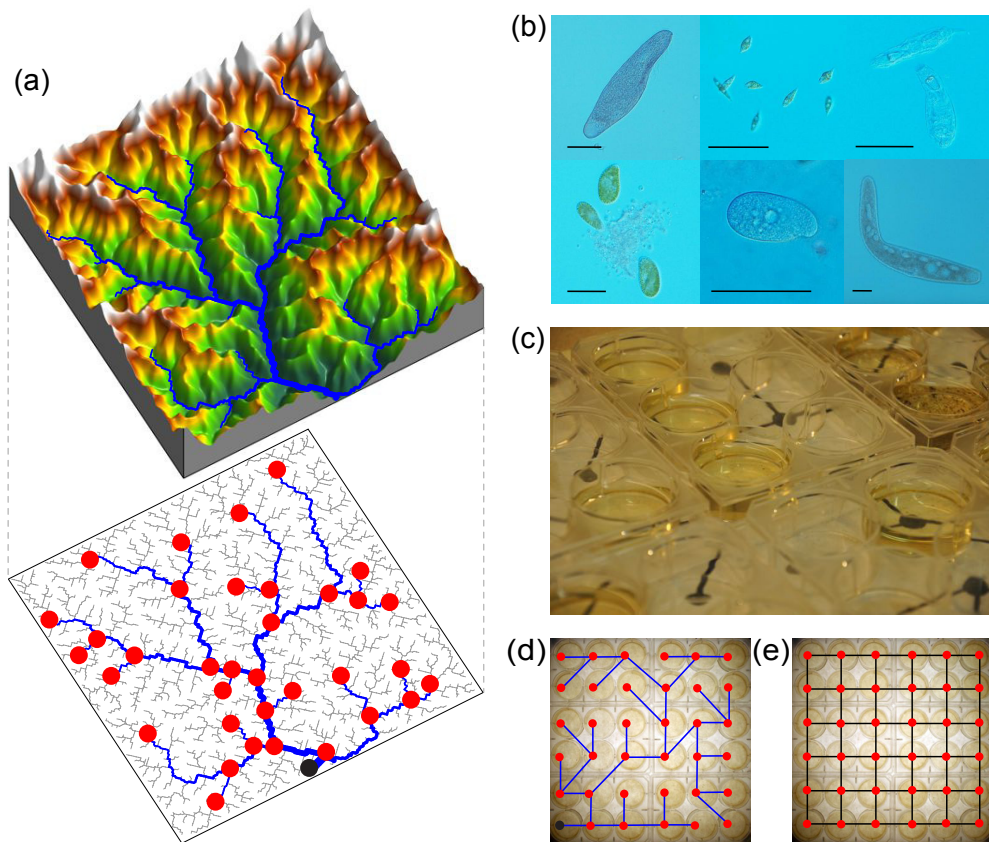


Figure 4.1: Design of the connectivity experiment. (a) The river network ('RN') landscape (bottom inset: red points label the position of LCs, the black point is the outlet) derives from a coarse-grained optimal channel network (OCN, see also Appendix A) which reflects the 3D structure of a river basin (top inset). (b–e) The microcosm experiment involves protists and rotifer species. (b) Subset of the species (in the order of the panels): *Blepharisma* sp., *Eug. gracilis*, *Cephalodella* sp. (first row from top left), *Paramecium bursaria*, *Colpidium* and *Spirostomum* sp. (second row, scale bars are 100 μm). In Table 4.1 the species' traits are summarized for the species pool. (c) Communities were kept in 36-well plates. Dispersal to neighboring communities follows the respective network structure: blue lines for RN (d), same network as in (a), black for '2D' lattice with four nearest neighbors (e).

from a natural pond (McGradySteed et al., 1997), and have also been used for other studies (Haddad et al., 2008; Altermatt et al., 2011a). The same nomenclature as in such studies is used, except for *Cephalodella* sp., which has been previously identified as *Rotaria* sp. All species are bacterivores whereas *Eug. gracilis*, *Eup. aediculatus* and *P. bursaria* can also photosynthesize. Furthermore, *Blepharisma* sp., *Euplotes aediculatus*, and *Spirostomum* sp. may not only feed on bacteria but can also predate on smaller flagellates. Twenty-four hours before inoculation with protozoans and rotifer, three species of bacteria (*Bacillus cereus*, *B. subtilis* and *Serratia marcescens*) were added to each community. LCs were located in 10 ml multiwell culture plates containing a solution of sterilized local spring water, 1.6 g l^{-1} of soil and 0.45 g l^{-1} of Protozoan Pellets (Carolina Biological Supply). Protozoan Pellets and soil provide nutrients for bacteria, which are consumed by protozoans. The experiment was conducted in a climatized room at 21°C under constant fluorescent light. On day 0, 100 individuals of each species were added, except for *Eug. gracilis* (500 ind.) and *Spirostomum* (40 ind.), which naturally occur respectively at higher and lower densities. Species' intrinsic growth rate r and carrying capacity K were determined in pure cultures, at identical conditions (see Species' traits below for details).

4.1.2 The landscapes

Each MC consisted of 36 LCs, connected according to two different schemes: a lattice network in which each LC has four nearest-neighbors with periodic boundaries ('2D' landscape), and a coarse-grained river network structure ('RN'), obtained from a 200×200 space filling optimal channel network (OCN, (Rodriguez-Iturbe et al., 1992; Rinaldo et al., 1992; Rodriguez-Iturbe and Rinaldo, 1997)), with an appropriate threshold on the drainage area (see *Modeling Riverine Connectivity* below for details). In the RN landscape a LC has either three nearest-neighbors ('Confluence', C) or one nearest-neighbor ('Headwater', H). Landscapes of these two dispersal treatments were replicated six times. Furthermore, MCs of 'Isolation' treatment were replicated three times.

'Isolation' treatment

Three MC replicates (108 LCs) without any disturbance-dispersal events were considered to test species coexistence in isolation ('Isolation' treatment, Figure 4.2). To avoid excessive deterioration of the medium in these isolated communities, on day 12 20% of old medium was replaced with fresh sterile medium. Figure 4.2 shows the three replicates for the Isolation treatment. It was already noticed that competition for resources and predation clearly disadvantaged certain species. Starting from the same initial conditions, only the same subset of species (*Cephalodella* sp. and the three photosynthetic ones, see Table 4.1 for species' traits) can persist without any kind of perturbation event.



Figure 4.2: α -diversity for the three replicates of the aquatic microcosm communities in ‘Isolation’ treatment. Specifically, *Euglena gracilis*, *Euplotes aediculatus*, *Paramecium bursaria* and *Cephalodella* sp. survived in all LCs of the three MCs, whereas *Paramecium aurelia* and *Blepharisma* sp. survived in a small fraction of them. Compare absolute numbers for local species richness (color coded) with Figure 4.6c, d.

4.1.3 Disturbance-dispersal events

In this section the experimental protocol for the microcosm metacommunities is described in detail. Spatio-temporal heterogeneity was introduced by disturbance events. Twice a week a disturbance-dispersal event was set-up, six times in total. Each time, 15 patches were randomly selected to be disturbed per metacommunity (MC). These patches were independently selected for each of the six replicates, but paired one RN and one 2D landscape to be disturbed along the same pattern.

A disturbance event consisted of the removing of all 10 ml of medium present in the local community (LC). To test the effectiveness of disturbance, one MC experienced disturbances but no dispersal. In this treatment, only in one LC (of 36 LCs) the persistence of two species was found: *Cephalodella* sp. and *Tetrahymena* sp. Thus, disturbance events were highly effective. After each disturbance event, dispersal was accomplished by manual transfer from every single LC to its nearest neighbors, without bias in directionality (isotropic dispersal) and happened simultaneously in well-mixed conditions, avoiding long-tailed dispersal events. This particular type of density-independent (diffusive) dispersal imposes equal per capita dispersal rates for all different species, and no competition-colonization trade-offs occur (Cadotte et al., 2006; Cadotte, 2007).

The following dispersal procedure was applied:

- thoroughly mixed the medium in every undisturbed LC;
- transferred from each LC in total 2 ml (20%) of medium to its nearest neighbors along the respective network on a ‘mirror’ landscape of 36 empty plates (Figure 4.3). Boundary

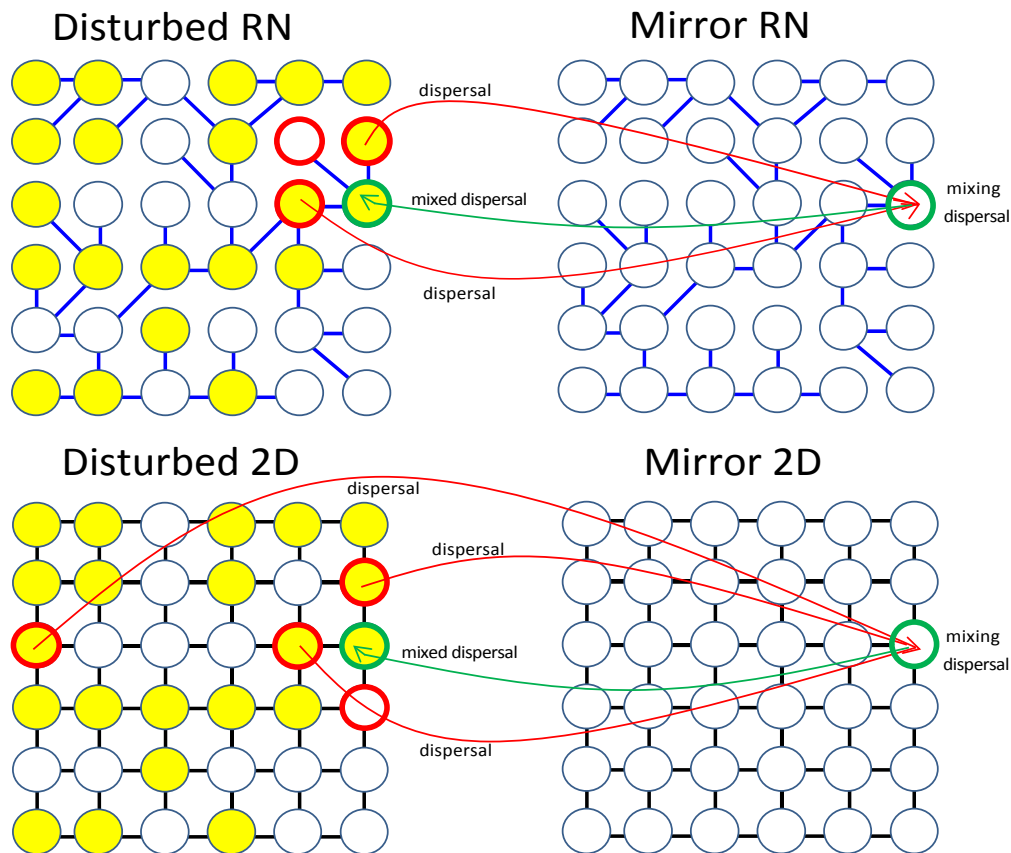


Figure 4.3: Dispersal protocol for the 'RN' and '2D' treatments. In this example: 1st replicate, 6th disturbance event. Yellow plates represent undisturbed LCs (the same for RN and 2D). Migrants were transferred from every undisturbed LC to its nearest neighbor(s) in 'mirror' landscape, where they were mixed. Then they were dispersed back to original position in 'real' landscape. Following this procedure the dispersal happened simultaneously. In the panels the dispersal are shown for red LCs migrants from green LC neighborhood for RN (closest upstream and downstream LCs) and 2D (four nearest neighbors, periodic boundaries) landscapes.

conditions are chosen for which headwaters dispersed only one third of medium (0.67 ml) dispersed by confluences in RN and LCs in 2D landscapes;

- collected and mixed dispersed medium in ‘mirror’ landscapes;
- re-transferred to the ‘real’ landscape;
- filled up every LC to 10 ml with fresh medium.

In this manner the dispersal happened simultaneously in well-mixed conditions, and long-tailed dispersal events were avoided. This particular type of density-independent (diffusive) dispersal, imposing equal per capita dispersal rates for all different species singles out the effects of connectivity on biodiversity patterns and no competition-colonization trade-offs occur (Cadotte et al. (2006); Cadotte (2007), see Figure 2.12 in chapter 2).

4.1.4 Biodiversity patterns

On day 24, after six disturbance-dispersal treatments, species presence-absence in each LC was checked. The entire LC was screened under a stereo-microscope, to avoid false-absences of the rarer species, obtaining the number of species present in every LC (α -diversity). Because of the nature of the last disturbance event, a few LCs could not be immediately recolonized by neighboring communities. Then, the spatial distribution of α -diversity and the number of LCs in which a species is present (species occupancy) was determined. To characterize β -diversity, the spatial decay of Jaccard’s similarity index (JSI) was considered, defined as $S_{ij}/(S_i + S_j - S_{ij})$, where S_{ij} is the number of species present in both LCs i and j , whereas S_i is the total number of species in LC i . The topological, rather than the euclidean, distances between community pairs was considered, because they represent the effective distance an individual has to disperse. The notation $\langle \cdot \rangle$ means a spatial average, while the $\bar{\cdot}$ represents an average over the six experimental replicates.

4.1.5 Species’ traits: size distribution

Protists were measured with a stereo-microscope (*Olympus SZX16*), on which a camera was mounted (*DP72*), and analyzed photographs via software (*cell3.2*). Exposure time and the magnification were optimized for each species. The length of 50 individuals of each species (longest body-axis) was measured to get size distributions (Table 4.1).

4.1.6 Species’ traits: population growth

Species-specific intrinsic growth rates and carrying capacities in pure cultures (Table 4.1) were measured, and these specific values were used in the stochastic model, without fitting parameters

Chapter 4. Connectivity rules

Table 4.1: Experimentally measured species' traits (mean \pm s.d.): body size, intrinsic growth rate, carrying capacity, and diffusion coefficient.

Species	Size [μm]	Growth rate [1/day]	Carrying capacity [ind/ml]	Diffusion mm^2/s
<i>Blepharisma</i>	471.3 \pm 57.1	0.67 \pm 0.07	59.5 \pm 4.7	0.113
<i>Cephalodella</i>	112.7 \pm 11.2	0.67 \pm 0.11	902.8 \pm 121.8	0.065
<i>Chilomonas</i>	23.3 \pm 3.7	0.98 \pm 0.13	1572.4 \pm 278.3	0.061
<i>Colpidium</i>	81.0 \pm 7.8	1.50 \pm 0.08	1379.2 \pm 76.6	0.156
<i>Eug. gracilis</i> [†]	36.7 \pm 6.4	0.87*	84578*	0.005
<i>Eup. aediculatus</i> [†]	85.4 \pm 8.6	0.43*	359*	0.012
<i>P.bursaria</i> [†]	101.3 \pm 12.9	0.23*	1639*	1.21
<i>P.aurelia</i>	111.6 \pm 15.1	0.86 \pm 0.02	111.1 \pm 2.6	0.372
<i>Spirostomum</i>	843.8 \pm 149.7	0.57 \pm 0.15	13.6 \pm 4.2	0.174
<i>Tetrahymena</i>	26.7 \pm 4.8	2.24 \pm 0.15	2996.8 \pm 196.1	0.011

*Data from Haddad et al. (2008)

[†]Mixotroph that can eat bacteria and photosynthesize.

(*Materials and Methods*). Even if estimates on growth rates and carrying capacities were already available for some species (Haddad et al., 2008), these experiments were repeated to get direct values for the specific experimental conditions, i.e., illumination, nutrient levels, chamber temperature, particular environment provided by well-plates (volume, ratio area/volume). For the growth experiment protists were cultivated in pure cultures at identical conditions used for the metacommunity experiment. Population density $\phi(t) = \langle n(t) \rangle / V$ grows in time following the Malthus-Verhulst differential equation (logistic curve)

$$\frac{d\phi_s}{dt} = r_s \phi_s \left(1 - \frac{\phi_s}{K_s} \right), \quad (4.1)$$

where $s = 1, \dots, 10$ is the species index, which has the following solution:

$$\phi_s(t) = \frac{\phi_{0,s} K_s e^{r_s t}}{K_s - \phi_{0,s} (1 - e^{r_s t})}, \quad (4.2)$$

where $\phi_{0,s}$ is the initial number of individuals per ml of medium, for species s . For every species the population growth curve in time was measured, averaging over six replicates. Every replicate was started at the same low density. Densities were measured daily for the first three days, subsequently measurements were taken depending on the species' growth rate r_s , till saturation of the curve, i.e., carrying capacity K_s . The complete results for all species are shown in Table 4.1.

4.1.7 Disentangling processes: ‘birth and death’ dynamics

The stochastic formulation of the logistic process [the one-step ‘birth and death process’ with space/food limitation (van Kampen, 2007)] is necessary when volumes of communities and/or number of individuals considered are small. The reader is referred to chapter 2 for an introduction to the stochastic ‘birth and death process’.

A theory-guided experiment may help to detect the strength of demographic stochasticity, endowing the metacommunity analysis key ingredients. Selected a time t_1 such that $n_0 e^{(b-d)t_1}$ is of order \sqrt{V} , for time $t < t_1$ the non-linear competition term in the master equation is of order $V^{-1/2}$ and may be neglected (van Kampen, 2007). The population is simply in its exponential malthusian growth phase $\langle n(t) \rangle = n_0 e^{(b-d)t}$ and $\langle n^2 \rangle - \langle n \rangle^2 = n_0 \frac{b+d}{b-d} [e^{2(b-d)t} - e^{(b-d)t}]$. To disentangle the two factors b and d hidden inside the macroscopic growth rate $r = b - d$, an analysis of variance among the six experimental replicates was performed: by calculating the macroscopic $\langle n(t) \rangle$ and the variance $\sigma^2(t)$ for time $t < t_1$, b and d can be inferred separately, knowing their sum and difference. The natural death rate for the protist species is $d_s \approx 0$.

4.1.8 Stochastic metacommunity model

The above arguments were generalized to the case of multiple species living in a patchy environment and competing for the same resources. The following discussion is valid for the LC k into the whole metacommunity. The nearest neighbors dispersal along the network is also simulated in a stochastic fashion. ‘Well-mixed’ conditions can not be assumed for individuals of all species, so each LC ideally divided in 100 cells and individuals in each of these cells were randomly distribute. Then 20 cells were randomly chosen to be dispersed to LCs nearest neighbors. The most conservative choice – in a pure competition for space framework among individuals of different species – is to consider the following null hypothesis. The competition term $\gamma_i(n_i - 1)/V \approx r_i(n_i - 1)/(K_i V)$, valid for species i in pure growth (see chapter 2), changes when taking into account the fact that the fraction of space occupied by an individual of species j is K_j/K_i times that of individual of species i . The transition probabilities for the birth and the death of an individual of the i th species, within a community with $\vec{n} = (n_1, n_2, \dots, n_i, \dots, n_S)$ individuals in species pool $P = (1, 2, \dots, i, \dots, S)$ respectively, read:

$$T(\vec{n} + \vec{e}_i | \vec{n}) = b_i n_i \quad (4.3)$$

$$T(\vec{n} - \vec{e}_i | \vec{n}) = d_i n_i + \frac{(b_i - d_i)n_i}{V} \left(\sum_{j \neq i} \frac{n_j}{K_j} + \frac{n_i - 1}{K_i} \right), \quad (4.4)$$

Chapter 4. Connectivity rules

where \vec{e}_i is a unit vector whose only i th component is not zero. The transition probabilities, when $d_i \equiv 0, \forall i \in P$ simplify to:

$$T(\vec{n} + \vec{e}_i | \vec{n}) = r_i n_i \quad (4.5)$$

$$T(\vec{n} - \vec{e}_i | \vec{n}) = \frac{r_i n_i}{V} \left(\sum_{j \neq i} \frac{n_j}{K_j} + \frac{n_i - 1}{K_i} \right). \quad (4.6)$$

The multivariate master equation (van Kampen, 2007) for the community is given by

$$\begin{aligned} \frac{dp(\vec{n}, t)}{dt} = & \sum_i \{ T(\vec{n} | \vec{n} + \vec{e}_i) p(\vec{n} + \vec{e}_i, t) + \\ & + T(\vec{n} | \vec{n} - \vec{e}_i) p(\vec{n} - \vec{e}_i, t) - \\ & - [T(\vec{n} + \vec{e}_i | \vec{n}) + T(\vec{n} - \vec{e}_i | \vec{n})] p(\vec{n}, t) \}. \end{aligned} \quad (4.7)$$

The resulting equations for the first moments are:

$$\frac{d\langle n_i \rangle}{dt} = r_i \left(\langle n_i \rangle - \sum_{j=1}^{S=10} \frac{\langle n_i n_j \rangle}{K_s V} \right), \quad (4.8)$$

that depends also on the second moments. Due to the limited LC volume $V = 10$ ml and the fact that the species' carrying capacity in some cases is small (less than hundred individuals per ml of medium), fluctuations around the macroscopic solutions may not be negligible. Thus, numerical simulations employing the Gillespie algorithm (Gillespie, 1977) were performed, which allows us to produce time series that exactly recover the solution of the multivariate master equation in Eq. (4.7) with transition probabilities in Eqs. (4.5) and (4.6). Edge effects in the lattice landscape are removed by imposing periodic boundary conditions. The dynamics of the system are stochastically perturbed to include diffusive dispersal of individuals across patches and spatially uncorrelated environmental disturbances, reflecting the experimental conditions. A simulation ends when the system has reached mono-dominance. Actually, at the experimental disturbance regime (and without any speciation process taken into account), only the species with the highest growth rate survives in the simulations.

4.1.9 Statistical analysis

Paired t-tests were performed to compare values from the six replicates for the RN and 2D treatments. Figure 4.4 shows the cumulative probability function of α -diversity for the different connectivity classes.

For the analysis in the RN, a ANOVA was performed with connectivity d , disturbance and ecological diameter l_i as factors, with random effects, due to the six different replicates. Seven

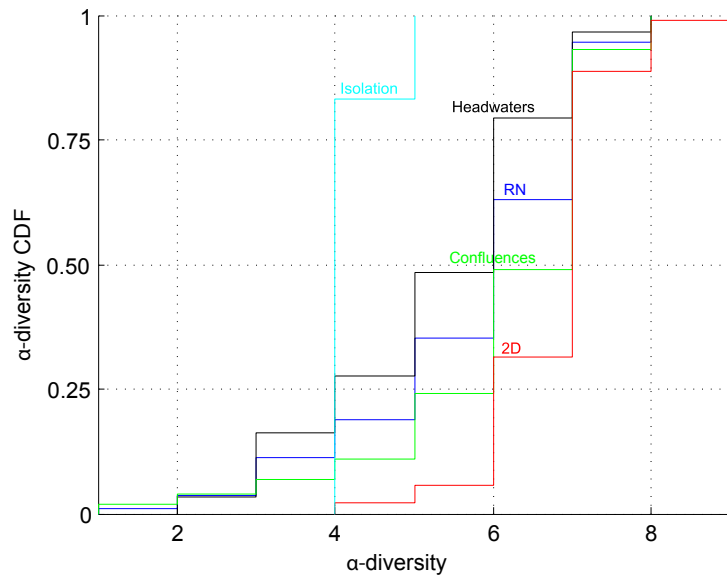


Figure 4.4: Cumulative density function (CDF) of α -diversity for different landscapes. The red and blue lines represent the α -diversity CDF for ‘2D’, ‘RN’, ‘Headwaters’ in black, ‘Confluences’ in green and ‘Isolation’ in cyan.

classes of disturbance were identified, according to the time to the last disturbance event to which a LC has been subjected. Actually, at the measurement time, the MCs have been exposed to six disturbance-dispersal events, but each LC exhibited different disturbance treatments (see *Materials and Methods* for disturbance protocol). In the class ‘0’ a LC has been subjected to the last disturbance, in the class ‘6’ a LC has never been disturbed. The ecological diameter is simply defined as the average distance $l_i = \langle d_{ij} \rangle_j$ of i from all the other LCs j in the RN, where d_{ij} represent the shortest (geodesic) distance between i and j (Newman, 2010). l_i was rounded to the nearest integer, thus identifying five classes (from 3 to 7) for the ecological diameter.

A temporal analysis of the disturbance events permits us to isolate the species that shows a disturbance-dependent behavior (Haddad et al., 2008). Every local community (LC) has a different ‘disturbance history’. LCs were divided in classes, in which every LC in a class has the same time from last disturbance event. The species occupancy distribution on these classes was obtained. If a species has a non-sensitive behavior to disturbances, its distribution should be constant over the different disturbance classes. This temporal analysis may reflect species competition rank: if a species is rarely found in a LC that has been disturbed long ago, it is very likely that its competition rank is low and vice versa.

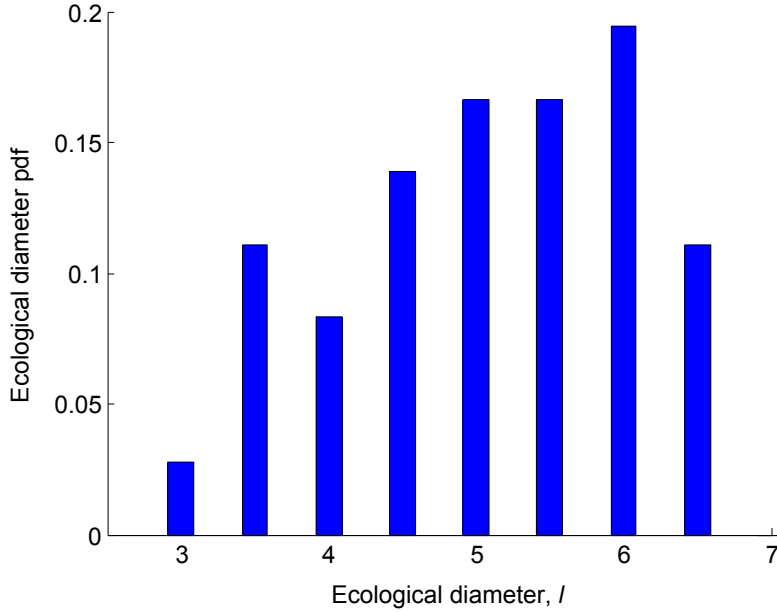


Figure 4.5: The probability density function (*pdf*) for the ecological diameter l_i for the RN landscape. In a 36-lattice landscape it is a delta function on $l_i^{2D} = l = 3$.

4.2 Results and Discussion

A significantly broader α -diversity distribution was found (Figs. 4.6 and 4.7a, b) in the RN compared to the 2D landscapes (measured as the coefficient of variation CV, $\overline{CV}_{RN} = 0.265$, $\overline{CV}_{2D} = 0.122$, paired t-test, $t_5 = 7.05$, $P = 0.0009$). Furthermore β -diversity, here described by the spatial decay of the Jaccard's similarity index (*Materials and Methods*), was higher in the RN compared to the 2D landscapes (Figure 4.7c). Mean local species richness in RN was significantly lower compared to 2D landscapes (Figure 4.6a–d, $\langle \alpha \rangle_{RN} = 5.72$, $\langle \alpha \rangle_{2D} = 6.72$, paired t-test, $t_5 = 9.23$, $P = 0.0003$). These results confirm theoretical predictions on the role of directional dispersal from both individual- or metacommunity-based models (Muneepeerakul et al., 2007, 2008a; Morrissey and de Kerckhove, 2009). Specifically, the anisotropy induced by directional dispersal has a strong impact on the spatial configuration of the species occupancy, reflected in α - and β -diversity (Figures 4.6a–d, 4.7e). This is a direct consequence of the radically different distributions of closeness centrality, i.e., the mean geometric geodesic distance (Newman, 2010) and the mean distance l between all LCs pairs (Figure 4.5) in RN vs. 2D landscapes ($l_{RN} = 5.33$, $l_{2D} = 3$). The model confirmed the experimental observations: a higher variability for α -diversity (Figure 4.6e, f) and a higher β -diversity (Figure 4.7c) in dendrites compared to lattice landscapes. These patterns were robust over a long time interval relative to species intrinsic growth rates (Figures 4.7d, 4.8). Furthermore, the patterns were consistent also at different spatial scales (Figure 4.7d).

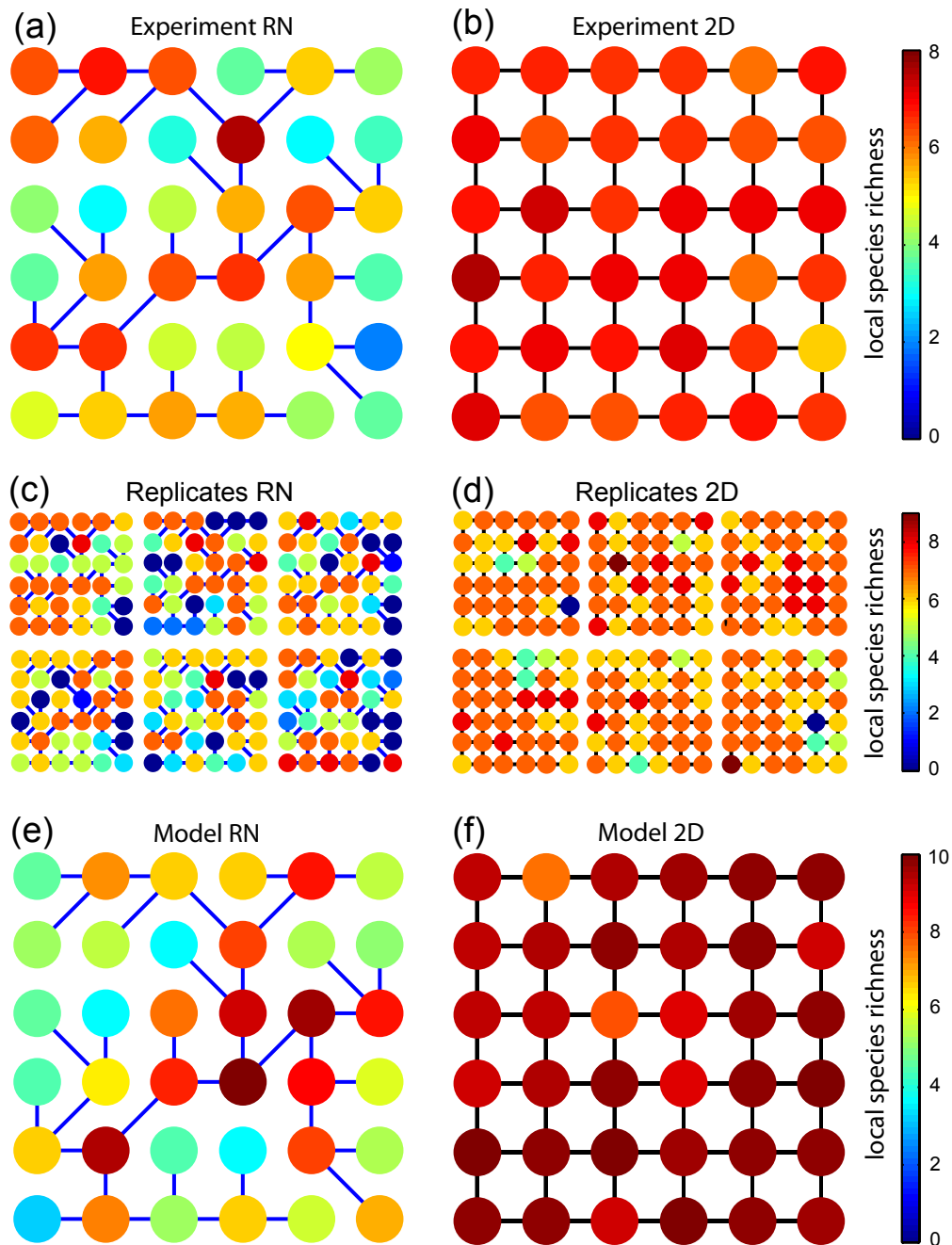


Figure 4.6: Experimental and theoretical local species richness in river network ('RN') and lattice ('2D') landscapes. (a, b) Mean local species richness (α -diversity, color coded; every dot represents a LC) for the microcosm experiment averaged over the six replicates. (c, d) Species richness for each of these replicates individually. (e, f) The stochastic model predicts similar mean α -diversity patterns (note different scales).

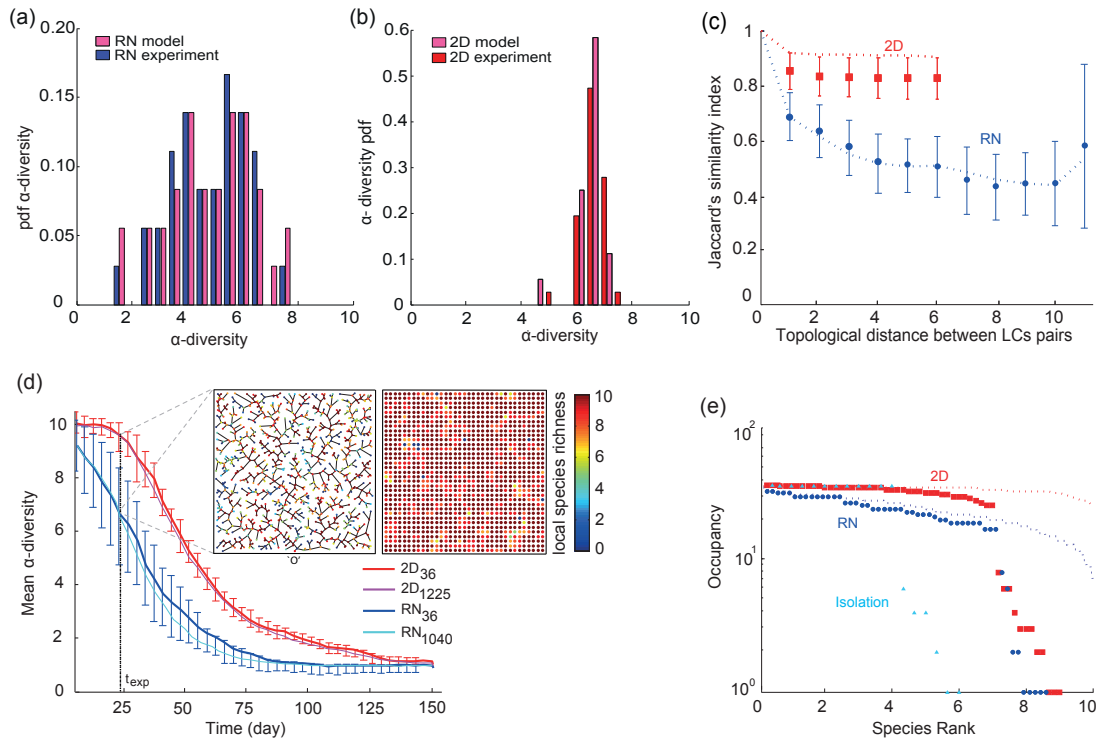


Figure 4.7: (a, b) Probability density function (*pdf*) of α -diversity for RN and 2D landscapes, with model distributions re-scaled to experimental averages. (c) β -diversity (JSI) in 2D (red) and in RN (blue), as a function of topological distance between LC pairs (mean \pm s.d. of experimental data, dotted lines are model predictions). Maximum geodesic distance in a 36 lattice is six, in the RN it is 11. (d) Predicted time behavior of mean \pm s.d. α -diversity for RN and 2D at two landscape sizes (36 and 1040 LCs for RN and 36 and 1225 LCs for 2D). Upper inset: α -diversity at $t_{exp} = 24$ day (black dashed line gives the experimentally measured time point) for a 1040 LCs RN landscape ('O' is the outlet), and for a 1225 LCs 2D landscape. (e) Rank-occupancy curve (red for 2D, blue for RN, and cyan for 'Isolation'), dotted lines are model predictions. Note the sharp decrease in occupancy for some protozoan species that the model does not predict, indicating stronger competition in the experiment (Figure 4.10).

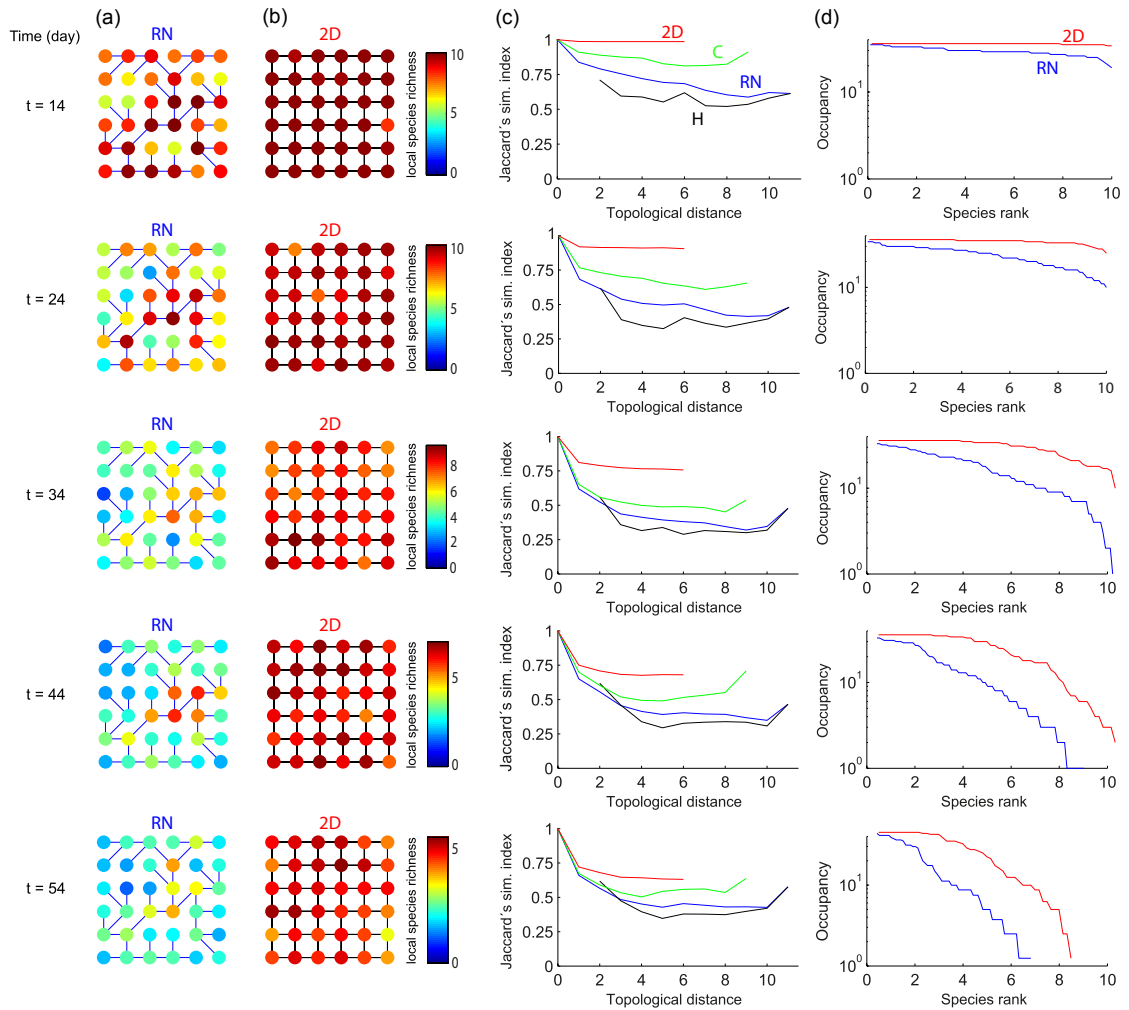


Figure 4.8: Average α -diversity (a, b), β -diversity (c), and rank-occupancy curve (d) at different time points. The patterns found in the experiment at $t_{exp} = 24$ day (Figure 4.6) are maintained for a long time interval in the stochastic metacommunity model. Moreover, in the isolation experiment, over temporal scales $t \approx t_{exp}$ the communities are driven by competition-exclusion dynamics to a lower biodiversity state.

4.2.1 Temporal dynamics

The experiments ended at day 24, after six disturbance-dispersal events. On day 24, data on presence-absence of metacommunity species were collected, observing different biodiversity patterns resulting from long-term community dynamics for the RN and 2D landscapes. But what about the patterns at different time scales? Through the combined approach of the microcosm experiments with the metacommunity model it is possible to answer this important question (Holyoak and Lawler, 2005). Having verified that the model predicts the biodiversity patterns at one particular time point, the behavior of the system may be inferred at different time scales (Figures 4.7d, 4.8). The dynamics of the system, stochastically perturbed to include diffusive dispersal of individuals across patches and spatially uncorrelated environmental disturbances, reflects the experimental conditions. A simulation ends when the system has reached monodominance, i.e. only one species survives in the metacommunity. Actually, as noted above, at the experimental disturbance regime (and with no speciation process), only the species with the highest growth rate survive in the simulations. Patterns hold in this entire time interval, while the average $\langle\alpha\rangle$ -diversity for the two landscapes decreases consistently in time (Figure 4.7d). Figure 4.8 shows the biodiversity patterns compared for the two landscapes, at different time points. The system is predicted to be in a long transient state (Hastings and Higgins, 1994). Experimental results are general over ecologically important time scales, meaning that the timescales are large relative to species generation time. Actually, the time interval in which the system has been analyzed corresponds to ≈ 50 – 300 generations, depending on the species' growth rate (Table 4.1).

4.2.2 Headwaters vs. confluences

The bimodal shape of the α -diversity distribution observed in both the model and experiment for the river network geometry (Figure 4.7a) called for an analysis based on the degree of connectivity, d , which gives the number of connected neighboring nodes to a LC. In the 'Headwater' class (H), LCs have $d_H = 1$ and are connected uniquely to their 'downstream' node whereas in the 'Confluence' class (C), LCs are characterized by $d_C = 3$ and are connected to two 'upstream' and one 'downstream' nodes. In this scenario, the terms 'downstream' and 'upstream' refer only to the position of the connected LC with respect to the outlet. They do not refer to a mass-flow as dispersal is not directionally biased (Muneepeerakul et al. (2008a), see *Materials and Methods*). The outlet of the network ('O'), connected only to its upstream node ($d_O = 1$), falls into the H class. The α -diversity distribution for Hs peaked at a significantly lower value compared to the peak of the Cs' distribution ($\overline{\langle\alpha\rangle}_H = 5.29$, $\overline{\langle\alpha\rangle}_C = 6.10$, paired t-test, $t_5 = 7.24$, $P = 0.0008$) and exhibits higher variability (Figure 4.9a). Figure 4.6a, e shows this pattern, in which the backbone of the river network exhibits on average a higher species richness with respect to peripheral communities. To explain the variability of the local species richness in the RN, two other factors were included in the analysis: the 'ecological diameter' l_i of the LC i (strictly related to its closeness centrality), and the temporal distribution of disturbance events. Connectivity significantly affected α -diversity in the RN landscape (ANOVA, $F_{1,5} = 12.09$, $P =$

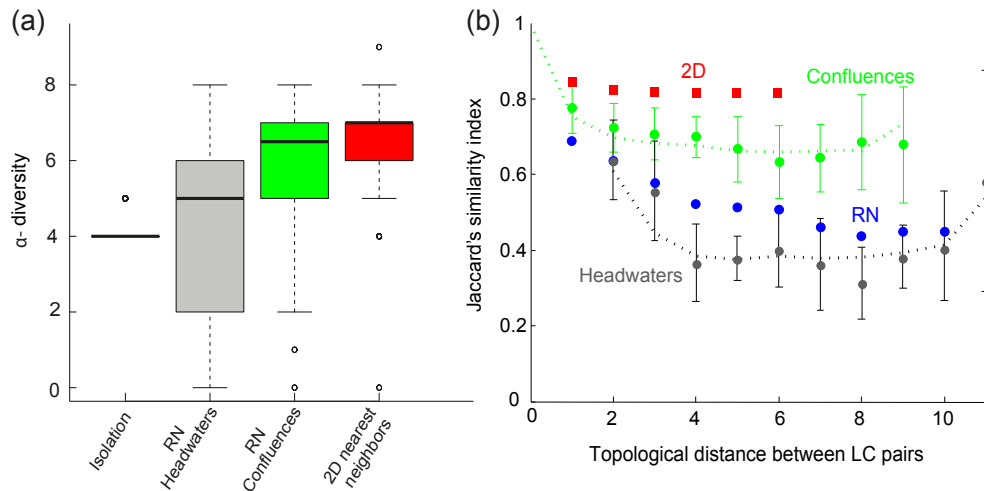


Figure 4.9: (a) Experimentally observed α -diversity as a function of the degree of connectivity (d), e.g. the number of connected neighboring nodes to a LC. For LCs in ‘Isolation’ treatment $d = 0$, in RN ‘Confluences’ (Cs) have $d = 3$ and ‘Headwaters’ (Hs) $d = 1$, whereas in 2D all LCs have $d = 4$. Larger d results in significantly higher species richness. Boxes represent the median and 25/75th percentile, whiskers extend to 1.5 times the interquartile range. (b) JSI for Cs (green), and for Hs (black) separately. Filled symbols represent the mean \pm s.d. of the experimental data, dotted lines the model predictions. For comparison, the JSI for the entire RN (blue) and that for the 2D (red) are shown.

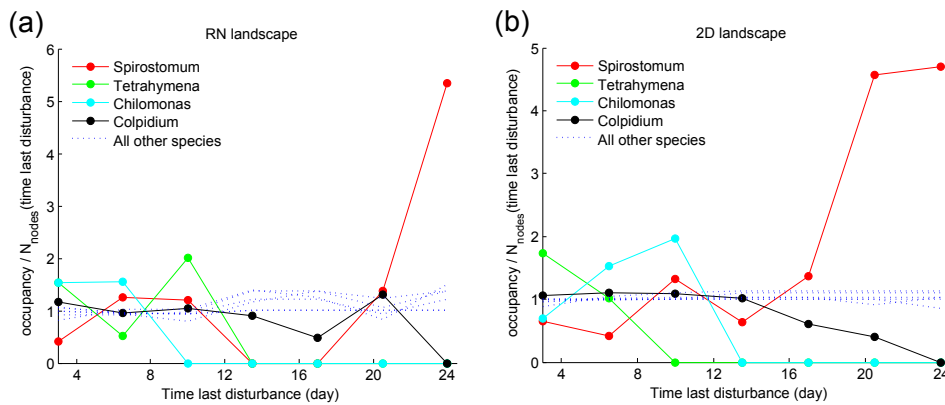


Figure 4.10: Distribution of species occupancies relative to the temporal distribution of disturbance events in ‘RN’ (a) and ‘2D’ (b) landscapes. Filled symbols represent deviations from a non-sensitive behavior to disturbance (dotted blue lines). Smaller protozoans (*Chilomonas* sp., *Tetrahymena* sp., and *Colpidium* sp., respectively cyan, green and black) occupied only sites that had been recently disturbed, suggesting that these species were competitively inferior. Opposite behavior was observed for *Spirostomum* sp. (red), which predominantly occupied patches that were disturbed relatively long ago.

0.0006), whereas neither time to the last disturbance nor network centrality significantly affected local species richness (ANOVA, $F_{6,5} = 1.66$, $P = 0.13$; and $F_{4,5} = 0.71$, $P = 0.59$, see Figure 4.10).

β -diversity was obtained separately for headwaters and confluences, to test the difference in species composition within the river network structure. Headwaters exhibited not only a higher variability in α -diversity, but also a higher β -diversity compared to confluences (Figure 4.9b), confirming patterns found in natural river basins (Fernandes et al., 2004; Clarke et al., 2008). Therefore, the difference in the loss of spatial correlation relative to lattice landscapes appeared even higher when only headwaters were considered in the comparison. These results reveal the crucial importance of headwaters as a source of biodiversity for the whole landscape. In natural systems other local environmental factors may play a role in structuring ecosystems (Brown and Swan, 2010). Nevertheless, this experimental approach sheds light on the effect of directional dispersal on biodiversity. Note that the patterns found in river network geometry are predicted to be even stronger in the presence of a downstream dispersal, which is typical for many passively transported riparian and aquatic species in river basins (Fér and Hroudová, 2008; Morrissey and de Kerckhove, 2009).

A lower mean α -diversity was observed in the experiment compared to the theoretical predictions ($\Delta\langle\alpha\rangle_{RN} = 37\%$, $\Delta\langle\alpha\rangle_{2D} = 42\%$), but a re-scaling to the experimental mean produced a consistent local species richness distribution (Figure 4.7a, b). Species occupancies are presented in Figure 4.7e as a rank-occupancy curve: both the model and the experiment revealed that well-connected 2D landscapes presented higher spatial persistence compared to river network environments, but the sharp decrease in experimental rank-occupancy curves observed in both landscapes suggests that some species are disadvantaged. It is likely that species competition in the experiment had stronger effects on the persistence of weaker species, than that generated in the model by pure competition for space (Figure 4.10).

4.2.3 Competitive exclusion dynamics

At this point of the discussion the following question arises: how does the system react over these spatio-temporal scales, without any disturbance-dispersal events? Species' ability to coexist was tested in an 'Isolation' treatment, under the same environmental conditions (*Materials and Methods*). Under stress (space saturation and reduced availability of bacteria) larger protozoans, such as *Blepharisma* and *Spirostomum* sp., could predate on smaller protozoans, such as *Chilomonas*, *Tetrahymena* and *Colpidium* sp. (Table 4.1 for species' traits, see chapters 2 and 3). The latter appeared to be strongly inferior competitors (Figures 4.2, 4.10). Note that predation could happen even at low protist densities and high bacterial densities. Figure 4.10 shows that smaller species (*Chilomonas*, *Tetrahymena*, and *Colpidium* sp.), that have high growth rates and carrying capacities, are almost absent in LCs classes disturbed long ago, therefore have low competition rank. This is also consistent with the results provided by the 'Isolation' treatment, in which the above three species have never been found in such isolated communities

at the end of the experiment. Thus, the spatio-temporal heterogeneity induced by disturbance and dispersal events has prevented competitive exclusion dynamics, which would have excluded the weaker species in long-term regimes. A consistent subset of four species survived at the end of the isolation experiment (Figure 4.2), whereas all other species went mostly extinct, resulting in lower values of both α - and β -diversity ($\overline{CV}_{Isolation} = 0.086$, $\overline{\alpha}_{Isolation} = 4.17$). The results confirmed the importance of dispersal and connectivity for maintaining higher level of biodiversity observed in fragmented landscapes (Damschen et al., 2006; Cadotte, 2006a), Figure 4.9a), at temporal scales over which competitive exclusion dynamics have emerged in isolated communities (Figure 4.2). Clearly, competition, although stronger than just for space and resources, has not altered the connectivity-induced patterns highlighted by both the theoretical and the experimental approaches.

Because the types of dispersal and disturbances employed in this system are not specific to riverine environments, the above results apply to a variety of heterogeneous and fragmented environments. Species constrained to disperse within dendritic corridors face reduced spatial persistence and higher extinction risks. On the other hand, heterogeneous habitats sustain higher levels of among-community biodiversity, that can be altered by modifying the connectivity of the system, with implications for community ecology and conservation biology since it may endow dendritic ecosystems with higher resilience to environmental change.

5 Disentangling habitat patch-size from hierarchical habitat capacity

5.1 Introduction

Biodiversity has been strongly affected by humans over the last decades. In many systems, diversity has been declining at all levels, with major consequences on ecosystem functioning and services (Vörösmarty et al., 2010). Anthropogenic alterations of the natural environment, such as land use changes and habitat fragmentation, directly threaten species (Fagan, 2002; Fahrig, 2003; Poff et al., 2007; Franzen and Nilsson, 2010; Gonzalez et al., 2011; Perkin and Gido, 2012). One of the main challenges in community ecology and conservation biology is the understanding of the interactions between local and regional factors controlling population demography and community composition (Sheldon, 1968; Chesson, 2000a; Hubbell, 2001; Holyoak et al., 2005), to eventually predict community dynamics (Fagan, 2002; Economo and Keitt, 2008).

Recent theoretical, experimental and comparative work suggests that dispersal constrained by specific habitat structures is a major determinant of the observed diversity patterns at both species and genetic level (Fagan, 2002; Muneeppeerakul et al., 2008a; Clarke et al., 2008; Morrissey and de Kerckhove, 2009; Brown and Swan, 2010; Finn et al., 2011; Carrara et al., 2012). Up to now, however, two major aspects have been neglected by most theoretical and experimental studies. First, landscape connectivity was generally considered independent of local environmental factors, such as habitat quality, patch-size, environmental disturbances, and intra- and inter-specific competition. While there are indeed cases for which this simplification is appropriate, such as forests (Hubbell, 2001), island archipelagos (MacArthur and Wilson, 1963), or natural ponds (Altermatt et al., 2008; De Bie et al., 2012), it does not represent many natural landscapes, such as fluvial and mountainous ecosystems, where local properties of the habitat and connectivity are intrinsically linked (Sheldon, 1968; Benda et al., 2004; Lowe et al., 2006). Second, past studies generally adopted constant dispersal rates, symmetric kernels and simplified landscape attributes (Warren, 1996; Gonzalez et al., 1998; Mouquet and Loreau, 2003; Matthiessen and Hillebrand, 2006; Altermatt et al., 2011b; Chisholm et al., 2011). Traditionally, many studies in stream ecology, influenced by the River Continuum Concept (Vannote et al., 1980), have considered linear conceptual models to analyze drainage basins. Such simplified linear environmental

Chapter 5. Disentangling habitat patch-size from hierarchical habitat capacity

matrices, however, may not completely capture biodiversity patterns within dendritic ecosystems (Fagan, 2002; Grant et al., 2007; Brown and Swan, 2010; Finn et al., 2011; Carrara et al., 2012).

In riverine ecosystems, landscape-forming discharges are related to total contributing drainage area, a by-product of spatial aggregation, depth, and width of the active river cross-section (Leopold et al., 1964; Rodriguez-Iturbe and Rinaldo, 1997; Benda et al., 2004). The river network not only provides suitable ecological corridors for individuals to disperse (Fagan, 2002; Rodriguez-Iturbe et al., 2009), but often dictates the availability of micro-habitats that species may eventually exploit (Cardinale, 2011). Habitat capacity (i.e., river width/depth, reflecting patch-size in rivers) scales with contributing area, dispersal is often biased downstream, and the distribution and intensity of disturbances are intrinsically linked with the position along the network through abrupt changes at confluences (Benda et al., 2004). Consequently, spatial correlations emerge between local properties and regional network descriptors in dendritic environments, where the hierarchical spatial organization of environmental heterogeneity is a fundamental driver of local species richness and community composition (Fernandes et al., 2004; Muneeppeerakul et al., 2007). Riverine ecosystems, which are among the most threatened ecosystems on Earth (Vörösmarty et al., 2010), are thus a prominent natural system in which disentangling the effect of local environmental conditions and connectivity of the landscape on diversity is needed (Lowe et al., 2006; Lake et al., 2007; Gonzalez et al., 2011; Grant et al., 2012). For example, habitat capacity and inter-annual streamflow variability are changed in rivers undergoing hydropower development or cross-basin connections (Poff et al., 2007; Grant et al., 2012; Ziv et al., 2012). Furthermore, land-use and agricultural practices in many countries are affecting riparian zones, foreseeing buffer zones on a fixed distance from the river bank only, irrespective of the spatial position within the river network (Gassner, 2006). Theoretical, empirical and comparative studies have suggested that the degradation of riparian vegetation structure and alteration of connectivity between the patches in the habitat mosaic may significantly reduce stream diversity at different trophic levels (Urban et al., 2006; Vörösmarty et al., 2010; Grant et al., 2012; Perkin and Gido, 2012; Ziv et al., 2012). However, most studies on ongoing habitat change and legal regulations regarding riverine landscapes are not considering the intrinsic link of habitat capacity and network position (Lake et al., 2007).

In this chapter, the interaction of dendritic connectivity and local habitat capacity on the diversity of microorganisms in dendritic metacommunities were experimentally singled out by modulating patch-size. Metacommunities were mimicking network structure and patch connectivity of natural river networks. Specifically, the individual influence of connectivity and habitat capacity on microbial diversity was singled out by using three different configurations of patch-sizes (*Riverine*, *Random* and *Homogeneous*), connected following a river network geometry (Figure 5.1, and *Material and Methods*). In *Riverine* landscapes local habitat capacity correlates with position along the network and distance to the outlet (Figure 5.2, Table 5.1). Larger downstream communities receive more immigrants from upstream communities, eventually having a combined positive effect on biodiversity. In the *Homogeneous* and *Random* landscapes, motivated by ongoing riverine habitat modifications, local habitat capacity (i.e., the patch-size) does not preserve the geomorphological scaling observed in natural river systems (Leopold et al., 1964;

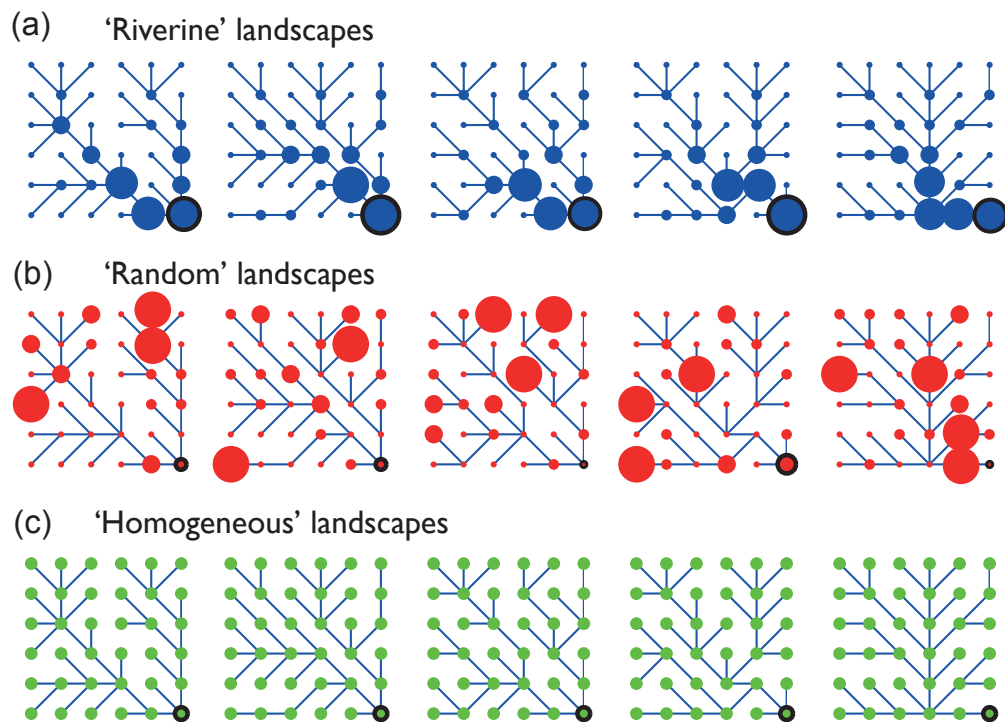


Figure 5.1: Spatial configuration of dendritic networks and corresponding patch-sizes in the microcosm experiment. (a) *Riv* landscapes (blue) preserved the observed scaling properties of real river basins; (b) *Ran* landscapes (red) had the exact values of volumes as in the *Riv* landscapes, randomly distributed across the networks; (c) in *Hom* landscapes (green) the total volume of the whole metacommunity was equally distributed to each 36 local communities. Patch-size (size of the circle) is scaled to the actual medium volume. Five unique river-like (dendritic) networks (columns) were implemented. Dispersal to neighboring communities followed the respective network structure, with a downstream bias in directionality towards the ‘outlet’ community (black circled dot).

Table 5.1: Correlations among network descriptors.

Landscape	Variable	d	v	o	A
<i>Riverine</i>	v	0.63*			
	o	-0.36*	-0.63*		
	A	0.48*	0.94*	-0.63*	
	l	-0.57*	-0.62*	0.55*	-0.54*
<i>Random</i>	v	-0.03			
	o	-0.36*	0.07		
	A	0.53*	0.09	-0.63*	
	l	-0.57*	0.13	0.55*	-0.54*
<i>Homogeneous</i>	v	-			
	o	-0.36*	-		
	A	0.54*	-	-0.64*	
	l	-0.57*	-	0.55*	-0.57*

Correlation matrix (*Pearson* correlation) among network descriptors (d = degree of connectivity; v = patch-size; o = distance to outlet; A = drainage area; l = ecological diameter), for the three network configurations. In *Random* landscapes patch-size loses correlation with the other network descriptors, compared with *Riverine* landscapes. Patch-size is constant by definition in *Homogeneous* landscapes.

* $p < 0.01$.

Rodriguez-Iturbe and Rinaldo, 1997). By measuring species' persistence and species' density diversity patterns were followed in terms of α -, β -, γ -diversity (local species richness, among-community dissimilarity and regional species richness), and community evenness in the above landscape configurations. Aquatic microcosms as employed here and in several other studies (e.g., Fukami and Morin (2003); Cadotte et al. (2006); Haddad et al. (2008); Carrara et al. (2012); Giometto et al. (2013)) offer a useful bridge between theoretical models and comparative field studies, to test for general macroecological principles (Holyoak and Lawler, 2005; Livingston et al., 2012). Findings from such laboratory experiments, even if not directly comparable to natural systems, may cast light on important underlying mechanisms that steer metacommunity dynamics in river systems.

5.2 Material and Methods

5.2.1 The Riverine landscapes

Each metacommunity (MC) consisted of 36 local communities grown in culture well-plates connected by dispersal. Communities, composed of nine protist and one rotifer species (see *Aquatic Communities*), were connected according to five different river network geometries (Figure 5.1). Dendritic network landscapes were derived from five different space filling Optimal Channel Networks (OCNs, Rinaldo et al. (1992); Rodriguez-Iturbe et al. (1992), known to reproduce the scaling properties observed in real river systems (Rinaldo et al., 2006). An appropriate

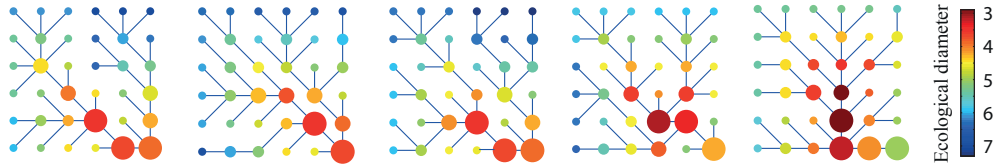


Figure 5.2: Spatial distribution of ecological diameter (color coded) for the five different river-network replicates in *Riverine* landscapes. Ecological diameter is defined as the average distance of a node from all the other nodes in the network. Closeness centrality, in network theory, is simply the inverse of ecological diameter. In our analysis, degree of connectivity, d , and patch-size, v , were used as local network descriptors. d_i and v_i are respectively the number of connected neighboring nodes and habitat capacity of LC i (size of the circle). Distance to the outlet, o , drainage area, A , and the ecological diameter, l , were used as regional network descriptors. d varies between 1 to 6, o between 0 to 7 (in units of topological distance), v falls in four size categories (2, 3.5, 6, 12 ml), and A varies over the range of 2 (headwater communities) to 136 ml (outlet of the river network). l varies in the range from $l_{min} = 2.7$ (central LC) to $l_{max} = 7.1$ (peripheral LC).

coarse-graining procedure was enforced to reduce a complex construct to an equivalent 6×6 patch network, preserving the characteristics of the original 3D basin. To have independent replication on the level of the networks, five different realization of river network configurations have been specifically chosen.

The habitat capacity of a MC is related to physical properties that affect persistence of species (Reche et al., 2005). The largest organism to be sustained by an ecosystem is known to depend on habitat size (see e.g., Banavar et al. (2007)), termed habitat capacity. Therefore habitat capacity conceptualizes the ability to rank different landscapes in terms of their capacity to support viable populations. Three different treatments of patch-size configurations were implemented in each of the five *OCN* landscapes (Figure 5.1): i) a '*Riverine*' landscape, in which the volume v_i (i.e., the patch-size) of the local community (LC) i preserves the scaling law observed in real river systems: $v_i \propto A_i^{1/2}$. A_i is the drainage area of the LC i defined as the sum over all the volumes v_j draining in that particular point; ii) a '*Random*' landscape, in which the exact values of patch volumes v_i as in the *Riverine* landscape were randomly distributed across the network; and iii) a '*Homogeneous*' landscape where the total volume of the whole MC was equal to the other two treatments, but each LC had a constant average value $\bar{v}_{hom} = 3.6 ml$ (*Riverine*=*Riv*, *Random*=*Ran*, *Homogeneous*=*Hom*). Values of v_i were binned based on their original drainage area, in four size categories (2, 3.5, 6 and 12 ml). In order to test species coexistence in isolation, 72 communities of '*Isolation*' treatment were initialized, in which the patch-sizes were equal to the first two replicates of the *Riv* configuration of the main experiment, but without dispersal.

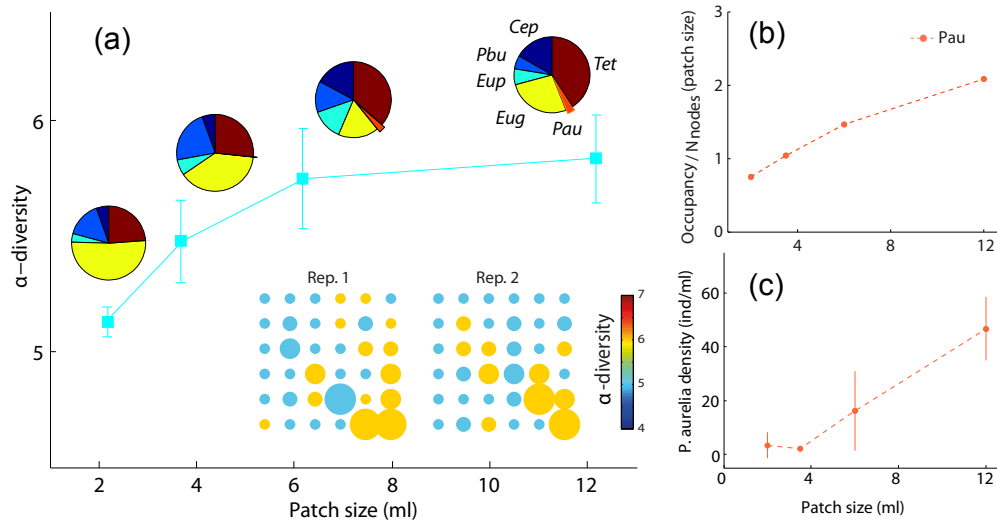


Figure 5.3: ‘Isolation’ treatment to test the effect solely of habitat capacity (patch-size). (a) α -diversity as a function of patch-size for the two replicates in the isolation treatment. Inset: pie charts show the average proportion of each species in the corresponding patch-size. Environmental conditions, dictated in the well-plates by the ratio of surface area to volume, are changing between communities with different patch-size, favouring different sets of species at a time. *Cep* is *Cephalodella* sp. (rotifer), *Eug* is *Euglena gracilis*, *Eup* is *Euplotes aediculatus*, *Pau* is *P. aurelia*, *Pbu* is *P. bursaria*, and *Tet* is *Tetrahymena* sp. (see relative increasing of *P. aurelia*, in orange, with increasing patch-size). (b, c) Distribution of occupancy relative to community patch-size for *P. aurelia*, which generally survived in bigger patch-sizes, with higher densities.

5.2.2 Aquatic communities

LCs were kept in multi-well culture plates containing a variable medium volume (2–12 ml), in a climatized room at 21°C under constant fluorescent light. Protozoan Pellets and soil provide nutrients for bacteria (*Bacillus cereus*, *B. subtilis* and *Serratia marcescens*), which are consumed by protists. Each LC within a MC initially contained nine protist species (*Blepharisma* sp., *Chilomonas* sp., *Colpidium* sp., *Euglena gracilis*, *Euplotes aediculatus*, *Paramecium aurelia*, *P. bursaria*, *Spirostomum* sp. and *Tetrahymena* sp.) and one rotifer species (*Cephalodella* sp., in the following included when speaking about protist). On day 0, $K_s/10$ individuals of each species were added, except for *Eug. gracilis* ($K_{Eug}/100$ ind.) which naturally occurs at higher densities. Species' specific carrying capacities K_s and intrinsic growth rates r_s were measured in pure cultures (Altermatt et al., 2011a; Carrara et al., 2012).

5.2.3 Patch-size effects

LCs were located in multiwell culture plates containing a solution of sterilized local spring water, 1.6 g l⁻¹ of soil and 0.45 g l⁻¹ of Protozoan Pellets (Carolina Biological Supply). In our species pool, *Blepharisma* sp., *Chilomonas* sp., and *Tetrahymena* sp. were supplied by Carolina Biological Supply Co., while all other species were originally isolated from a natural pond (McGradySteed et al., 1997). All species are bacterivorous whereas *Eug. gracilis*, *Eup. aediculatus* and *P. bursaria* can also photosynthesize. Furthermore, *Blepharisma* sp., *Cephalodella*, *Eup. aediculatus*, *Spirostomum* sp. may not only feed on bacteria but can also predate on smaller flagellates, which are always present and remain unidentified.

Two replicates (72 local communities) were run without emigration events to test species coexistence in isolation and dependence of community composition on patch-size. Patch-sizes were the same as adopted for the first two replicates of the *Riverine* configuration treatment of the main experiment (Figure 5.3).

5.2.4 The dispersal events

After the onset of the experiment, a dispersal event occurred every three days, in total eight times. Each time, half of the individuals of each community emigrated. Emigration happened by transfer of the individuals in the medium in well-mixed conditions, and proportion dispersing was thus density independent. The dispersers were manually transferred from every single LC to the nearest neighbors along the network, with absorbing boundary conditions. Emigration and subsequent immigration happened simultaneously across the landscape in well-mixed conditions. This specific type of density-independent (diffusive) dispersal, chosen to avoid long-tailed dispersal events, imposes equal per capita dispersal rates for all species. By applying eight one-step dispersal events, individuals from any population may disperse at most the average maximum size of the networks. In the dispersal procedure, a bias in directionality was imposed,

Chapter 5. Disentangling habitat patch-size from hierarchical habitat capacity

i.e., the probability for an individual to be dispersed into a downstream direction was double than dispersing into upstream directions. A dispersal-induced mortality was introduced into the system by discarding half of the emigrating individuals (equal to 25% of LC). The landscapes was enforced to maintain the initial spatial volume configuration, by adding fresh medium to LC with a negative balance after the dispersal, or by disregarding immigrating individuals in exceedance (see also Figure 4.3 of chapter 4 for a detailed description of the method). Dispersal was accomplished by manual transfer of medium from every single local community (LC) to its nearest neighbors, with downstream bias in directionality (non-isotropic dispersal). The following dispersal procedure was applied:

- thoroughly mixing the medium in every LC
- selecting 50% of medium from each LC for emigration
- discarding 50% of emigrating medium (25% of the original volume, fixed disturbance rate $d_E = 0.5$)
- transferring the remaining medium to its nearest neighbors along the network on a ‘mirror’ landscape of 36 empty plates. The downstream migration was always twice as great as the upstream migration. Absorbing boundary conditions were chosen, in which dispersal from headwaters/outlet was only two thirds/one third respectively of the medium dispersed by confluences
- collecting and mixing dispersed medium in ‘mirror’ landscapes
- re-transferring to the ‘real’ landscape from the mirror landscapes, eventually disregarding the exceedance medium in order to maintain a constant community volume over time (see Eq. (5.1))
- filling up every LC to its original volume with fresh medium to maintain the distribution of initial volume in each treatment (volume conservation)

In this manner the dispersal happened simultaneously, imposing equal per capita dispersal rates for all different species in well-mixed conditions, and long-tailed dispersal events were avoided.

Given two communities i and j , the probability P_{ij} to disperse from i to j is $P_{ij} = P_{down}$, if $i \rightarrow j$, $P_{ij} = P_{up}/d_{up}(i)$, if $i \leftarrow j$, $P_{ij} = 0$, if $i \leftrightarrow j$, where $d_{up}(i)$ is the number of upstream communities connected to i , $P_{up} = 1/3$, and $P_{down} = 2/3$. The system was enforced to maintain the initial spatial volume configuration, by adding new medium in each location, V_i^{new} , or by disregarding a fraction m_{ji} of immigrating individuals from community j in exceedance, before re-transferring from the mirror to the real landscape (see procedure above). Solving a balance equation for every LC i , imposing the volume $v_i(t+1) = v_i(t)$ after every dispersal events, one can derive the following equation for new medium, V_i^{new} or for mortality, m_{ji} :

$$\Theta(\xi_i)V_i^{new} = \Delta l \sum_j [\Theta(-\xi_i)P_{ji}v_j m_{ji}] - \xi_i, \quad (5.1)$$

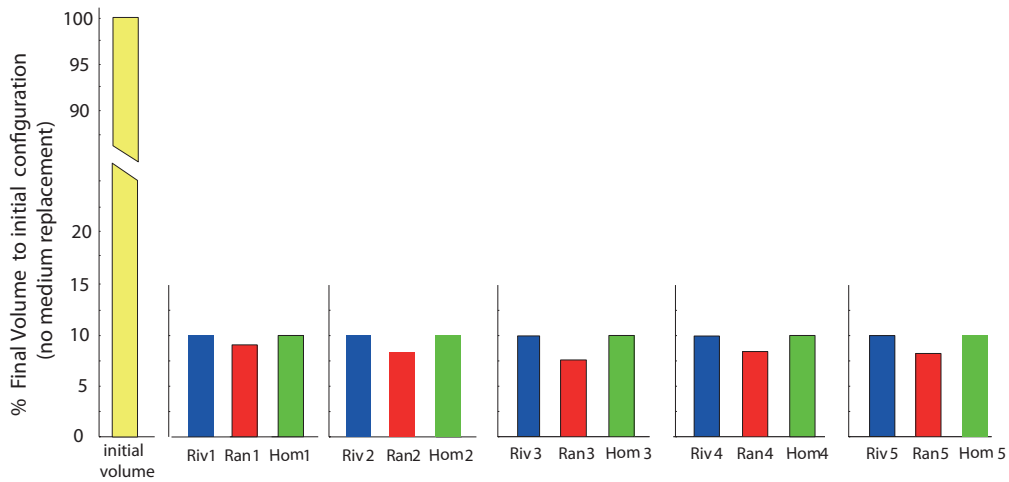


Figure 5.4: Hypothetical final volume of medium (or abundances of individuals in the case of non reacting particles) relative to initial volume conditions (in yellow) after eight dispersal treatments, without replacing medium (i.e., not maintaining volume conservation). Dispersal was simulated as in the experiment, but without replacing medium. The volume/abundances drop to $\sim 10\%$ of the initial volume, due to the migration mortality that was implemented into the dispersal procedure. Differences in final volume/abundances among the three landscapes are within 20% in the five experimental replicates (*Riverine*, *Random* and *Homogeneous*; blue, red and green respectively).

where Θ is the Heaviside step function, $\xi_i = v_i - (1 - d_E) \sum_j P_{ji} v_j$, $d_E = 0.5$ is the fixed disturbance rate, and P_{ji} is given above.

Figure 5.4 shows the final relative concentration of initial medium after the eight dispersal treatments, for a passive diffusion over the network (no reaction at the nodes, abundance dropped to $\sim 10\%$ of the initial abundances). The *Riverine* networks, by definition, are suffering a slightly lower disturbance rate due to emigration mortality, i.e., m_{ji} in Eq. (5.1) are minimized due to the spatial autocorrelation of hierarchical patch-sizes. The highest disturbance rate is found in *Random* networks with a difference of 10-20% between *Riv/Ran*. Such experimental assumptions will be relaxed in next sections, by suitably adjusting the dispersal rates in order to equalized the disturbance rates m_{ji} among the three treatments.

5.2.5 Biodiversity patterns

On day 27, three days after the last dispersal-disturbance treatment, species richness and species abundance were measured (on a logarithmic scale) for each LC. This time interval corresponds to ≈ 10 -100 generations, depending on the species' intrinsic growth rate, and the dynamics occurs over ecologically significant time scales (Carrara et al., 2012). The entire culture-plate was screened under a stereo-microscope (Olympus SZX16) to avoid false-absences of the rarer

Chapter 5. Disentangling habitat patch-size from hierarchical habitat capacity

species. Estimation of species density were obtained by following a standard procedure (Haddad et al., 2008; Altermatt et al., 2011b) by direct microscope observation of 0.5 ml of medium. The number of species present in the MC (γ -diversity) and in every single LC (α -diversity), and the spatial distribution of α -diversity were obtained.

β -diversity patterns

For β -diversity, Jaccard's dissimilarity index, β_J , based on species presence-absence, together with an index based on species abundances, β_A were considered. β_J is defined as $1 - S_{ij}/(S_i + S_j - S_{ij})$, where S_{ij} is the number of species present in both local communities i and j , whereas S_i is the total number of species in LC i . β_A is defined as $\frac{\sum_{k=1}^S w_k |x'_{ik} - x'_{jk}|}{\sum_{k=1}^S w_k} - \beta_J$, where x_{jk} is the abundance of species k in the LC j , $x'_{jk} = \log x_{jk} + 1$, whenever $x_{jk} \neq 0$, w_k is a weight to take into account joint absences, and $S = 10$ is the species pool. β_J only looks at compositional differences in species identities, whereas β_A studies the compositional differences in abundances, and is not bounded between 0 and 1. Their sum gives the modified Gower's index, β_{MG} (Anderson et al., 2006). Thereby, the effects of species richness on β -diversity were distinguished.

5.2.6 Local and regional evenness

Local community evenness (LC-evenness) is described by

$$E_i = 1 - 2/\pi \cdot \arctan \left[\frac{\sum_{s=1}^S (\log x_{is} - \sum_{t=1}^S \log x_{it}/S)^2 / S}{\sum_{s=1}^S \log x_{is}} \right]. \quad (5.2)$$

This defines an index bounded between 0 and 1, independent of species richness (Smith and Wilson, 1996). Regional evenness was calculated from species' populations in the whole network.

5.2.7 Modeling metcommunities in dendritic environments

Biological communities of multiple species living in a patchy environment of varied patch-size and competing for the same resources were simulated. Intrinsic growth rates and carrying capacities were chosen similar to the empirically known species-specific traits, measured in Carrara et al. (2012). A generalization to multiple interacting species of the one-step 'birth and death process' (the stochastic formulation of the logistic process, see chapter 2) has been performed. Each individual of species s has a natural death rate d_s and a probability b_s per unit time to reproduce. To insure that the Markov property holds, d_s and b_s are assumed to be fixed and independent of the age/size of the individual (van Kampen, 2007). Moreover, competition gives rise to an additional death rate $\alpha(\vec{n}(i))/V$, which depends on individuals present in community i .

A pure inter-specific competition-for-space framework is considered to provide a null hypothesis for the effects of dispersal-habitat configuration interaction, not considering competitive hierarchy among species. The competition term reflects the fraction of space occupied by an individual of species s compared to that of individuals of species r , that is, K_s/K_r . A metacommunity is composed of an ensemble \mathcal{N} of $T = 36$ nodes, $\mathcal{N} = (1, 2, \dots, i, \dots, T)$, with the same spatial configuration of patch-sizes as in the experiment (*Riverine, Random, Homogeneous*). The transition probabilities for birth, death and migration of an individual of the r th species within community i (with $\vec{n}(i) = (n_1, n_2, \dots, n_r, \dots, n_I)$ individuals in species pool $\mathcal{P} = (1, 2, \dots, r, \dots, I)$ respectively) read:

$$T(\vec{n}(i) + \vec{e}_{ri} | \vec{n}(i)) = b_r(i)n_r(i) + l_r \sum_{j=1}^T [P_{ji}m_{ji}n_r(j)] \quad (5.3)$$

$$\begin{aligned} T(\vec{n}(i) - \vec{e}_{ri} | \vec{n}(i)) &= [d_r(i) + l_r(i)]n_r(i) + \\ &+ \frac{1}{v_i} [b_r(i) - d_r(i)]n_r(i) \left(\sum_{s \neq r}^I \frac{n_s(i)}{K_s} + \frac{n_r(i) - 1}{K_r} \right), \end{aligned} \quad (5.4)$$

where \vec{e}_{ri} is a unit vector whose only r th component in community i is not zero, and l_r is the dispersal rate of species r , kept constant in the network. The multivariate master equation for the whole metacommunity is given by

$$\begin{aligned} \frac{\partial}{\partial t} p(\vec{n}, t) &= \sum_j \sum_r \{ T(\vec{n}(j) | \vec{n}(j) + \vec{e}_{rj}) p(\vec{n}(j) + \vec{e}_{rj}, t) + \\ &+ T(\vec{n}(j) | \vec{n}(j) - \vec{e}_{rj}) p(\vec{n}(j) - \vec{e}_{rj}, t) - \\ &- [T(\vec{n}(j) + \vec{e}_{rj} | \vec{n}(j)) + T(\vec{n}(j) - \vec{e}_{rj} | \vec{n}(j))] p(\vec{n}(j), t) \}. \end{aligned} \quad (5.5)$$

Numerical simulations employing the Gillespie algorithm (Gillespie, 1977) were performed, which allow, as seen already in previous chapters, to the generation of time series that exactly recover the solution of the multivariate master equation in Eq. (5.5), with transition probabilities in Eqs. (5.2.7). As ‘well-mixed’ conditions for individuals of all species can not be postulated, the nearest neighbor dispersal along the network is also simulated in a stochastic procedure, following the experimental procedure, with discrete temporal steps. At each dispersal time step (every three days), individuals were randomly distributed in 100 cells, then 50 cells were randomly chosen to be dispersed to LCs nearest neighbors (emigration rate). From the emigrating pool, individuals from 25 randomly selected cells were disregarded (emigration mortality):

$$\begin{aligned} \vec{n}(i, t+1) &= (1 - \Delta l_i) \vec{n}(i, t) + F \sum_{j=1}^T (\Delta l_j P_{ji} m_{ji} \vec{n}(j, t)) + \vec{b}(i, \vec{n}(i, t)) \cdot \vec{n}(i, t) - \\ &- \vec{d}(i, \vec{n}(i, t)) \cdot \vec{n}(i, t), \end{aligned} \quad (5.6)$$

where Δl_i is the fraction of individuals to be dispersed at each time step from community i , which depend on the node i , $F = 1 - d_E$ is the survival probability during emigration, and m_{ji} is the mortality rate imposed to keep the volume configuration constant over time, given in Eq. (5.1). ‘Neutral’ and ‘non-neutral’ metacommunities were simulated, composed of 35 species with equal carrying capacity, $K = 350$ individuals ml^{-1} . Species in neutral communities shared the same intrinsic growth rate, $r_s = 1$. Non-neutral metacommunities had species with a variable intrinsic growth rates, in the range from 0.1 to 3.5 day^{-1} , with a 0.1 step. The system was observed over 72 days, a time window that covered three times the experimental duration.

In the model, the disturbance rate among the three different spatial configurations were equalized by varying the dispersal rate (node specific dispersal rate instead of node specific disturbance rate), in order to have the same amount of disturbance at the metacommunity level.

5.2.8 Statistical analysis

In the analysis, degree of connectivity, d , and patch-size, v , were the local network descriptors. d_i is defined as the number of connected neighboring nodes to the LC i , whereas v_i represent its habitat capacity. Distance to the outlet, o , drainage area, A , and the ecological diameter, l , were the regional network descriptors. o_i is calculated as the shortest path connecting i to the outlet community. The specific spatial arrangement of patch-sizes upstream of LC i defines A_i . The average distance of i from all other communities in the river network defines $l_i = \langle d_{ij} \rangle_j$, where d_{ij} represents the shortest topological distance between i and j . Thus l_i is the inverse of the closeness centrality of community i (Newman, 2010), and in riverine landscapes defines network positioning (Figure 5.2, Table 5.1).

An analysis of covariance (ANCOVA) was performed with configuration treatments as categorical fixed effects, OCNs as random effect, and the above described network descriptors (continuous variables) as fixed effects. Normality and constancy of variance in α -diversity and LC-evenness over covariates were verified with Bartlett’s test. A parallel analysis performed with a generalized linear mixed model (GLMM) framework was conducted, giving qualitatively consistent results. However, as model assumptions on error structure were better fulfilled by the ANCOVA compared to a GLMM with Poisson error structure, the analysis was conducted with the former. Models were hierarchically simplified in a stepwise algorithm, starting with the full model and removing non-significant terms, with highest-level interactions first. The overall effect of the configuration treatment on α -diversity and LC-evenness was analyzed. Individual ANCOVAs within each landscape configuration were used to disentangle the effect of individual network properties on biodiversity indicators for each landscape configuration separately. Kolmogorov-Smirnov tests (K-S test) were performed on the cumulative density functions of α -, β -diversity and LC-evenness of the three landscapes configurations.

Mantel tests (999 permutations, Kendall correlation) were performed in order to statistically analyze β -diversity (Anderson et al., 2011). The explanatory variables adopted in our analysis

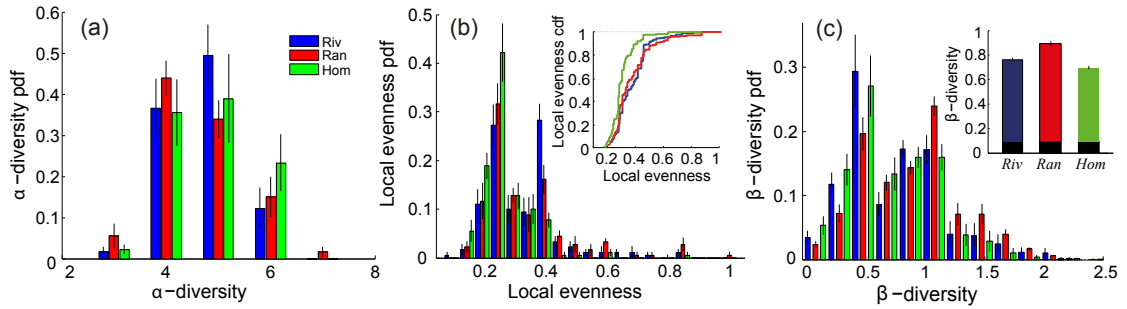


Figure 5.5: Probability density function (*pdf*) for α -diversity (a), local evenness (b), and β -diversity (c) in *Riv* (blue) *Ran* (red), and *Hom* (green) configurations, over the five replicated dendritic landscapes. The insets give the cumulative density function (*cdf*) of local evenness (b), and the mean \pm s.e.m. of β -diversity (c), decomposed in an abundance-based index (β_A , upper colored-coded part), and presence-absence based index (β_J , black, bottom part).

were the topological distance between community pairs (real distance along the network), the environmental distance, calculated as the difference in patch-size between community pairs, and the centrality distance, calculated as the difference between the ecological diameters between community pairs. Differences in environmental conditions and network positioning were captured by taking respectively, for two focal communities i and j , the absolute differences in patch-sizes, $|v_i - v_j|$, and in ecological diameters, $|l_i - l_j|$. The notation in the main text $\langle \cdot \rangle$ means a spatial average over the nodes, while the $\bar{\cdot}$ represents an average over the five landscape replicates.

5.3 Results

The spatial distribution of hierarchical patch-size significantly affected community composition in dendritic environments (for all full ANCOVA-results, see Tables 5.2–5.5, data are deposited in the Dryad Digital Repository: doi:10.5061/dryad.15np2, Carrara et al. (2013b)).

α -diversity and LC-evenness were significantly different across the three landscape configurations, *Riv*, *Ran* and *Hom* (ANCOVA α -diversity, $F_{2,4} = 7.99$, $p = 0.0006$, Figure 5.5a; ANCOVA LC-evenness, $F_{2,4} = 4.65$, $p = 0.01$, Figure 5.5b). Regionally, at the landscape-scale, γ -diversity and mean α -diversity did not vary significantly across the three different landscape configurations ($\bar{\gamma}_{riv} = 5.8$, $\bar{\gamma}_{ran} = 6.2$, $\bar{\gamma}_{hom} = 6$, $\langle \bar{\alpha} \rangle_{riv} = 4.72$, $\langle \bar{\alpha} \rangle_{ran} = 4.63$, $\langle \bar{\alpha} \rangle_{hom} = 4.83$, p -values of all pairwise K-S tests on different configuration treatments were $p > 0.1$). LC-evenness was higher for the configuration treatments in which spatial heterogeneity was introduced by varying patch-sizes, i.e., *Riv* (K-S test, $p < 10^{-5}$, $K = 0.33$) and *Ran* landscapes (K-S test, $p < 10^{-5}$, $K = 0.26$) compared to *Hom* landscapes (inset Figure 5.5b). No significant difference was instead detected between *Riv* and *Ran* landscapes (K-S test, $p = 0.45$, $K = 0.09$). β -diversity (Modified Gower's β_{MG} -index) was higher in the two heterogeneous landscape configurations (*Riv*, *Ran*)

Chapter 5. Disentangling habitat patch-size from hierarchical habitat capacity

Table 5.2: Effects of network descriptors on α -diversity.

Variable	<i>d.f.</i>	<i>F</i>	<i>P</i>
<i>R</i>	1	0.11	0.977
<i>N</i>	2	7.99	< 0.001
<i>d</i>	1	77.50	< 0.001
<i>v</i>	1	15.80	0.001
<i>o</i>	1	4.92	0.088
<i>d * o</i>	1	12.05	< 0.001
<i>N * d</i>	2	6.30	0.002
<i>N * o</i>	2	8.03	< 0.001
<i>R * N</i>	2	6.89	< 0.001
<i>R * d</i>	1	1.40	0.232
<i>R * v</i>	1	3.23	0.012
<i>R * o</i>	1	1.69	0.151
Error	523		

Replicated landscapes (*R*, reflecting independent network configurations) were specified as random effects, whereas network configurations (*N*) as categorical fixed effects. The analysis was made taking into account the network descriptors in table 5.1 (introduced in *Material and Methods*). Variables *l* (ecological diameter), and *A* (drainage area) were eliminated from the model because of non-significant effects on α -diversity.

Table 5.3: Effects of network descriptors on local community-evenness.

Variable	<i>d.f.</i>	<i>F</i>	<i>P</i>
<i>R</i>	1	1.00	0.405
<i>N</i>	2	4.77	0.009
<i>v</i>	1	3.62	0.071
<i>A</i>	1	11.49	0.005
<i>l</i>	1	0.10	0.769
<i>N * l</i>	2	4.14	0.016
<i>R * N</i>	2	3.20	0.002
<i>R * v</i>	1	0.24	0.917
<i>R * A</i>	1	0.19	0.946
<i>R * l</i>	1	1.12	0.347
Error	526		

The analysis was made taking into account the network descriptors in table 5.1 (introduced in *Material and Methods*), replicates (*R*) and network configurations (*N*) factors. The model was simplified in a stepwise procedure (Crawley 2007).

Table 5.4: α -diversity patterns.

Landscape	Variable	<i>d.f.</i>	<i>F</i>	<i>P</i>
<i>Riverine</i>	<i>R</i>	1	1.53	0.196
	<i>d</i>	1	44.26	0.002
	<i>v</i>	1	0.42	0.55
	<i>o</i>	1	8.75	0.041
	<i>R * d</i>	1	0.54	0.706
	<i>R * v</i>	1	1.12	0.347
	<i>R * o</i>	1	3.09	0.017
	Error	172		
<i>Random</i>	<i>R</i>	1	0.99	0.417
	<i>d</i>	1	32.56	< 0.001
	<i>v</i>	1	17.78	< 0.001
	<i>o</i>	1	0.49	0.518
	<i>d * v</i>	1	5.86	0.016
	<i>R * d</i>	1	1.05	0.381
	<i>R * v</i>	1	0.85	0.496
	<i>R * o</i>	1	1.44	0.222
Error	171			
<i>Homogeneous</i>	<i>R</i>	1	0.55	0.156
	<i>d</i>	1	30.59	0.005
	<i>o</i>	1	12.61	0.021
	<i>R * d</i>	1	3.38	0.011
	<i>R * o</i>	1	0.57	0.681
	Error	174		

Three separate ANCOVA analyses were performed for each landscape configuration. Landscape replicates (*R*) were specified as random effects, whereas network configurations (*N*) as categorical fixed factors.

Chapter 5. Disentangling habitat patch-size from hierarchical habitat capacity

Table 5.5: Local community-evenness patterns.

Landscape	Variable	<i>d.f.</i>	<i>F</i>	<i>P</i>
<i>Riverine</i>	<i>R</i>	1	1.12	0.349
	<i>v</i>	1	10.08	0.004
	<i>o</i>	1	0.37	0.55
	<i>v * o</i>	1	5.22	0.024
	<i>R * v</i>	1	1.23	0.298
	<i>R * o</i>	1	0.92	0.453
	Error	173		
	<i>Random</i>	<i>R</i>	1	1.52
<i>v</i>		1	2.87	0.152
<i>o</i>		1	2.96	0.135
<i>l</i>		1	3.16	0.138
<i>R * v</i>		1	0.21	0.932
<i>R * o</i>		1	1.92	0.110
<i>R * l</i>		1	2.24	0.068
Error		172		
<i>Homogeneous</i>	<i>R</i>	1	2.11	0.081
	<i>d</i>	1	0.001	0.964
	<i>o</i>	1	1.80	0.224
	<i>l</i>	1	0.89	0.385
	<i>A</i>	1	0.74	0.433
	<i>R * d</i>	1	0.89	0.469
	<i>R * o</i>	1	1.42	0.231
	<i>R * l</i>	1	1.41	0.232
<i>R * A</i>	1	0.56	0.691	
Error	170			

Three separate ANCOVA analyses were performed for each landscape configuration. Landscape replicates (*R*) were specified as random factors, whereas network configurations (*N*) as categorical fixed factors.

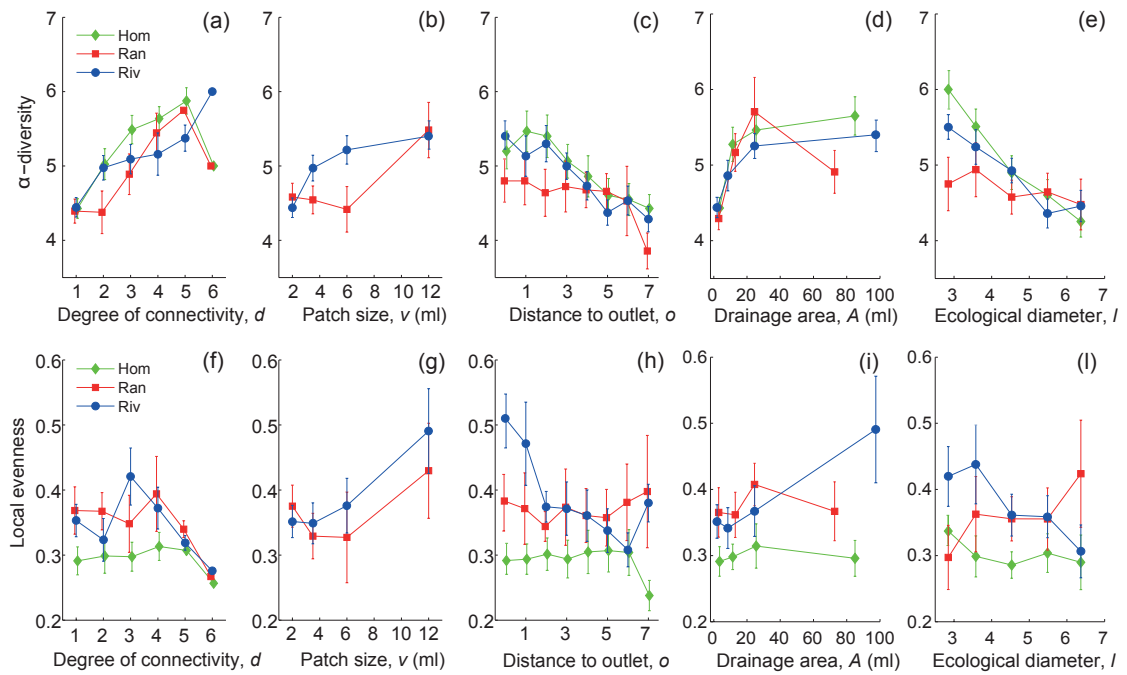


Figure 5.6: α -diversity (upper panels) and local evenness (lower panels) in dendritic landscapes for the three different configuration treatments (*Riv* landscapes in blue, *Ran* landscapes in red, and *Hom* landscapes in green), depending on local (connectivity, patch-size) and regional network descriptors (distance to outlet, drainage area, ecological diameter). (a, f) α -diversity and local evenness as a function of degree of connectivity, (b, g) as a function of the patch-size, (c, h) as a function of distance to the outlet, (d, i) as a function of drainage area, (e, l) as a function of ecological diameter. Symbols represent the mean \pm s.e.m. of the experimental data over the five experimental replicates.

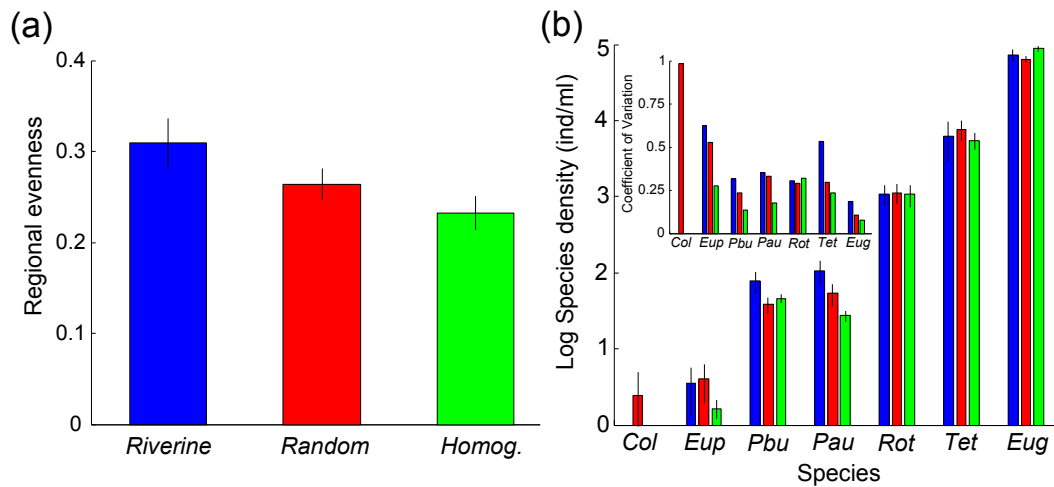


Figure 5.7: Community composition at metacommunity scale in *Riv* (blue) *Ran* (red), and *Hom* (green) configurations. (a) Regional evenness was significantly higher in *Riv* landscapes compared to *Ran* and *Hom* landscapes (average \pm s.e.m. over the five experimental replicates). (b) Species' density of the seven species detected at the end of the experiment for the three landscape configurations, sorted in increasing order of abundances (log scale). Values represent the mean \pm s.e.m. across the five replicated landscapes. Inset: coefficient of variation for the same species over the five replicates (*Col* is *Colpidium* sp., *Eup* is *Euplotes aediculatus*, *Pau* is *Paramecium aurelia*, *Pbu* is *Paramecium bursaria*, *Cep* is *Cephalodella* sp., *Tet* is *Tetrahymena* sp., and *Eug* is *Euglena gracilis*).

compared to the *Hom* landscapes (K-S tests, both $p < 10^{-5}$, Figure 5.5c). *Ran* landscapes showed the highest values of β_{MG} (K-S test, $p < 10^{-5}$, $K = 0.16$), but considering only β_J , no significant differences between the three configurations were found (inset Figure 5.5c).

In the *Isolation* treatment, species richness increased with increasing patch-size. Larger protist species (especially *P. aurelia* but also *P. bursaria*) preferentially occupied patches with larger sizes. α -diversity was significantly affected by the degree of connectivity ($F_{1,4} = 77.5$, $p < 10^{-5}$, Figure 5.6a) and by patch-size ($F_{1,4} = 15.8$, $p = 0.001$, Figure 5.6b). A significant interaction was observed between connectivity and patch-size on α -diversity ($F_{1,4} = 12.05$, $p = 0.0006$), whereas distance to the outlet, ecological diameter and drainage area had no overall significant effect on α -diversity. LC-evenness was significantly affected by drainage area only ($F_{1,4} = 11.49$, $p = 0.005$, Figure 5.6i).

5.3.1 α -diversity patterns

Because of the significant interaction between configuration treatment (i.e., *Riv*, *Ran* and *Hom*) and individual network descriptors (Tables 5.2, 5.3), three separate *ANCOVA* analyses were needed to address within-landscape relationships (one for each landscape configuration, Table 5.4). In the following, the three analyses (*Riv*, *Ran* and *Hom*) are compared separately for each network descriptor. α -diversity significantly increased with increasing degree of connectivity ($p_{riv} = 0.002$; $p_{ran} < 10^{-5}$; $p_{hom} = 0.005$), although with different slopes ($\bar{m}_{riv} = 0.26$; $\bar{m}_{ran} = 0.28$; $\bar{m}_{hom} = 0.40$, Figure 5.6a). Patch-size significantly determined α -diversity in *Ran* landscapes ($p_{ran} = 0.0002$, Figure 5.6b), where it also interacted with connectivity ($p_{ran} = 0.016$). Distance to the outlet significantly affected α -diversity in *Riv* and *Hom* landscapes ($p_{riv} = 0.041$; $p_{hom} = 0.021$), where α -diversity decreased with increasing distance to the outlet ($\bar{m}_{riv} = -0.22$, $\bar{m}_{hom} = -0.18$, Figure 5.6c). No dependence of α -diversity on distance to the outlet was observed in the *Ran* landscapes ($\bar{m}_{ran} = -0.022$, Figure 5.6c). Drainage area A and ecological diameter l (Figure 5.2), two regional network descriptors (*Material and Methods*), did not significantly affect α -diversity (Figure 5.7d, e).

5.3.2 Evenness patterns

In *Riv* landscapes, LC-evenness depended significantly on patch-size ($p_{riv} = 0.004$, Figure 5.6g). There was also a significant interaction of patch-size and distance to the outlet in determining local evenness ($p_{riv} = 0.02$, Table 5.5). Instead, LC-evenness in *Ran* and *Hom* landscapes did not show any significant dependence on any of the network descriptors (Figure 5.6f–i, Table 5.5). Importantly, the dependence of LC-evenness on patch-size in *Riv* landscapes at the local scale contributed to shape a significantly higher evenness values at the regional scale, compared to *Ran* (paired t -test, $t_4 = 2.95$, $p = 0.041$, Figure 5.7a) or *Hom* landscapes (paired t -test, $t_4 = 3.36$, $p = 0.028$, Figure 5.7a). A higher variability in terms of coefficient of variation was detected in *Riv* landscapes across the five replicates (inset in Figure 5.7b). In *Riv* landscapes species which presented low numbers of individuals in pure cultures, with higher body sizes and lower intrinsic growth rates persisted at higher densities (Figures 5.7b, 5.8).

5.3.3 β -diversity patterns

In *Riv* landscapes, β_{MG} increased with increasing pairwise topological distance between community pairs. No such pattern was found in the two other landscapes, and β -diversity showed a flat behavior (5.9a).

Differences in community composition did not significantly depend on topological distance: Mantel tests revealed that there was no spatial dependence of β -diversity in any of the three configurations (Figures 5.9a, 5.10a, and Table 5.6). Changes in patch-size, instead, significantly affected β -diversity in *Riv* and *Ran* landscapes (Figures 5.9b, 5.10b, and Table 5.6). Changes in ecological diameter, capturing the difference in network positioning (Figure 5.2), had a significant

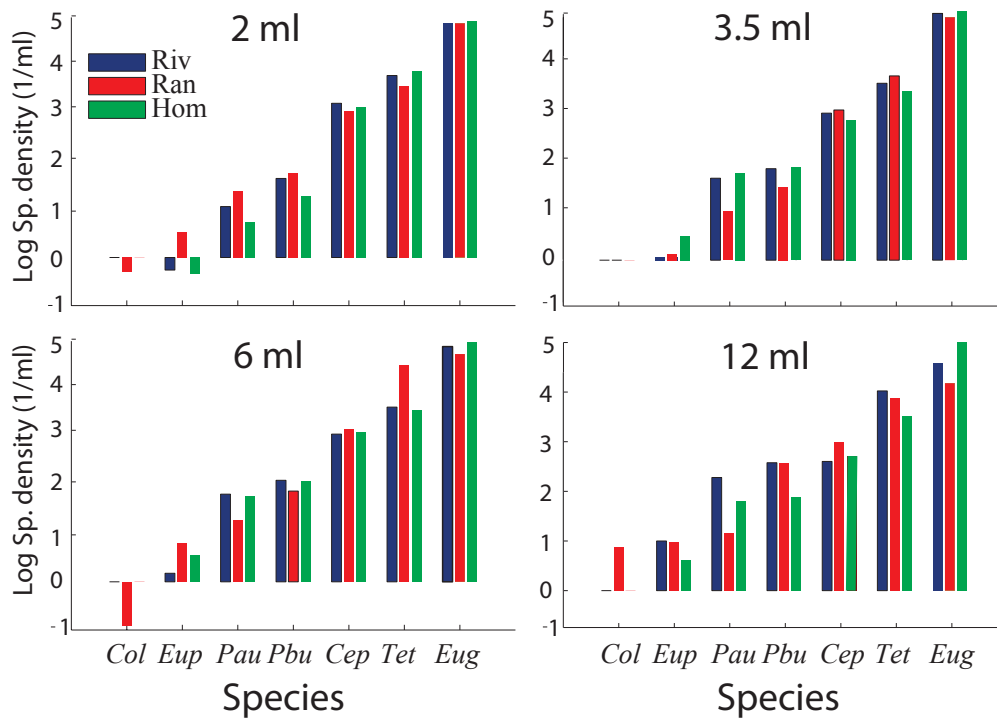


Figure 5.8: Species' density, sorted in increasing order of abundances (log scale) for the seven species detected at the final stage of the experiment for the three patch-size configurations (*Riverine* in blue, *Random* in red, and *Homogeneous* in green), averaged over similar community patch-sizes and over the five replicates. *Col* is *Colpidium* sp., whereas the other names correspond to species as in Figure 5.7. *Homogeneous* communities were considered in the comparison by averaging over the same nodes as in *Riverine* landscapes. Only in *Random* landscapes *Colpidium* sp., a weak competitor but a fast grower, was observed.

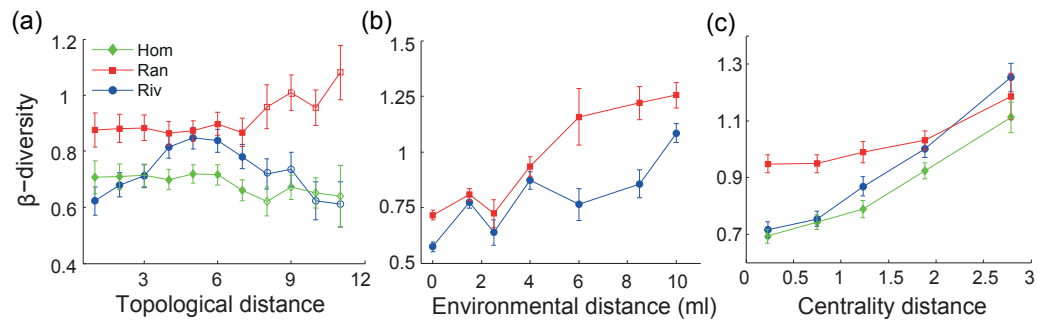


Figure 5.9: β -diversity as a function of the topological (a), environmental (b), and centrality distance (c) between local community pairs, in *Riv*, *Ran*, and *Hom* configurations of patch-size. Symbols represent the mean \pm s.e.m. of the β_{MG} -diversity data over the five experimental replicates. Open symbols in panel (a) indicate the points where the statistical significance is lower (topological distance ≥ 8 , Figure 5.10).

effect on β -diversity only in *Riv* and *Hom* landscapes (Figures 5.9c, 5.10c, Table 5.6, $\bar{m}_{riv} = 0.74$, $\bar{m}_{ran} = 0.16$, $\bar{m}_{hom} = 0.59$).

5.4 Discussion

The aquatic microcosm experiment disentangled the interaction between dendritic connectivity and hierarchical patch-size on biodiversity of communities and showed that biodiversity patterns in river-like metacommunities significantly depend on the spatial covariance between dendritic connectivity, patch-size and position along the network.

5.4.1 α -diversity patterns

Highly connected nodes, irrespective of the local environmental factors such as patch-size, disturbances and interspecific competition among species, sustained higher levels of local species richness compared to more peripheral communities (Finn et al., 2011; Carrara et al., 2012; Perkin and Gido, 2012). Such a correlation is predicted by network theory (Newman, 2010), where individuals on a random walk will be found in community i proportionally to the degree of connectivity of i on a connected network. In all three landscape configurations (Figure 5.1), α -diversity increased with increasing connectivity. Similar results are obtained from a neutral model employed in spatially explicit networks (Economio and Keitt, 2010). Neutral models focus on the spatial structure and dispersal limitation constrained by the specific landscape connectivity (Economio and Keitt, 2008; Muneeppeerakul et al., 2008a; Economio and Keitt, 2010) suggesting that dispersal in our experiment was a driving factor of α -diversity.

Table 5.6: Mantel tests on β -diversity.

Landscape	Replicate	Topology	Environment	Centrality
		r	r	r
<i>Riverine</i>	1	0.028	0.22**	0.21**
	2	0.002	0.2**	0.38**
	3	0.12**	0.09	0.14**
	4	-0.005	0.32**	0.1*
	5	-0.03	0.32**	0.29**
<i>Random</i>	1	0.13**	0.18*	0.034
	2	-0.002	0.13	0.034
	3	0.05	0.19**	0.082
	4	0.04	0.37**	0.034
	5	-0.05	0.17*	0.11*
<i>Homogeneous</i>	1	0.026	—	0.09*
	2	-0.09	—	0.11**
	3	0.023	—	0.1**
	4	-0.11	—	0.21**
	5	-0.05	—	0.33**

Environmental distance is always zero by definition in *Homogeneous* landscapes (fixed patch-size).

* $p < 0.05$.
 ** $p < 0.01$.

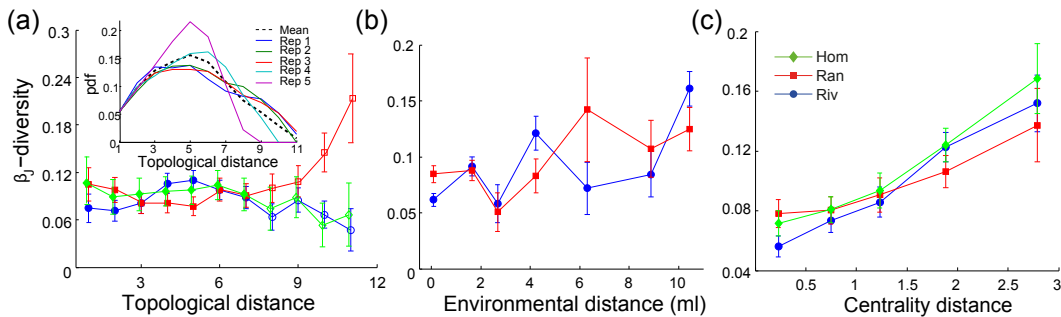


Figure 5.10: β_J -diversity as a function of the topological (a, environmental (b) and centrality (c) distance between local community pairs, in *Riverine* (blue) *Random* (red), and *Homogeneous* (green) configurations of patch-size. Symbols represent the mean \pm s.e.m. of the β_J -diversity data over the five experimental replicates. Inset in panel (a) shows the probability density function (*pdf*) of topological distance for the five different river-network replicates adopted in the experiment. Open symbols in panel (a) and in Figure 5.9a represent community pairs where topological distance is ≥ 8 . At these distances, pdf starts to decline and statistical power too.

In *Riv* landscapes a consistent increase in α -diversity was observed for larger patch-sizes. Overall, in hierarchical *Riv* environments patch-size is not significant because of the spatial covariance between patch-size with the other network descriptors (Table 5.1), which better describe the variation in local species richness. Only in *Ran* landscapes patch-size, controlling formation and composition of micro-habitats (Figure 5.3), significantly affected α -diversities. Our results show that species richness in dendritic landscapes with spatially uncorrelated patch-size was determined largely by local drivers (i.e., degree of connectivity and patch-size). The significant interaction between degree of connectivity and patch-size in *Ran* landscapes (Table 5.4) is suggesting that in intermediate-patches (patch-size 3.5 and 6 *ml*), or in linear branches (connectivity $d = 2$), the detrimental effects of disturbances (i.e., mortality due to emigration) on local species richness are enhanced (Figure 5.6a, b). In *Ran* landscapes, the largest patches sustained higher abundances and thereby maintained a high α -diversity irrespective of position (Figure 5.6b), as found in aquatic bacterial communities in mountain lakes (Reche et al., 2005). Previous protist studies identified species' specific responses to disturbances (Haddad et al., 2008; Carrara et al., 2012), and found that a high intrinsic growth rate is the most important factor in promoting a species' ability to survive a disturbance (Haddad et al., 2008). Such model systems cover substantial biological complexity in terms of species interactions and trophic levels that cannot be entirely captured by any model. Species with low reproductive number are prone to suffer more from environmental disturbances and require larger and well-connected habitats to persist (Staddon et al., 2010; Perkin and Gido, 2012). In our experiment *Eup. aediculatus*, *P. aurelia*, and *P. bursaria* have lower intrinsic growth rates and lower carrying capacities in pure cultures (Altermatt et al., 2011a; Carrara et al., 2012). Because absolute numbers of individuals are lower for these species, demographic stochasticity plays an important role in affecting populations dynamics. In *Ran* landscapes the negative effect of disturbances related to emigration on the survival of species with low reproductive rates was aggravated by the alteration of the natural hierarchical patch-size configuration.

Regional network descriptors, i.e., drainage area and ecological diameter (Figure 5.2), provide a synthesis of the above dynamics (Figure 5.6d, e). In *Riv* and *Hom* landscapes α -diversity increased with increasing contributing drainage area. In *Ran* landscapes, a local peak at intermediate values of total contributing area was instead observed, with a decline in α -diversity for the largest values (Figure 5.6d). A likely explanation for this pattern is that in *Ran* metacommunities high-capacity patches are displaced also in peripheral zones of the network (Figure 5.1b), thereby acting as local sources of immigrants for the neighboring communities in the sub-basin. Through mass effects, the displaced high-capacity patches maintained species populations in the less favorable small or peripheral habitats (Figure 5.6b). In general, such mechanism of population survival is important in determining metapopulation dynamics. For example, in a plant pollinator system exposed to habitat fragmentation, it was found that high-quality patches with large size were essential for bees' persistence (Franzen and Nilsson, 2010). It is a characteristic of natural riverine landscapes that high-capacity communities are placed at network position that have a high closeness centrality (Fernandes et al. (2004), Figure 5.2 and Table 5.1). These populations are thus strongly affecting the overall MC dynamics (Muneepeerakul et al., 2007)

(Figure 5.6e). It has been demonstrated how breaking the natural link between patch-size and connectivity at local scales destroys the regional pattern in species richness observed in *Riv* and *Hom* landscapes. In *Ran* configuration, local species richness did not increase while approaching the outlet community (Figure 5.6c), despite the converging character of the network structure and downstream-biased dispersal (Muneepeerakul et al., 2008a). This suggests that in rivers the positioning of high-capacity patches has a higher significance for biodiversity (Lowe et al., 2006; Grant et al., 2007) than in other types of landscapes, such as ponds, islands or lakes (De Bie et al., 2012). Even though habitat capacity and interannual streamflow variability, which are altered in rivers undergoing hydropower development (Poff et al., 2007; Grant et al., 2012; Ziv et al., 2012), may not exactly correspond to our *Ran* landscapes, proof of principles has been provided for how altering the hierarchical patch-size configuration in dendritic systems may impact on important biodiversity patterns of aquatic microbial communities.

5.4.2 Community composition

Locally (i.e., at the patch-scale), variation in patch-size configuration in dendritic networks altered community composition. Theory suggests that species that are better competitors in a particular environmental condition eventually spread along the system, impeding other species' growth, and thus exposing them to higher extinction levels (Hillebrand et al., 2008; Cardinale, 2011). Accordingly, in our experiment a predominance of *Eug. gracilis* (best competitor of our species pool, see chapters 2 and 3) was observed in *Hom* landscapes, whereas populations of larger species (*Eup. aediculatus*, *P. aurelia* and *P. bursaria*) were reduced compared to heterogeneous configurations (Figure 5.7b). Habitat heterogeneity in *Riv* and *Ran* landscapes promoted both local species evenness (Figure 5.5b) and persistence of β -diversity (Figure 5.5c), compared to *Hom* landscapes. This gives a causal, experimental proof of principles on how homogenization of habitat size along river networks can affect diversity (Lowe et al., 2006).

At regional spatial scales, the consequences of the spatial configuration of patch-sizes on community composition in terms of degree of dominance and species turnover were subtle. Only in *Riv* landscapes, LC-evenness increased consistently with increasing patch-size and decreasing distance to the outlet (Figure 5.6g, h). This highlights the structuring power of hierarchy (Figure 5.6i, l). Spatial environmental autocorrelation resulted in higher levels of regional evenness in *Riv* ecosystems (Figure 5.7a), by increasing the population size of some of the rarer species and at the same time decreasing the total biomass of the more abundant species (Figure 5.7b). Possibly, rare species with lower growth rates were able to track their specific niche requirements more efficiently in *Riv* landscapes (Cardinale, 2011). Thereby, the rarest species grew to higher population densities in *Riv* landscapes compared to the *Ran* landscapes where the spatial autocorrelation was disentangled.

In parallel to the experiment, a suite of metacommunity models have been developed, thus complementing and extending the experimental findings. This included a purely diffusive model, maintaining the dispersal characteristics and network structures as in the experiment.

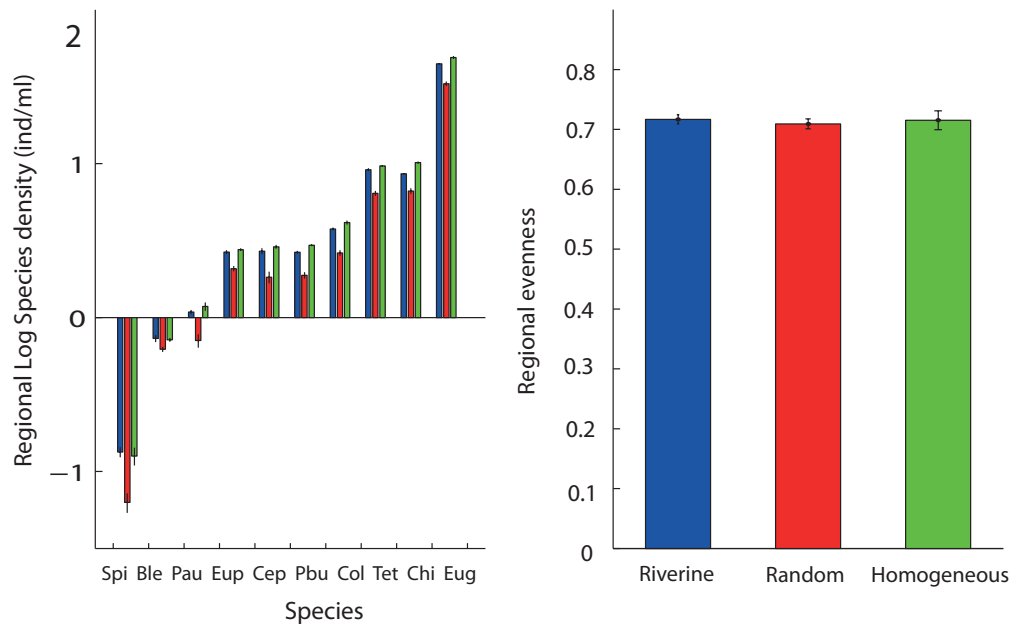


Figure 5.11: Results from stochastic metacommunity simulations adopting no-growth particles. Species abundance (left) and community evenness (right) were simulated using non-reactive, diffusive dispersal along the network structure only. In the initial set-up of the model, species started with identical abundance as in the experiment (reflecting species-specific carrying capacities), and dispersal-disturbance rates were identical as in the experiment and across the three treatments (*Riverine*, *Random* and *Homogeneous*; blue, red and green respectively).

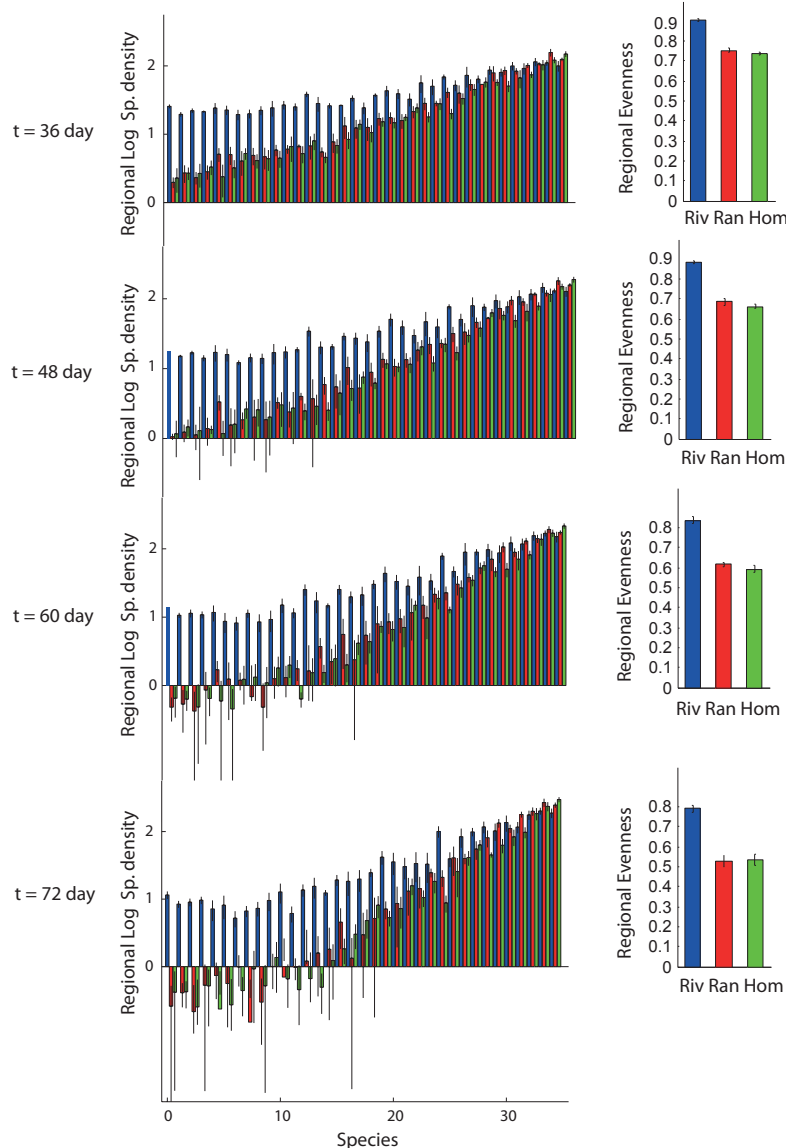


Figure 5.12: Results from stochastic metacommunity simulations: species abundances (left panels) and regional evenness (right panels), averaged over the metacommunity, and over the five different realization of the five river networks adopted in the main experiment (*Riverine*, *Random*, *Homogeneous*, blue, red and green respectively). Non-neutral communities consisted of 35 species with varying growth rates over the range (from 0.1 to 3.5 day⁻¹, and same carrying capacities $K = 350$ ind ml⁻¹). Species are ordered from left to right with increasing growth rate, which is reflecting directly in biomass production, as the interaction is only for space. Initial conditions were the same across the three landscapes, with each species starting with the same number of individuals. The *Riverine* landscapes maintain higher abundances of the rarer species over time, compared to *Random* and *Homogeneous* landscapes. The more common species on the right part of the graph, with higher intrinsic growth rate, were instead equally abundant in the three landscapes. This results into a higher regional evenness, reflecting the results found in the main experiment, where some of the rarer species had higher abundances in *Riverine* landscapes (Figure 5.7).

A non-reactive particle dispersion model (refer to Section 5.2.7 in *Materials and Methods*) showed that disturbance affected the abundance of species, but the relative frequency across treatments was the same for all species. Thus, the suggested higher loss in random is indeed observable (and to be expected) in the particle model, but very different from our experimental work (Figure 5.7 and Figure 5.12). There is no effect on the regional community composition across the three treatments when there are only conservative, non-interacting particles considered (Figure 5.12b). Thus, the observed effects of the interaction between network structure and patch-size position is indeed non-trivial and not just to be expected from a diffusion-only model. Specifically, the key results on the rarer vs. more common species, and different ‘niche use’ of species in these three landscape treatments can not be driven or explained by a conservative particle model. An overall disturbance rates of 25% (our disturbance rate) in the disturbance rates does not affect such communities, as already experimentally shown by previous studies (Altermatt et al., 2011a). In fact, the recovery from disturbances is much faster than the time between disturbances. Only at very high disturbance rates (90 – 98%) the differences in disturbance rates become effective (Altermatt et al., 2011b). Thus, as our disturbances were well below that threshold, the disturbance difference could not explain the observed patterns, and species-interactions over the intra-disturbance time-periods in differently-sized patches were driving the observed dynamics.

Regional evenness was not impacted in neutral metacommunities by the spatial configuration of community sizes. In non-neutral metacommunities, regional evenness was indeed higher in *Riv* landscapes with hierarchical patch-size distribution (Figure 5.12), and the effect was consistent over time (Figure 5.13). In *Riv* landscapes, species with lower intrinsic growth rate occurred at higher abundances compared to *Ran* and *Hom* landscapes, with a similar trend to that highlighted in the main experiment, where much more biological complexity is captured (Figure 5.7). Species with a low intrinsic growth rate, which are suffering most by the disturbances due to emigration mortality, are possibly tracking more efficiently the environmental variation in autocorrelated *Riv* environments, compared to landscapes where the environmental variation in patch-size was disentangled (*Ran*) or kept equal across the landscape (*Hom*).

The experimental and theoretical analyses presented in this chapter suggest that alterations of river-like landscapes may have strong effects on MC dynamics, and impact important regional diversity and evenness properties (Hillebrand et al., 2008).

5.4.3 β -diversity patterns

The modified Gower’s β_{MG} was mostly driven by its abundance component β_A (inset of Figure 5.5c), indicating that empirical and theoretical studies in community ecology and conservation biology have to consider species abundances. β -diversity increased in *Riv* landscapes with increasing topological distance along the network (Figure 5.9a). Such a pattern is commonly observed in comparative studies on riverine diversity (Muneepeerakul et al., 2008a; Brown and Swan, 2010). No spatial correlation of LC similarity was found in *Ran* and *Hom* landscapes (Figure 5.9a), suggesting that a combination of patch-size and network position is needed to reproduce this pattern.

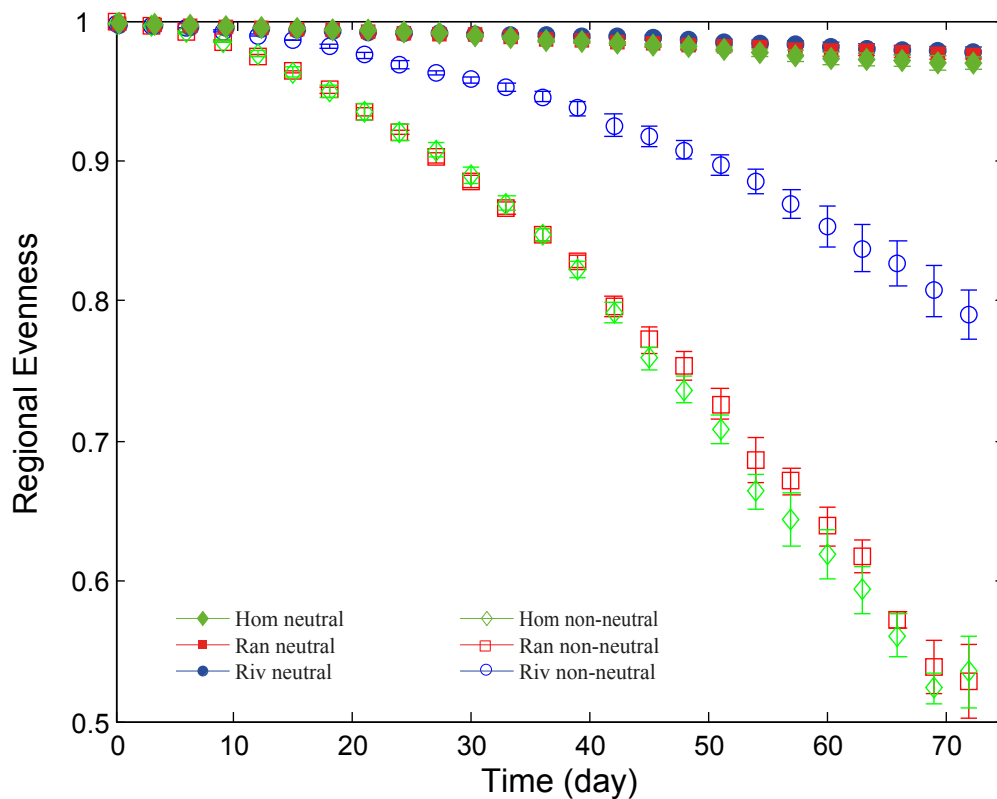


Figure 5.13: Stochastic metacommunity simulations with neutral and non-neutral dynamic: regional evenness as a function of time, for the three spatial configurations adopted in the main experiment (*Riverine*, *Random*, *Homogeneous*, blue, red and green respectively). Filled symbols show regional evenness for metacommunities with 35 neutral species (same intrinsic growth rate, $r = 1$, and same carrying capacities, $K = 350 \text{ ind ml}^{-1}$). Open symbols represent regional evenness for non-neutral metacommunities of 35 species with varying growth rates over the range from 0.1 to 3.5 day^{-1} , and same carrying capacities $K = 350 \text{ ind ml}^{-1}$. The neutral metacommunities maintain the same regional evenness (as diffusive particles, without reaction at the nodes, Figure 5.11). Interestingly, the non-neutral metacommunities show differentiations between the configuration treatments, with *Riverine* having higher evenness compared to *Random* and *Homogeneous* landscapes, an effect that was found also in the experiment. The decline in regional evenness reflects the increasing abundance imbalance of rare versus common species over time (Figure 5.12).

The flat behaviour of β -diversity against topological distance reflected the prominent role of local environmental conditions in structuring communities through species sorting and competition. Dispersal limitation alone cannot reproduce such an effect on community differentiation (Brown and Swan, 2010; Astorga et al., 2012). Priority effects, reflecting colonization history, did not play an important role in community assembly as species were present everywhere at the start of the experiment. Randomizing patch-size, i.e., altering the hierarchical riverine structure, is an analog of fragmenting the landscapes (see effects on α -diversity, Figure 5.6a, b, d). At the same time it is opening up more diversified spatiotemporal niches (Chesson, 2000b), and producing more distinct species compositions. Interestingly, β -diversity depended on centrality in the *Hom* landscapes with fixed habitat-capacity. This strongly indicates that dendritic connectivity *per se* shapes both α and β -diversity (Carrara et al., 2012), as already found in chapter 4 with constant patch-size. Community-composition turnover along centrality gradient was maximized for *Riv* landscapes, and hierarchical patch-size distribution enhanced the turnover provided by dendritic connectivity itself (Figure 5.9c, Table 5.6).

5.4.4 Broader implications for aquatic organisms in streams

The work presented in chapter 4, which was done with a similar model system, focused only on effect of connectivity (Carrara et al., 2012). The present study implemented a more realistic realization of natural rivers with varied patch-size and biased dispersal kernel (Fagan, 2002; Grant et al., 2007; Muneeppeerakul et al., 2007). For the first time, the effects of the intrinsic link of network position and habitat patch-size on diversity and community evenness and of the alteration of riverine structure were singled out. By looking at the effects on common vs. rare species, the interaction between species traits and population responses to spatiotemporal gradients of local environmental conditions in spatially structured habitats has also been highlighted. For example, fast population growth, allowing rapid population responses to a more unpredictable environment, might favour species with higher intrinsic growth rates and vice versa. Our protist species are naturally co-occurring in freshwater habitats and cover a wide range of intrinsic growth rates, body sizes, and other important biological traits, such as dispersal ability (Altermatt et al., 2011a; Carrara et al., 2012). Such experiments, as in similar model systems (Cadotte, 2006a; Haddad et al., 2008; Livingston et al., 2012), are conceptualized versions of natural ecosystems and do not allow direct extrapolation of our results to natural rivers. However, they enhance our understanding of complex systems in nature, where multiple processes are interacting on different scales (Holyoak and Lawler, 2005). Dispersal rate, dispersal mode and the strength of directionality are important factors in determining community patterns in theoretical models (Mouquet and Loreau, 2003; Morrissey and de Kerckhove, 2009) and natural communities (Clarke et al., 2008). In analogy to our experiments, recent comparative studies (Brown and Swan, 2010; Astorga et al., 2012; De Bie et al., 2012; Heino, 2013) showed that different dispersal abilities, controlled by body size and dispersal mode, determine a change in the response of community similarity to environmental variation and geographic distance. This suggests that the relative importance of the two structuring forces may depend on the group of organisms and the spatial scale. In riverine ecosystems the river network itself provides at the same time the

primary habitat for the species and suitable ecological corridors for individuals to disperse (Fagan, 2002; Grant et al., 2007; Rodriguez-Iturbe et al., 2009), resulting in a close match between the physical and the ecological scales (Grant et al., 2007). This correspondence is recognized as important for the ecosystems' resilience at different levels of ecological complexity (Gonzalez et al., 2011). For a variety of species living in natural riverine systems, out-of-network movements are likely to occur, leading to inter-catchment dispersal (Clarke et al., 2008; Brown and Swan, 2010). In macroinvertebrates, active dispersers with a terrestrial stage should track environmental heterogeneity better than passive dispersers with only an aquatic stage (Heino, 2013). Moreover, the strength of directionality in river systems might be much stronger for passive dispersers, as bacteria and protists, compared to macroinvertebrates, amphibians, or fishes (Astorga et al., 2012; De Bie et al., 2012). For example, a neutral metacommunity model showed that a symmetric dispersal kernel suitably described fishes' biodiversity patterns in Missisipi-Missouri river system (Muneepeerakul et al., 2008a). Thus, when comparing or extrapolating our results to natural systems, one needs to carefully examine whether taxon specific aspects of dispersal have to taken into account. Patterns and processes may not scale directly across all species and landscapes sizes. In our experiment, adopting a diffusive downstream-biased dispersal between isolated habitat patches and at discrete-time intervals (*Material and Methods*), different dispersal strategies could not naturally arise. Competition-colonization trade-offs were documented in protist studies which were adopting similar species (Cadotte, 2006a), but see (Haddad et al., 2008). Such mechanism of species coexistence, together with the storage effect (Chesson, 2000b), may interact with the spatial structure to shape diversity and ecosystem productivity, as tested in bacterial metacommunities (Livingston et al., 2012). As the system was continuously perturbed away from stationarity by dispersal and emigration mortality, community dynamics was likely in a transient state (Hastings and Higgins, 1994). The duration of transient dynamics in our networks may depend non-trivially on the different patch-sizes, which are sustaining different population sizes. System relaxation time to equilibrium could be investigated by implementing a metacommunity model with salient features of our experiment, but it goes beyond the scope of the present study.

5.5 Conclusions

Understanding the effects of fragmentation and patch-size distribution on communities is crucial, especially in highly diverse riverine systems. Hierarchical riverine habitats, characterized by a natural spatiotemporal heterogeneity, sustain higher levels of diversity (Muneepeerakul et al., 2007; Carrara et al., 2012). Because dispersal is constrained by the network pathway, the river network may become a trap for species when the dendritic system is exposed to habitat fragmentation and patch-size alterations (Fahrig, 2003). Protecting highly connected communities could help to avoid extinctions of species with low reproductive rates. These species are prone to suffer more from environmental disturbances and require larger and well-connected habitats to persist. By preserving the natural hierarchy of spatiotemporal heterogeneity along river networks, fast growing species and weak competitors alike are better able to persist. Our results not

only causally demonstrate general ecological principles, but also give insights for developing theoretical metacommunity models in dendritic environments and for future empirical studies focusing on riverine ecosystems.

6 The mid-altitude effect in river landscapes: patterns and processes

6.1 Introduction

The search for the mechanisms determining the distribution of life on Earth has long been a challenge for ecologists and biogeographers (Brown, 1995; Gaston, 2000). Developing conservation strategy requires an improved knowledge of biodiversity patterns and processes and the linking between them (Hanski and Ovaskainen, 2000). Recently, an increase of distribution-mapping campaigns dedicated to assess the current status of biodiversity has provided researchers with a wealth of data over different clades (Hubbell, 2001; BDM Coordination Office, 2009; Taberlet et al., 2012). Figure 6.1 illustrates one such example regarding a survey of macroinvertebrates in the Swiss river basins. This increased availability of data permits to have tested ecological theories at a higher degree of sophistication (Kraft et al., 2011), and has boosted the development of new analytical tools applied to spatial ecology, borrowed from other fields of research, such as statistical mechanics, network theory and the theory of stochastic processes (Harte et al., 1999; Azaele et al., 2006; Volkov et al., 2009; Bertuzzo et al., 2011).

A important and traditional area of ecological research (MacArthur and Levins, 1967; MacArthur, 1972) is dedicated to the study of species richness depending on gradients across space or environmental conditions (Gaston, 2000). Empirical evidence strongly supports the presence of a hump-shaped pattern in local species richness in an elevational gradient, across different types of organisms and different types of habitats, ranging from forest, to grassland and river-ecosystems (Rahbek, 1995; Nogues-Bravo et al., 2008; Bryant et al., 2008; McCain, 2009; Altermatt et al., 2013). Several factors change predictably with increasing elevation, such as temperature, precipitation, anthropogenic pressure (Nogues-Bravo et al., 2008) and geometric constraints (MacArthur, 1972). All these factors contribute synergistically to shape the observed patterns of diversity. Perhaps, the most important driver is temperature, because it directly controls the productivity of communities (Brown et al., 2004; Barry, 2008). However, a too simplistic association of the elevation gradient with the temperature gradient in mountainous ecosystems led researchers to the misleading null expectation of a decline of species richness with increasing altitude (MacArthur, 1972). This expectation is appealing because elevation

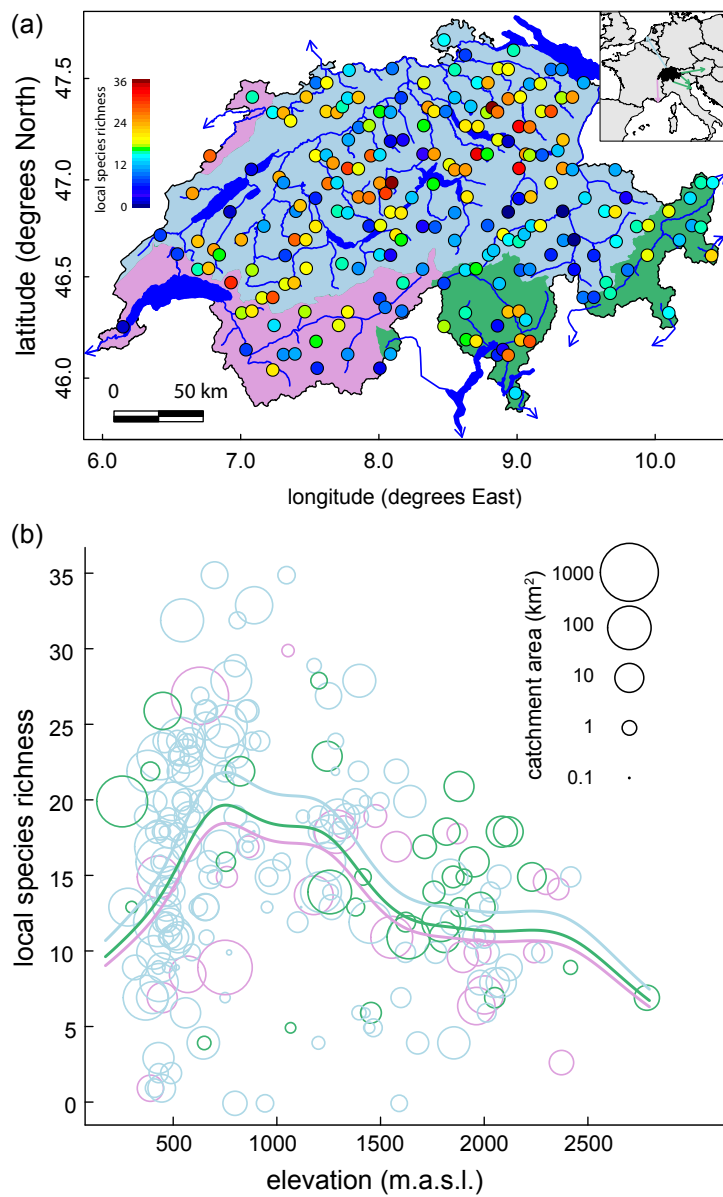


Figure 6.1: (a) Local species richness of macroinvertebrates collected in 217 sampling sites in the Swiss river basins. (b) Relationship between elevation of a sampling site and local species richness, showing a hump-shaped pattern. Circle colors refer to the three main Swiss rivers shown in map a). Figure redrawn from Altermatt et al. (2013).

gradient would mirror the latitudinal gradient (Willig et al., 2003), i.e. the decline of species richness from the equator to the poles. However, it is inconsistent with empirical observations, usually showing a hump-shaped pattern, rather than a monotonically decreasing pattern (Rahbek, 1995; Nogues-Bravo et al., 2008). Nogues-Bravo et al. (2008) correlated the low species richness at low elevation with human disturbance. Another possible cause of this pattern is the so called mid-domain effect (MDE). In this case species distribution is determined by simple stochastic processes operating within geometrically constrained boundaries (Jetz and Rahbek, 2001; Rahbek and Graves, 2001). Specifically, if species' ranges are randomly distributed over a bounded geographic range free of environmental gradients, ranges overlap increasingly over the center of the domain, thus creating the characteristic observed peak in species richness (Colwell et al., 2004). Applying the same principle to an altitudinal rather than geographic range, Rahbek (1995) explained the hump-shaped pattern of local species richness along elevation gradients.

A possible source of misinterpretation in most of previous studies was that the environmental matrix and the elevational gradients were considered disconnected, which represents an over-simplified interpretation of the landscape structure (Figure 6.2a). In fact, deriving species distribution patterns directly from altitudinal gradients of environmental conditions implicitly assumes a one dimensional dynamics which contrasts with the high complexity and dimensionality of a typical real-life mountainous regions (Figure 6.2b). In chapters 4 and 5, this procedure of using one dimensional domains has already been highlighted as too simplistic if not erroneous, in particular when considering ecosystems, like river landscapes, that naturally embed a high degree of complexity in forms and structures. Environmental conditions and landscape connectivity have been shown to shape characteristic patterns of diversity in an intricate manner, as per the interaction with species ecological traits in determining different community responses to environmental drivers (Carrara et al., 2012, 2013a).

Recently, mechanistic approaches were applied to link the causes and the consequences of the intriguing natural mid-elevation peak pattern (Thuiller et al., 2008; Colwell et al., 2009). In this context, the present chapter investigates the possible geomorphologic origins of the mid-elevation peak in local species richness, recently observed also for macroinvertebrates in Swiss river basins (Altermatt et al., 2013), by implementing a zero-sum metacommunity model (Rosindell et al., 2011) and by comparing the patterns emerging from the simulations in a simple slope (Figure 6.2a) and in a mountainous landscape (Figure 6.2b). The model has been formalized by invoking the "minimum-set-of-assumptions principle" (Rosindell et al., 2011). Specifically, the following set of rules has been implemented: i) individuals of each species have a preference depending on altitude; this preference varies among species; ii) there is no preferential altitude at the metacommunity scale; iii) dispersal is isotropic (towards the four nearest neighbors in a two dimensional landscape); iv) environmental conditions are constant over the entire domain. As such, the observational scale here adopted can be thought as an intermediate scale between local and continental scale approaches, where other kind of factors, such as latitudinal gradients, should be considered (Ricklefs, 2004). The hypothesis that the complex structure of landscapes shaped by river erosion processes can lead to non trivial species richness patterns even in the absence of species preferential altitude or environmental condition gradients is here tested. Mountainous

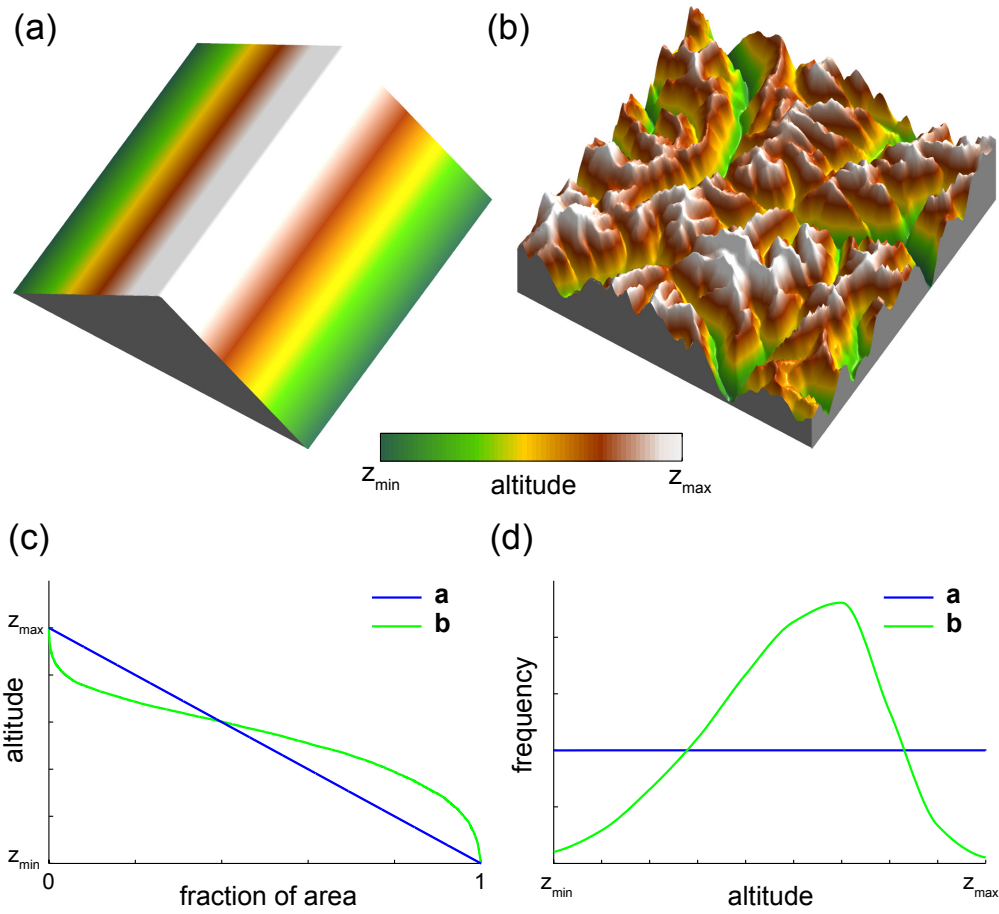


Figure 6.2: Comparison between an oversimplified model of altitudinal gradient (a) and a real-life altitudinal field of a mountain area (b). Hypsographic curves of the two landscapes (c). Points along the curve indicate the fraction of area that exceeds a certain altitude. Comparison between the frequency distributions of altitudes of the two landscapes (d).

landscapes display, in fact, two distinctive characteristics that can affect the distribution of species along an altitudinal gradient. First, differently from the simple planar slope (Figure 6.2a), the frequency distribution of elevation in real-life landscapes is non-uniform with a peak at mid-altitude (Figure 6.2c, d). This pattern is ubiquitous in mountainous areas (when a sufficient large region and not a single slope is considered) and it changes only if large portions of plain are included in the domain. Second, patches of sites at different altitude have very different connectivity. Figure 6.3 clearly shows how valley (low altitude sites) and mountain tops (high altitude sites) form fragmented patches isolated from each other, whereas mid-altitude patches are far more connected. As individuals of different species selectively prefer different altitudes, patches of sites within a certain altitude range directly translate into habitat patches. Therefore, the proposed scheme embeds essential features of metapopulation and metacommunity theory, such as the landscape patchiness (Hanski, 1998; Holyoak et al., 2005). It is thus expected that communities at low (high) altitude exhibit, being more isolated, lower species richness than those at mid-altitude. A similar effect has already been discussed in chapters 4 and 5 regarding the isolation of headwaters.

6.2 Methods

In order to investigate the role of the mountainous landscapes in shaping altitude gradient of species richness, a zero-sum metacommunity model is adopted (Hubbell, 2001; Rosindell et al., 2011). In this framework, the system comprises N local communities which are characterized by their position in space and by their mean altitude. Only communities organized in an equally spaced two dimensional lattice will be considered; however the model could be readily adapted to account for other connectivity structures like those investigated in the previous chapters. Each local community assembles n individuals. The system is assumed to be at saturation (zero-sum assumption, Rosindell et al. (2011)). Thus, at any time, the system is populated by $N \cdot n$ individuals belonging to S different species. Each species is characterized by a specific altitude niche which expresses, in this context, how the ability of a species to exploit resources varies with the altitude. This relationship is modelled as a gaussian function:

$$c_i(z) = c_{max_i} e^{-\frac{(z-z_{opt_i})^2}{2\sigma_i^2}}, \quad (6.1)$$

where $c_i(z)$ reflects the competitive ability of the individuals of species i at altitude z , z_{opt_i} is the optimal altitude of species i , that is where $c_i(z)$ equals its maximum c_{max_i} . The parameter σ_i controls the dispersion of the gaussian function. In this chapter the analysis is limited to the case where all the species have the same parameters $\sigma_i = \sigma$ and $c_{max_i} = c_{max}$. Figure 6.4 illustrates how the niches of different species are modelled. To avoid edge effects (Jetz and Rahbek, 2001), species that have an optimal elevation outside the altitude range of the system are also considered. Specifically, the range of optimal elevation used is twice that of the system simulated. While species differ for their altitudinal niches, all the other ecological traits (namely birth, death and dispersal rates) are identical like in the classical ecological neutral dynamics

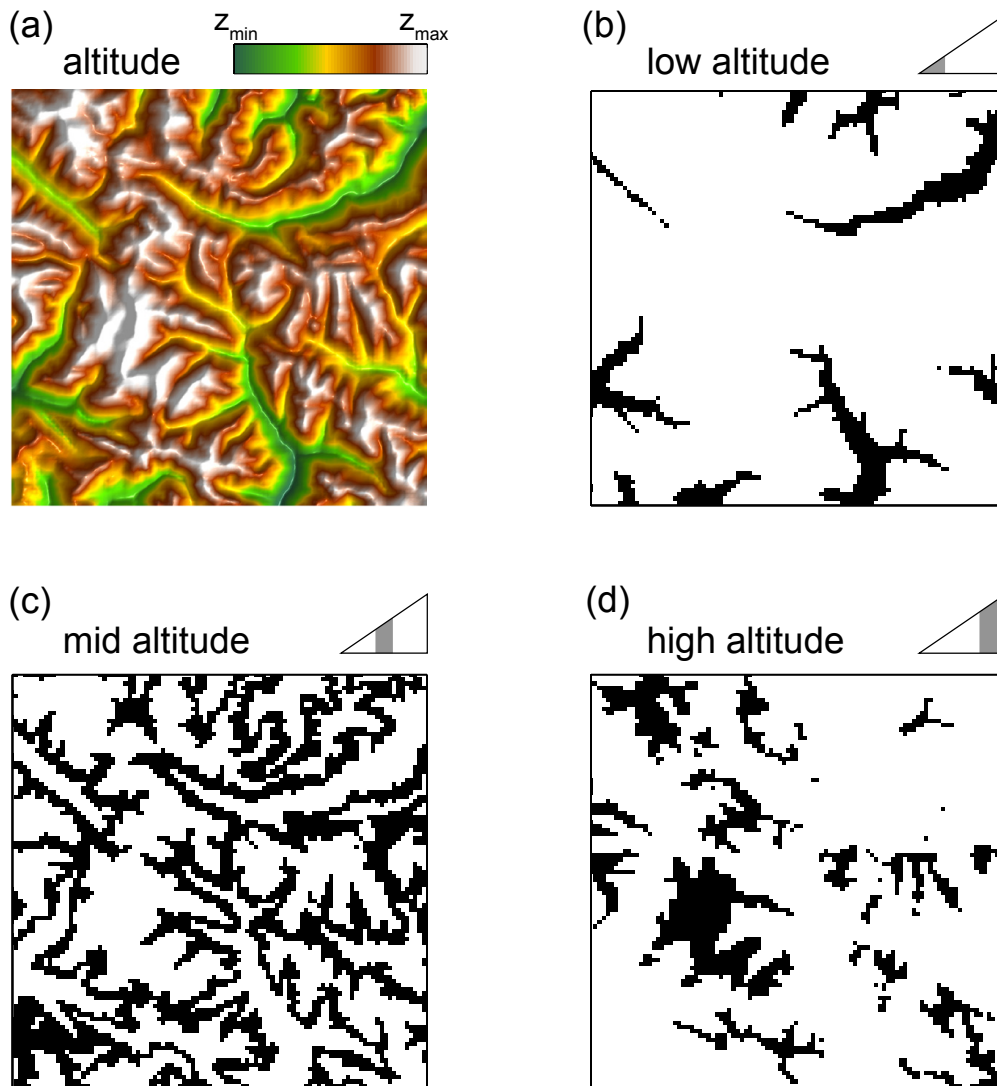


Figure 6.3: Connectivity of patches with similar altitude. Panel a shows the altitude map of the landscape shown also in Figure 6.2b. Patches with low elevation (b), mid-elevation (c) and high elevation (d) are shown in black. The altitude range is indicated at the top-right corners of panels (b–d).

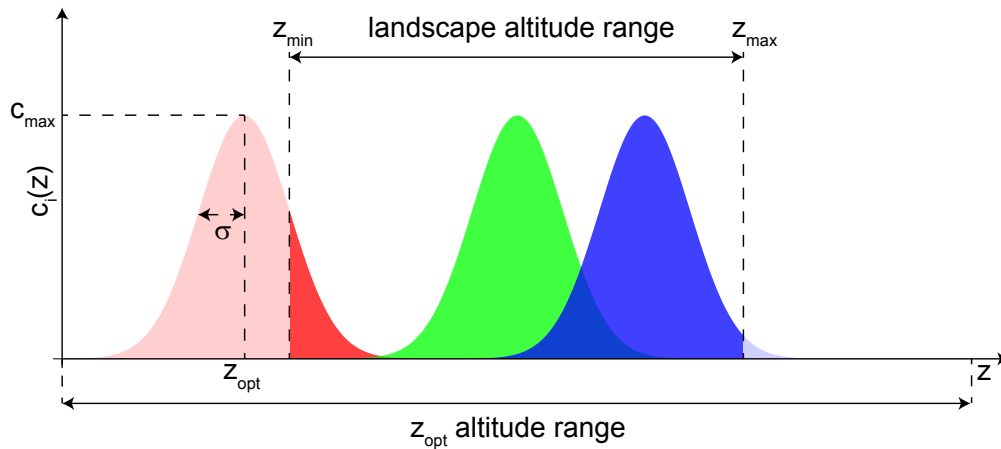


Figure 6.4: Altitude niches. Different species have different altitude niches which are modelled by a gaussian function with parameter z_{opt_i} , c_{max_i} and σ_i . The three species have σ_i equal to the 10% of the altitude range of the system. To avoid edge effects, species that have an optimal elevation z_{opt_i} outside the altitude range of the simulated system (e.g. the orange-coded area of the red species) are also considered. The range of optimal elevation is twice the range of the simulated system.

(Hubbell, 2001; Volkov et al., 2003). Ecological interactions among individuals are simulated as follows. At each time step, a randomly selected individual dies and the resources are freed up and available for colonization. The empty site is occupied by an offspring of one of the individuals occupying either the local community of the dead individual or one of the four nearest-neighbour communities (von Neumann neighborhood). The offspring is selected randomly with a probability proportional to $c_i(z)$ of all the candidate colonizing individuals evaluated at the elevation z of the local community of the dead individual. At each time step, with probability v , an additional individual, belonging to a species not currently present in the system, engages in the competition for colonizing the free spot. The optimal altitude z_{opt_i} of this individual is drawn from a uniform distribution spanning twice the altitude range of the system as described before (see also Figure 6.4). This introduction of new species is aimed at modelling both speciation and immigration from external communities.

In addition to the two landscapes illustrated in Figure 6.2, the model is simulated also in the three dimensional structure shown in Figure 6.5 which has the same frequency distribution of site elevation (i.e. the same hypsographic curve) of the mountainous landscape shown in Figure 6.2b. In the following, these landscapes will be referred as: planar slope (PS, Figure 6.2a), hypsographic slope (HS, Figure 6.5) and mountainous landscape (ML, Figure 6.2b). With such design it is possible, analyzing sequentially the results in the three landscapes, to quantify and disentangle the effects of a finite range of elevation (PS), of an uneven distribution of elevation (HS) and of the fractal structure of river landscapes (ML). All the landscapes are constructed

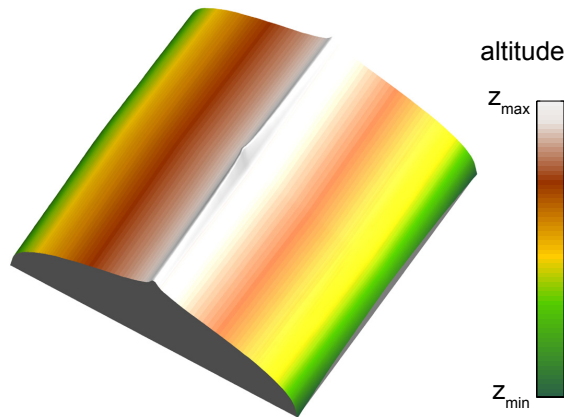


Figure 6.5: Hypsographic slope. A landscape that conceptualizes the one dimensional view of an altitudinal gradient. The particular profile is derived imposing that the frequency distribution of site elevation is that of the landscape shown in Figure 6.2b.

by gridding different elevation maps in a regular 100×100 lattice ($N = 10^4$). The structure in Figure 6.2b has been obtained using a real-life elevation map where each pixel embeds the mean altitude of a 500×500 m region. The local community size n is set to 100. The system is initially populated by single species and it is simulated until a statistically steady state is reached (10^5 generations, where a generation is $N \cdot n$ time steps). Periodic boundaries conditions are prescribed for both landscapes. Notice that model results do not depend on the actual altitude range ($[z_{min}, z_{max}]$) but only on the ratio $\sigma / (z_{max} - z_{min})$.

6.3 Results and Discussion

Figure 6.6 shows the patterns of local species richness (α -diversity) resulting from the simulations of the zero-sum metacommunity model in the three landscapes. In the planar slope (Figure 6.6a, b) α -diversity is relatively constant along the elevation gradient except for a decrease at the boundaries of the altitude interval. This effect is due to the finiteness of the elevation range. In fact, while sites in the middle of the altitude range can be potentially colonized by species that live at (and have a preference for) higher and lower altitude, sites at the lower (higher) extreme are only subject to the colonizing pressure from higher (lower) altitude. The boundaries of the elevation interval should not be confused with those of the spatial extent of the domain, whose possible effect is avoided using periodic boundaries conditions. The α -diversity pattern in the hypsographic slope (Figure 6.6c, d) exhibits a more pronounced edge effect. It is deemed that this particular pattern is the result of the combination of finiteness of the elevation range and the non-uniform distribution of altitude. Notice in fact how species richness is higher in the top half of the altitude interval, a pattern which resembles the frequency distribution of elevation (Figure 6.2d). Finally, the pattern of α -diversity in the mountainous landscape, which combines

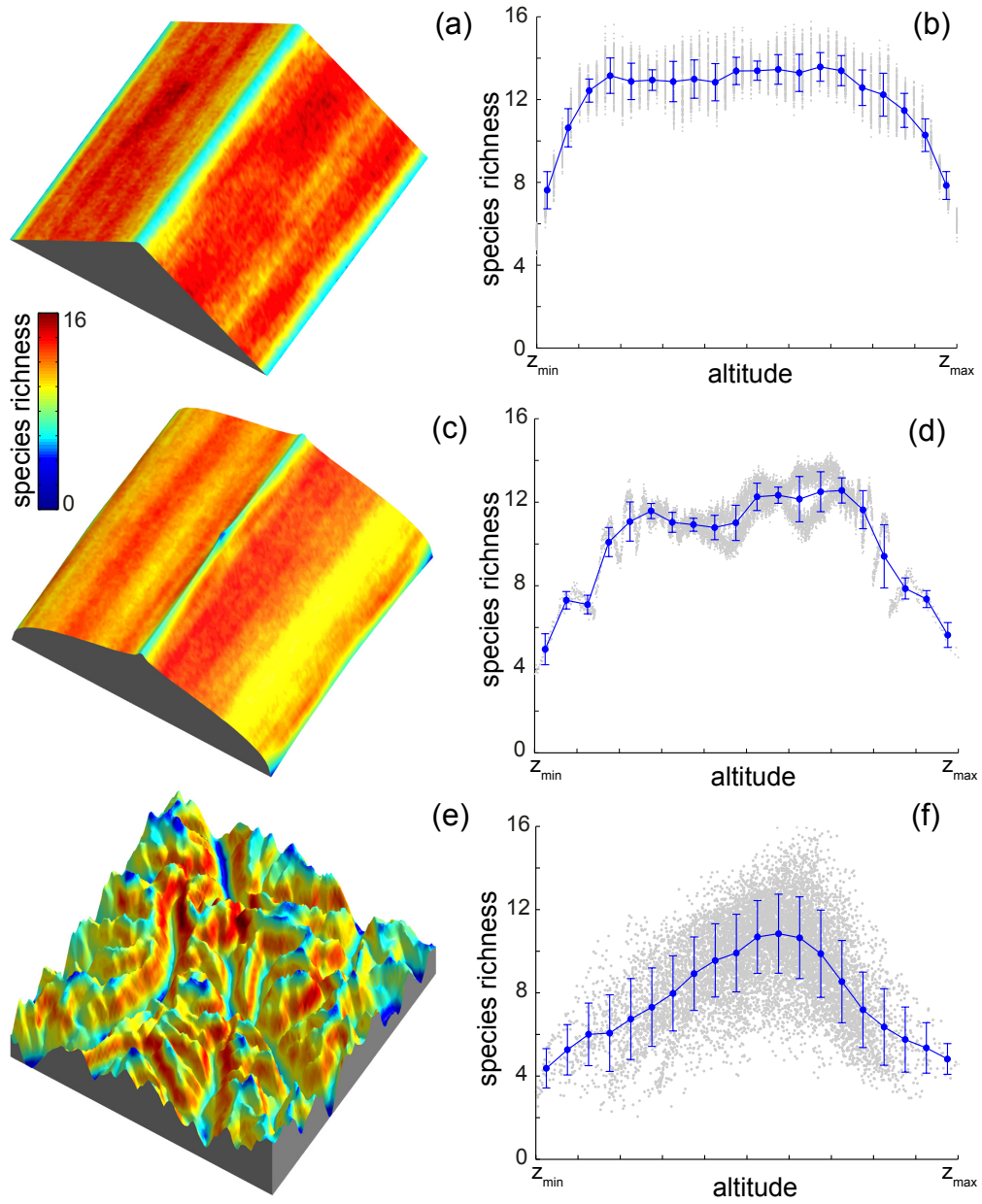


Figure 6.6: α -diversity patterns in the three landscapes. Species richness as a function of the spatial position (a, c, e) and altitude (b, d, f) for the planar slope (a, b), the hypsographic slope (c, d) and the mountainous landscapes (e, f). Averages over 40 realizations are shown. Parameters employed are: $N = 10^4$, $n = 100$, $\sigma/(Z_{max} - Z_{min}) = 0.1$, $nu = 0.5$.

the effects discussed before with the fractal geometry, presents a peak for mid-elevation sites (Figure 6.6e, f). The map in Figure 6.6e reveals a clear spatial pattern with valleys and mountain tops characterized by low species richness. Moreover, species richness gradients in the slopes (PS and HS) are much more predictable (smaller variance) than the one in the realistic landscape.

Also the analysis of classical macroecological indicators reveals notable differences among the biodiversity patterns in the different landscapes. While the mean α -diversity decreases as the complexity of the environmental matrix increases (12.1 for the PS, 11.3 for the HS and 9.3 for the ML), the γ -diversity, that is, the total number of species in the system, follows an opposite trend (653 for the PS, 750 for the HS and 972 for the ML). This directly implies a higher β -diversity (between communities diversity) for the more complex landscapes, a result similar to that obtained in chapter 4. Dispersal employed in the simulations is isotropic to the four nearest neighbors, that is, there is no constraint on dispersing only along the river network pathway. Clearly, the effect on species richness is only due to the specific spatial organization of the river basin. Habitat maps depending on altitude (Figure 6.3) help in the interpretation of this result. Habitats patches near the borders of the elevation domain (panels b, d) are rather disconnected compared to the habitat available for species adapted to the mid-range elevations.

Figure 6.7 sheds more light on the mechanisms underlying the formation of such different α -diversity patterns in different landscapes. It shows how the relative abundance of a subset of species whose optimal elevation falls within a certain range varies with the elevation. The envelope containing all the altitudinal niches of the species considered is also shown. These two profiles can be interpreted as the theoretical (the latter) and the realized (the former) niche. As expected, the realized niche is narrower than the theoretical one because of the competition with other species. It is interesting to note, however, how the realized niche in the mountainous landscape is wider than the one in the hypsographic slope. Moreover, the relative abundance within the range of altitude selected is less than one in the ML. These two results imply that the structure of the ML favors the coexistence of species with a wider range of optimal altitude. Intuitively, this effect can be explained by the 'environmental disorder' derived by the specific geomorphological signatures of the river basin (Rodríguez-Iturbe and Rinaldo, 1997). The intrinsic fractality of such environments may buffer ecosystems from stationarity and synchronization, promoting among-community dissimilarity and regional evenness. On the contrary, the biogeography of species embedded in the theoretical slopes result more predictable, and arguably with dynamics more prone to synchronization (note the persistent lines with the same colors in Figure 6.6c).

A preliminary exploration of metacommunities patterns suggests that the specific spatial arrangement of sites in mountainous regions at different elevation can induce a baseline mid-altitude effect on species richness. This does not imply that other gradients of abiotic factors (e.g., temperature, precipitation, human activity) are not important. However they act on top of this baseline patterns and they can possibly enhance it, distort it or eventually becloud it. The mid-altitude peak observed for local species richness in the simulation results is entirely due to the dynamics emerging from the zero-sum metacommunity model in river basin. In fact, species' altitudinal range was randomly selected with a particular procedure in order to minimize the effects of the

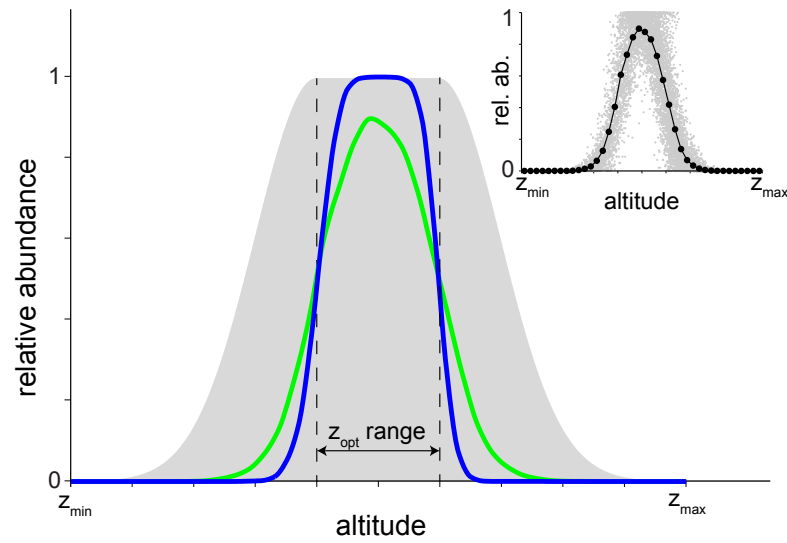


Figure 6.7: Relative abundance of a subset of species whose optimal elevation falls within a certain range (arrow) as a function of the altitude for the mountainous landscapes (green line) and the hypsographic slope (blue line). Pattern for the planar slope is very close to that of the HS (result not shown). The gray shaded area represents the envelope containing all the altitudinal niches of the species considered. The inset describes how this pattern is computed. First, the relative abundance for each site is calculated as the sum of the relative abundance of all the species considered (gray dots). Second, the different sites are binned based on their altitude and the mean relative abundance of each bin is calculated.

Chapter 6. The mid-altitude effect in river landscapes: patterns and processes

boundary conditions (see section *Methods* 6.2).

The above considerations are interconnected with the problem of scales in ecology (Ricklefs, 2004; Rahbek, 2005; Nogues-Bravo et al., 2008). In this framework, based on a simple assumptions on the species altitude preferences, the distribution of area at a given altitude naturally translates into 3-D species-habitat maps. Organisms with different dispersal abilities may experience different habitat size or connectivities. This may have important implications because the dispersal and the geographic range of a species are clearly interconnected. It is thus obvious to ask how the appearance of a mid-altitude pattern in species richness is related to the dispersal ability (Bryant et al., 2008). Under this null framework, the prediction is that the smaller the dispersal ability of the species, the larger the effect of the isolation due to the environmental matrix. Also, quantification of changes in species habitat maps after a translation in the optimal niche due to climate change will be possible (Lenoir et al., 2008). This allows speculating about likely scenarios of species' habitat modifications and derivation of the ensuing extinction debts (Hanski and Ovaskainen, 2000; Hanski, 2013) under the pressure of environmental change (Araujo and Rahbek, 2006).

Finally, extending the analysis to aquatic organisms dispersing along river networks, the mid-altitude effect is predicted to be even stronger, as can be inferred from the results presented in chapter 4 of the effects of dendritic connectivity on metacommunity patterns.

7 Conclusions and perspectives

This thesis presents results of theoretical and empirical nature aimed at understanding the mechanisms that maintain diversity in biological communities, with a particular focus on dendritic ecosystems. The combination of theory-guided experiments with theoretical investigations has been pursued consistently from a local perspective to the metacommunity scale.

The main conclusions of the thesis can be summarized as follows:

- Chapter 2 has introduced in detail the theoretical tools and the experimental model system adopted along all the research work. It is shown how a stochastic implementation of population dynamics is considered as a fundamental tool for the derivation of key community properties, such as species persistence and community stability. In what follows, the spatial extension of the stochastic community model was applied to the characterization of dendritic ecosystems.
- In chapter 3 key aspects of biodiversity-ecosystem functioning research have been addressed, where all pairwise interactions in a pool of 11 species of eukaryotes (10 protists and one rotifer), belonging to three functional groups, were measured in a replicated multi-generation experiment. This approach builds upon more traditional experimental investigations, which generally focused on one trophic level. The diversity-productivity and diversity-stability relationships were explored in a local perspective, showing the crucial role played by functional diversity in the maintenance of species coexistence and productivity in microbial communities. A positive relationship between functional diversity and total biomass production was experimentally detected and confirmed in the stochastic simulations. Communities composed of species from a single or two functional groups were less productive compared to communities where species belonged to the three functional groups. Moreover, looking at species coexistence of communities initially composed by the same species richness level across a functional diversity gradient, a higher final species richness for communities with a higher initial functional diversity was observed. This pattern is reflected in higher community productivity and a generally higher stability.

To our knowledge, these results represent the first attempt in disentangling, through a mechanistic-based approach, the effect of functional diversity and species richness on stability and productivity properties of trophically structured communities, answering to a precise need from community ecology research.

- Diversity and ecosystem functioning of riverine systems are highly threatened due to a combination of habitat modification, invasive species and changes in river connectivity. To mitigate these negative effects, an understanding of factors driving riverine diversity patterns is of the highest priority. As a consequence, the main contribution of this thesis has been obtained by experimentally showing that spatially constrained dendritic connectivity interact with the hierarchical organization of habitat capacity in driving community composition and population persistence in riverine landscapes. Specifically, chapter 4 shows that connectivity *per se* shapes key components of biodiversity in microcosm metacommunities. By conducting an experiment in aquatic microcosms landscapes, the effects of directional dispersal imposed by the habitat-network structure on the biodiversity of metacommunities have been investigated. Spatially heterogeneous metacommunities following a river network geometry were compared with spatially homogeneous metacommunities, in which every local community has 2-D lattice four nearest neighbors. Experimental findings were reproduced and extended with a stochastic metacommunity model. Local dispersal in isotropic lattice landscapes homogenizes local species richness and leads to pronounced spatial persistence. On the contrary, dispersal along dendritic landscapes leads to higher variability in local diversity and among-community composition. Although headwaters exhibit relatively lower species richness, they are crucial for the maintenance of regional biodiversity.
- The effect of local habitat capacity (i.e., the patch size) and dendritic connectivity on biodiversity in aquatic microcosm metacommunities was experimentally disentangled in chapter 5, by suitably arranging patch sizes within river-like networks. The individual influence of patch size and connectivity was disentangled by using three different configurations of local community volumes, connected following a river-network geometry. These treatments were i) a riverine landscape maintaining the intrinsic link of position and patch size, ii) a random landscape, with spatial random permutation of the patch volumes in above riverine configuration, and iii) a homogeneous landscape, with equal distribution of volumes (total volume is conserved in all cases). It is there shown that species coexistence and community assembly depend on intricate, non-trivial interactions of local community capacity and network positioning. Furthermore, an interaction of spatial arrangement of habitat capacity and dispersal along river-like networks is also affecting a key ecosystem descriptor, namely regional evenness. High regional evenness in community composition is found only in landscapes preserving geomorphological scaling properties of patch sizes. In riverine environments some of the rarer species sustained regionally more abundant populations and were better able to track their own niche requirements compared to landscapes with homogeneous patch size or landscapes with spatially uncorrelated patch size. All the experimental results were supported (and extended) by a theoretical analysis where the

above mechanisms have been generalized.

- Guided by empirical observations on diversity of macroinvertebrates in Swiss river basins, a theoretical ansatz was provided in chapter 6, which captures the essential geomorphological drivers and controls relating species-fitness to altitude. The investigation of the causes for the mid-altitude effect was accomplished following the conceptual thread of the previous chapters, where dispersal limitation and species' adaptation to altitude are the crucial drivers. It provided a synthesis of this thesis work in combining aspects from niche-theory, usually considered in spatially implicit model, as in chapters 2 and 3, in a spatial context, from a typical real-life mountainous region.

A zero-sum metacommunity model was adopted to describe the community dynamics happening in river basins, where the landscape is sculpted by well-known geomorphological signatures. Specifically, species were assigned with a fitness-dependence on altitude and dispersed to the four nearest-neighbors (isotropic dispersal). The well-known mid-domain effect is revisited under the light of the appropriate consideration of the spatial environmental matrix. A possible source of misinterpretation in most of previous studies was in considering the environmental matrix and the elevational gradients as disconnected, which represents an over-simplified interpretation of the landscape structure. In fact, deriving species distribution patterns directly from altitudinal gradients of environmental conditions implicitly assumes a one dimensional dynamics, which contrasts with the high complexity and dimensionality of a typical real river basin. In fact, the amplification to multiple spatial scales of the boundary effects on local species richness in chapter 6 is entirely due to the fractal organization of the river landscape. The mid-elevation effect in local species richness was much less pronounced in a landscape preserving the same hypsographic slope of the river landscape for an appropriate comparison, or even a planar slope, that is the standard procedure in most of ecological research on this topic. In chapters 4 and 5, this procedure of using a simplified dimensional domain has already been highlighted as too simplistic if not erroneous, in particular when considering ecosystems, like river landscapes, that naturally embed a high degree of complexity in forms and structures. Both environmental conditions and landscape connectivity shaped characteristic patterns of diversity in an intricate manner, as per the interaction with species ecological traits in determining different community responses to environmental drivers.

An overarching pattern of the present thesis consisted in a higher among-community dissimilarity (captured by several measures of β -diversity) of communities embedded in heterogeneous landscapes compared to more homogeneous landscapes. Also in chapter 6 the source of spatial and environmental heterogeneity typical of mountainous landscapes, which was captured in the model, resulted in higher beta-diversity patterns, and in a higher regional γ -diversity. The 'environmental disorder' derived by the specific geomorphological signatures of the river basin may buffer ecosystems from stationarity and synchronization, promoting among-community dissimilarity and regional evenness. Also, this reflects a wider realized geographic range in the river landscape compared to the two simplified realizations, with implications on the assessment of species' geographic range. The precise interconnections between habitat geomorphology and species habitat maps

Chapter 7. Conclusions and perspectives

may provide predictions in the changes on species habitats, as species altitudinal range are documented to shift towards higher elevations. Thus, it endows ecosystem management with a solid null assumption.

There is a need in ecology to further our understanding of the links between patterns and processes. Evidence is provided in this thesis of the usefulness of applying ecological theories that capture a few key details of ecosystems to explain various aspects of biodiversity. This is a crucial step in order to provide a predictive science that should inform a proper management of the ecosystems. This thesis offers insight into the ecological forces structuring natural communities such as riverine habitats and suggests principles that can be further tested in theoretical metacommunity models and real riverine ecosystems. Taken together, the analyses show how the structure of ecological networks interacts with the spatial environmental matrix in determining biodiversity patterns and the functioning of biological communities. In a nutshell, the proposed analyses suggest that altering the natural linkage between dendritic connectivity and patch size strongly affects community properties at multiple scales. By combining theoretical models with experimental and empirical evidence, a unified approach for the understanding of the origins and the maintenance of diversity within river networks has been proposed. It is argued that the approach may be relevant to ecology, conservation biology and environmental sciences, with implications for a management oriented to the preservation of ecosystem processes and preservation of endangered species in ecosystems exposed to habitat fragmentation and environmental change.

Chapter 6 presents results of preliminary analyses. Different sets of parameters are under investigation, involving the role of speciation/immigration processes, the breadth of the altitude-niche, the dispersal kernel, and a more accurate assessment of the boundary conditions has been planned. Also, the model will be used for a more specific characterization of the biodiversity patterns of macroinvertebrates (BDM dataset), where an analysis based on taxa will be performed, by performing a hierarchical analyses that is considering the phylogenetic tree. Measures of spatial β -diversity will be contrasted to phylogenetic distance in order to understand the balance between dispersal limitation, environmental filtering, and competitive exclusion dynamics in structuring macroinvertebrates communities. Future work may focus on the analysis and the characterization of species' dispersal ability. In fact, the dispersal ability for Ephemeroptera, Plecoptera, and Trichoptera (EPT) species is almost unknown notwithstanding much effort dedicated to this crucial behavioral aspect affecting natural communities. This approach will be complemented by and profit from a parallel analysis currently performed by researchers at Eawag.

With regard to the experimental system, there are two possible directions to pursue: i) at the local scale, the study of the effects of a temperature gradient on the species interactions and, more generally, communities properties such as productivity, stability and species coexistence; ii) the study of the spreading of invasive species along the network already filled with a resident species at stationarity. Important priority effects are predicted to occur for the succession of the spreading depending on the initial position of spreading process (e.g., headwater vs. outlet) and a better

understanding of the role played by directionality is needed. The experimental analysis could be extended to other organisms than protists, such as bacteria, which would allow one investigation of eco-evolutionary dynamics in realistic dendritic landscapes.

A Modeling riverine ecosystem connectivity

To describe topological and metric properties of river network connectivity generally, stationary states of the general landscape evolution equation are reproduced through the static model known as the optimal channel network (OCN, Rinaldo et al. (1999, 2006) for a review). The OCN model was originally based on the ansatz that configurations occurring in nature are those that minimize a functional describing the dissipated energy and on the derivation of an explicit form for such a functional. A later proof (Banavar et al., 1997, 2001) confirmed that optimal networks are exactly related to the stationary solutions of the basic landscape evolution equation to leading order in the small gradient approximation. In particular, any configuration that minimizes total energy dissipation, within the framework of general dynamical rules, corresponds, through a slope-discharge relation, to an elevation field that is a stationary solution of the basin landscape evolution equation. Thus spanning, loopless network configurations characterized by minimum energy dissipation are obtained by selecting the configuration, say s , that minimizes

$$E(s) = \sum_j a_j^\gamma, \quad (\text{A.1})$$

where j spans the lattice and $a_i = \sum_j W_{j,i} a_j + 1$ is the value of the drainage area $a_i \forall i$. $W_{j,i}$ is the element of the connectivity matrix spanning all nodes and determining uniquely, in a spanning loopless tree. The exponent γ is exactly $\gamma = 1/2$ in the small gradient approximation and it is crucial that one has $\gamma < 1$ from the physics of the problem (Banavar et al., 2001).

The global minimum (the ground state) of the functional in the Eq. A.1 is exactly characterized by known mean field exponents. Thus any stationary solution of the landscape evolution equation must locally satisfy the slope-area relationship.

The 3D drainage basin can be reconstructed using the rule of steepest descent, that is, the flux at a point j has the direction of the maximum gradient of the elevation field (the direction toward the lowest among all nearest neighbors to j). Moreover, the channelized part of the landscape is necessarily (but not sufficiently) identified by topographically concave areas where the above assumption holds strictly. Thus one can uniquely associate any landscape with an

Appendix A. Modeling riverine ecosystem connectivity

oriented spanning graph on the lattice, i.e., an oriented loopless graph passing through each point. Identifying the flux in a point i with the total area A_i drained in that point, one can reconstruct the field of landscape-forming fluxes corresponding to a given oriented spanning graph. From the fluxes, a field of elevation can be defined using the above relation with the local slope.

In chapter 4, Figure 4.1a shows a local minimum of E in Eq. (A.1), obtained by moving from an initial configuration s . A site is then chosen at random, and the connectivity W (hence the configuration s) is perturbed by disconnecting a link, which is reoriented to produce a new configuration s' . If the new configuration lowers total energy dissipation, i.e., $E(s') \leq E(s)$, the change is accepted and the procedure is restarted. Figure 4.1A is obtained through the same procedure where an annealing procedure has been implemented, i.e., unfavorable changes may also be accepted with probability $\propto \exp(-[E(s) - E(s')]/T)$, where T assumes the role of temperature in a gas or a spin glass. Only changes that retain the loopless character are retained because every local minimum of the functional (3) is a tree (Banavar et al., 1999, 2000, 2001). Iteration to convergence in the connectivity structure W thus produces the desired planar and 3D landforms. The final number of nodes in the network is obtained by considering from the original space filling configuration (all pixels in the landscape domain are channelized) only those nodes with a drainage area $A_i > A_t$, where A_t denotes an adequate threshold.

In network theory, an important measure of centrality is provided by the closeness centrality, defined as the average of the inverse distances from a vertex to other vertices

$$C_i = \frac{1}{n-1} \sum_{(j \neq i)} \frac{1}{d_{ij}}. \quad (\text{A.2})$$

It is directly related to the ‘ecological diameter’ l_i , defined in the main text, which measures the mean distance from a LC to all other LCs. In chapter 4, Figure 4.5 shows the ecological diameter distribution for the RN (in a 36-lattice landscapes it is simply a delta function on $l_i^{2D} = l^{2D} = 3$).

A.1 Synchronization in river networks

In aquatic ecological research quite peculiar procedures are often chosen to construct networks in trying to mimick natural river network seen as ecological corridors for biological communities. For example, Bethe lattices (Bethe, 1935) or Cayley trees (are tree-like structure¹ emanating from a central node, with all the nodes arranged in shells around the central one) are considered (Figure A.1). The central node may be identified with the root/outlet of the lattice. Bethe tree is an infinite connected cycle-free graph where each node is connected to z neighbours, where z is called the coordination number. The number of nodes in the k th shell is given by $N_k = z(z-1)^{k-1}$. Due to its distinctive topological structure, the statistical mechanics of lattice models on this graph are often exactly solvable (Baxter, 1982). While it allows an analytical tractability, this procedure removes important properties of the natural river network (e.g., Rodriguez-Iturbe & Rinaldo

¹Bethe tree is the thermodynamic limit of Cayley tree, hence in Cayley trees, surface effects/boundary conditions become important

1997). Mainly, all the tributaries are confined on the last level in the hierarchy, not allowing the presence of small tributaries also on lower sites. In real rivers, smaller level tributaries (Strahler order 1) can drain directly into all higher levels. For example, a Strahler order 1 tributary can drain directly into an arbitrary level, and not only into a Strahler level 2. The chosen model of river networks only allows Strahler level 1 tributaries to drain into Strahler level 2.

This unrealistic definition of river networks may have a strong and potentially important impact on the synchronization property of the network, that is the subject of the following analysis. Synchronization, in preventing rescue effects in metapopulations, is a crucial component of stability in patchy environments. By using the master stability framework developed in Barahona and Pecora (2002) the stability property of the synchronization state for an arbitrary (completely connected) graph is made by looking at the eigenratio Λ_{max}/Λ_2 of the Laplacian matrix (Type I of synchronization criteria). This type of analyses can be performed irrespective of the particular dynamics on the nodes (Arenas et al., 2008).

Different network topologies were contrasted: i) the optimal channel networks (OCN) used as conceptual thread in all the present Thesis; ii) a deterministic Cayley tree with constant coordination number z ; iii) a modified version of Cayley tree, where the tree is built up from the outlet and at each bifurcation process the coordination number z is extracted from a Poisson distribution (Poisson bifurcation process). It therefore maintains the deterministic shell structures, where all leaves are located at the external shell; and iv) a modified Cayley tree, built as in the previous framework, in which the leaves can be located also in internal shells (Poisson bifurcation process tree and random shell structure, Figure A.1, right panels).

Higher stability for the synchronous state was obtained for deterministic and stochastic Cayley trees (Figure A.1), comparing the Laplacian eigenratio-number of network nodes relationship. The synchrony of the whole river network is deeply affected and different contributions are responsible for the increasing eigenvalue ratios. Multiple network characteristics are changing in between the different network topologies, e.g., maximum degree of connectivity, betweenness centrality, closeness centrality, and average geodesic distance. The behaviour of the smallest non-zero eigenvalue is affected, where its bounds depends on the above network characteristics (Arenas et al., 2008). Increasing river complexity/fractality properties, which coincides in preserving the natural geomorphic features of natural river basins, is also increasing the potential for an unstable synchronous state, with implications for the stability properties of metapopulations of species living in the ecological corridors provided by the river network.

Appendix A. Modeling riverine ecosystem connectivity

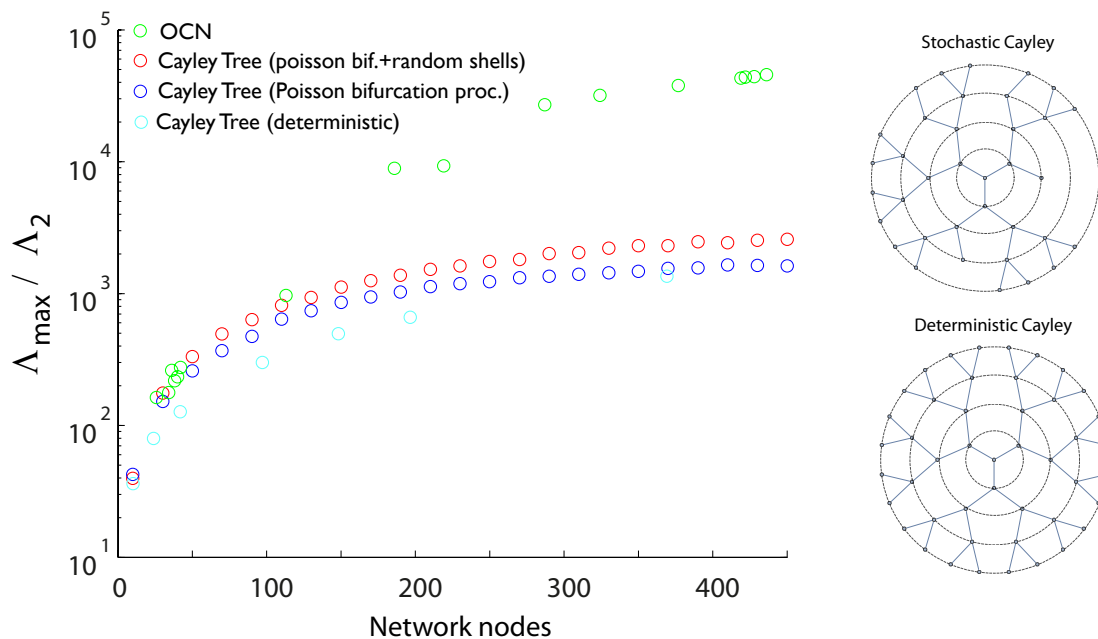


Figure A.1: Synchronization (captured by the eigenratio Λ_{max}/Λ_2) is enhanced in more regular structures, compared to optimal channel networks (OCN), suggesting that the degree of environmental disorder introduced by the fractality of natural river structure is buffering the system away from synchrony.

Bibliography

- Adler, P., HilleRisLambers, J., and Levine, J. (2007). A niche for neutrality. *Ecology Letters*, 10:95–104.
- Allan, E., Weisser, W., Weigelt, A., Roscher, C., Fischer, M., and Hillebrand, H. (2011). More diverse plant communities have higher functioning over time due to turnover in complementary dominant species. *Proceedings of the National Academy of Sciences of the United States of America*, 108:17034–17039.
- Allesina, S., Alonso, D., and Pascual, M. (2008). A general model for food web structure. *Science*, 320:658–661.
- Allesina, S. and Levine, J. (2011). A competitive network theory of species diversity. *Proceedings of the National Academy of Sciences of the United States of America*, 108:5638–5642.
- Allesina, S. and Tang, S. (2012). Stability criteria for complex ecosystems. *Nature*, 483:205–208.
- Altermatt, F., Bieger, A., Carrara, F., Rinaldo, A., and Holyoak, M. (2011a). Effects of connectivity and recurrent local disturbances on community structure and population density in experimental metacommunities. *Plos One*, 6: e19525.
- Altermatt, F., Pajunen, V., and Ebert, D. (2008). Climate change affects colonization dynamics in a metacommunity of three daphnia species. *Global Change Biology*, 14:1209–1220.
- Altermatt, F., Schreiber, S., and Holyoak, M. (2011b). Interactive effects of disturbance and dispersal directionality on species richness and composition in metacommunities. *Ecology*, 92:859–870.
- Altermatt, F., Seymour, M., and Martinez, N. (2013). River network properties shape α -diversity and community similarity patterns of aquatic insect communities across major drainage basins. *Journal of Biogeography*, in press.
- Amarasekare, P. (2002). Interference competition and species coexistence. *Proceedings of the Royal Society B-Biological Sciences*, 269:2541–2550.
- Anderson, M., Crist, T., Chase, J., Vellend, M., Inouye, B., and Freestone, A. *et al.* (2011). Navigating the multiple meanings of beta diversity: a roadmap for the practicing ecologist. *Ecology Letters*, 14:19–28.

Bibliography

- Anderson, M., Ellingsen, K., and McArdle, B. (2006). Multivariate dispersion as a measure of beta diversity. *Ecology Letters*, 9:683–693.
- Araujo, M. and Rahbek, C. (2006). How does climate change affect biodiversity? *Science*, 313:1396–1397.
- Arenas, A., Diaz-Guilera, A., Kurths, J., Moreno, Y., and Zhou, C. (2008). Synchronization in complex networks. *Physics Reports-Review Section of Physics Letters*, 469:93–153.
- Astorga, A., Oksanen, J., Luoto, M., Soininen, J., Virtanen, R., and Muotka, T. (2012). Distance decay of similarity in freshwater communities: do macro- and microorganisms follow the same rules? *Global Ecology and Biogeography*, 21:365–375.
- Ayala, F., Gilpin, M., and J.G., E. (1973). Competition between species - theoretical models and experimental tests. *Theoretical Population Biology*, 4:331–356.
- Azaele, S., Pigolotti, S., Banavar, J., and Maritan, A. (2006). Dynamical evolution of ecosystems. *Nature*, 444:926–928.
- Banavar, J., Colaiori, F., Flammini, A., Giacometti, A., Maritan, A., and Rinaldo, A. (1997). Sculpting of a fractal river basin. *Physical Review Letters*, 78:4522–4526.
- Banavar, J., Damuth, J., Maritan, A., and Rinaldo, A. (2007). Scaling in ecosystems and the linkage of macroecological laws. *Physical Review Letters*, 98:068104.
- Banavar, J., F., C., Flammini, A., Maritan, A., and Rinaldo, A. (2001). Scaling, optimality and landscape evolution. *Journal of Statistical Physics*, 104:1–33.
- Banavar, J., Maritan, A., and Rinaldo, A. (1999). Size and form in efficient transportation networks. *Nature*, 399:130–134.
- Banavar, J., Maritan, A., and Rinaldo, A. (2000). Topology of the fittest network. *Physical Review Letters*, 84:4745–4748.
- Barahona, M. and Pecora, L. (2002). Synchronization in small-world systems. *Physical Review Letters*, 89:054101.
- Barry, R. G. (2008). *Mountain whether and climate*. Cambridge University Press, Cambridge, UK.
- Bastolla, U., Fortuna, M., Pascual-Garcia, A., Ferrera, A., Luque, B., and Bascompte, J. (2009). The architecture of mutualistic networks minimizes competition and increases biodiversity. *Nature*, 458:1018–1021.
- Bastolla, U., Lassig, M., Manrubia, S., and Valleriani, A. (2005). Biodiversity in model ecosystems, i: coexistence conditions for competing species. *Journal of Theoretical Biology*, 235:521–530.
- Baxter, R. J. (1982). *Exactly solvable models in statistical mechanics*. Academic Press, London.

- BDM Coordination Office (2009). *The state of biodiversity in Switzerland. Overview of the findings of Biodiversity Monitoring Switzerland (BDM) as of May 2009*. State of the Environment. Federal Office for the Environment, Bern.
- Benda, L., Poff, N., Miller, D., Dunne, T., Reeves, G., Pess, G., and Pollock, M. (2004). The network dynamics hypothesis: How channel networks structure riverine habitats. *Bioscience*, 54:413–427.
- Berlow, E., Navarrete, S., Briggs, C., Power, M., and Menge, B. (1999). Quantifying variation in the strengths of species interactions. *Ecology*, 80:2206–2224.
- Berlow, E., Neutel, A., Cohen, J., de Ruiter, P., Ebenman, B., Emmerson, M., Fox, J.W. *et al.* (2004). Interaction strengths in food webs: issues and opportunities. *Journal of Animal Ecology*, 73:585–598.
- Bertuzzo, E., Suweis, S., Mari, L., Maritan, A., Rodriguez-Iturbe, I., and Rinaldo, A. (2011). Spatial effects on species persistence and implications for biodiversity. *Proceedings of the National Academy of Sciences of the United States of America*, 108:4346–4351.
- Bethe, H. A. (1935). Statistical theory of superlattices. *Proceedings of the Royal Society London Series A*, 150:552–575.
- Brown, B. and Swan, C. (2010). Dendritic network structure constrains metacommunity properties in riverine ecosystems. *Journal of Animal Ecology*, 79:571–580.
- Brown, J. (1995). *Macroecology*. The University of Chicago Press, Chicago.
- Brown, J., Gillooly, J., Allen, A., Savage, V., and West, G. (2004). Toward a metabolic theory of ecology. *Ecology*, 85:1771–1789.
- Bryant, J. A., Lamanna, C., Morlon, H., Kerkhoff, A. J., Enquist, B. J., and Green, J. L. (2008). Microbes on mountainsides: Contrasting elevational patterns of bacterial and plant diversity. *Proceedings of the National Academy of Sciences of the United States of America*, 105:11505–11511.
- Bulleri, F., Bruno, J., and Benedetti-Cecchi, L. (2008). Beyond competition: Incorporating positive interactions between species to predict ecosystem invasibility. *Plos Biology*, 6:1136–1140.
- Cadotte, M. (2006a). Dispersal and species diversity: A meta-analysis. *American Naturalist*, 167:913–924.
- Cadotte, M. (2006b). Metacommunity influences on community richness at multiple scales: A microcosm experiment. *Ecology*, 87:1008–1016.
- Cadotte, M. (2007). Competition-colonization trade-offs and disturbance effects at multiple scales. *Ecology*, 88:823–829.

Bibliography

- Cadotte, M. (2013). Experimental evidence that evolutionarily diverse assemblages result in higher productivity. *Proceedings of the National Academy of Sciences of the United States of America*, 110:8996–9000.
- Cadotte, M., Mai, D., Jantz, S., Collins, M., Keele, M., and Drake, J. (2006). On testing the competition-colonization tradeoff in a multispecies assemblage. *American Naturalist*, 168:704–709.
- Cardinale, B. (2011). Biodiversity improves water quality through niche partitioning. *Nature*, 472:86–89.
- Cardinale, B., Duffy, J., Gonzalez, A., Hooper, D., Perrings, C., Venail, P. *et al.* (2012). Biodiversity loss and its impact on humanity. *Nature*, 486:59–67.
- Carrara, F., Altermatt, F., Rodriguez-Iturbe, I., and Rinaldo, A. (2012). Dendritic connectivity controls biodiversity patterns in experimental metacommunities. *Proceedings of the National Academy of Sciences of the United States of America*, 109:5761–5766.
- Carrara, F., Rinaldo, A., Giometto, A., and Altermatt, F. (2013a). Complex interaction of dendritic network structure and hierarchical patch-size on biodiversity in river-like landscapes. *American Naturalist*, in press.
- Carrara, F., Rinaldo, A., Giometto, A., and Altermatt, F. (2013b). Data from: Complex interaction of dendritic connectivity and hierarchical patch-size on biodiversity in river-like landscapes. *American Naturalist*, Dryad Digital Repository:10.5061/dryad.15np2.
- Case, T. and Bender, E. (1981). Testing for higher-order interactions. *American Naturalist*, 118:920–929.
- Ceola, S., Hoedl, I., Adlboller, M., Singer, G., Bertuzzo, E., Mari, L., Botter, G., Waringer, J., Battin, T., and Rinaldo, A. (2013). Hydrologic Variability Affects Invertebrate Grazing on Phototrophic Biofilms in Stream Microcosms. *Plos One*, 8: e60629.
- Chesson, P. (1994). Multispecies competition in variable environments. *Theoretical Population Biology*, 45:227–276.
- Chesson, P. (2000a). General theory of competitive coexistence in spatially-varying environments. *Theoretical Population Biology*, 58:211–237.
- Chesson, P. (2000b). Mechanisms of maintenance of species diversity. *Annual Review of Ecology and Systematics*, 31:343–367.
- Chesson, P. and Kuang, J. (2008). The interaction between predation and competition. *Nature*, 456:235–238.
- Chisholm, C., Lindo, Z., and Gonzalez, A. (2011). Metacommunity diversity depends on connectivity and patch arrangement in heterogeneous habitat networks. *Ecography*, 34:415–424.

- Clarke, A., Mac Nally, R., Bond, N., and Lake, P. (2008). Macroinvertebrate diversity in headwater streams: A review. *Freshwater Biology*, 53:1707–1721.
- Colwell, R., Gotelli, N., Rahbek, C., Entsminger, G., Farrell, C., and Graves, G. (2009). Peaks, plateaus, canyons, and craters: the complex geometry of simple mid-domain effect models. *Evolutionary Ecology Research*, 11:355–370.
- Colwell, R., Rahbek, C., and Gotelli, N. (2004). The mid-domain effect and species richness patterns: What have we learned so far? *American Naturalist*, 163:E1–E23.
- Condit, R., Ashton, P., Baker, P., Bunyavejchewin, S., Gunatilleke, S., Gunatilleke, N., and Hubbell, S. *et al.* (2000). Spatial patterns in the distribution of tropical tree species. *Science*, 288:1414–1418.
- Condit, R., Pitman, N., Leigh, E., Chave, J., Terborgh, J., Foster, R. *et al.* (2002). Beta-diversity in tropical forest trees. *Science*, 295:666–669.
- Damschen, E., Haddad, N., Orrock, J., Tewksbury, J., and Levey, D. (2006). Corridors increase plant species richness at large scales. *Science*, 313:1284–1286.
- Darwin, C. (1859). *On the origin of species*. John Murray, London.
- de Aguiar, M., Baranger, M., Baptestini, E. M., Kaufman, L., and Bar-Yam, Y. (2009). Global patterns of speciation and diversity. *Nature*, 460:384–387.
- De Bie, T., De Meester, L., Brendonck, L., Martens, K., Goddeeris, B., Ercken, *et al.* (2012). Body size and dispersal mode as key traits determining metacommunity structure of aquatic organisms. *Ecology Letters*, 15:740–747.
- de Mazancourt, C., Isbell, F., Larocque, A., Berendse, F., De Luca, E., Grace, J.B. *et al.* (2013). Predicting ecosystem stability from community composition and biodiversity. *Ecology Letters*, 16:617–625.
- DeLong, J. and Vasseur, D. (2012). Size-density scaling in protists and the links between consumer-resource interaction parameters. *Journal of Animal Ecology*, 81:1193–1201.
- Donohue, I., Petchey, O., Montoya, J., Jackson, A., McNally, L., Viana, M. *et al.* (2013). On the dimensionality of ecological stability. *Ecology Letters*, 16:421–429.
- Dublin, L. I. and Lotka, A. J. (1925). On the true rate of natural increase. *Journal of the American Statistical Association*, 20:305–339.
- Duffy, J., Cardinale, B., France, K., McIntyre, P., Thebault, E., and , M. (2007). The functional role of biodiversity in ecosystems: incorporating trophic complexity. *Ecology Letters*, 10:522–538.
- Economu, E. P. and Keitt, T. H. (2008). Species diversity in neutral metacommunities: a network approach. *Ecology Letters*, 11:52–62.

Bibliography

- Economo, E. P. and Keitt, T. H. (2010). Network isolation and local diversity in neutral metacommunities. *Oikos*, 119:1355–1363.
- Fagan, W., Unmack, P., Burgess, C., and Minckley, W. (2002). Rarity, fragmentation, and extinction risk in desert fishes. *Ecology*, 83:3250–3256.
- Fagan, W. F. (2002). Connectivity, fragmentation, and extinction risk in dendritic metapopulations. *Ecology*, 83:3243–3249.
- Fahrig, L. (2003). Effects of habitat fragmentation on biodiversity. *Annual Review of Ecology Evolution and Systematics*, 34:487–515.
- Faust, K. and Raes, J. (2012). Microbial interactions: from network to models. *Nature Reviews Microbiology*, 10:538–549.
- Fenchel, T. (1974). Intrinsic rate of natural increase - relationship with body size. *Oecologia*, 14:317–326.
- Fenchel, T. (1980). Suspension feeding in ciliated protozoa: feeding rates and their ecological significance. *Microbial Ecology*, 6:13–25.
- Fér, T. and Hroudová, Z. (2008). Detecting dispersal of *nuphar lutea* in river corridors using microsatellite markers. *Freshwater Biology*, 53:1409–1422.
- Fernandes, C., Podos, J., and Lundberg, J. (2004). Amazonian ecology: Tributaries enhance the diversity of electric fishes. *Science*, 305:1960–1962.
- Finke, D. and Snyder, W. (2008). Niche partitioning increases resource exploitation by diverse communities. *Science*, 321:1488–1490.
- Finlay, B., Corliss, J., Esteban, G., and Fenchel, T. (1996). Biodiversity at the microbial level: The number of free-living ciliates in the biosphere. *Quarterly Review of Biology*, 71:221–237.
- Finlay, B. and Esteban, G. (1998). Freshwater protozoa: biodiversity and ecological function. *Biodiversity and Conservation*, 7:1163–1186.
- Finn, D., Bonada, N., Murria, C., and Hughes, J. (2011). Small but mighty: headwaters are vital to stream network biodiversity at two levels of organization. *Journal of the North American Benthological Society*, 30:963–980.
- Foster, K. and Bell, T. (2012). Competition, not cooperation, dominates interactions among culturable microbial species. *Current Biology*, 22:1845–1850.
- Fox, J. and McGrady-Steed, J. (2002). Stability and complexity in microcosm communities. *Journal of Animal Ecology*, 71:749–756.
- Franzen, M. and Nilsson, S. (2010). Both population size and patch quality affect local extinctions and colonizations. *Proceedings of the Royal Society B-Biological Sciences*, 277:79–85.

- Freilich, S., Zarecki, R., Eilam, O., Segal, E., Henry, C., Kupiec, M. *et al.* (2011). Competitive and cooperative metabolic interactions in bacterial communities. *Nature Communications*, 2:589.
- Fukami, T. (2001). Sequence effects of disturbance on community structure. *Oikos*, 92:215–224.
- Fukami, T., Dickie, I., Wilkie, J., Paulus, B., Park, D., Roberts, A. *et al.* (2010). Assembly history dictates ecosystem functioning: evidence from wood decomposer communities. *Ecology Letters*, 13:675–684.
- Fukami, T. and Morin, P. (2003). Productivity-biodiversity relationships depend on the history of community assembly. *Nature*, 424:423–426.
- Gassner, A. (2006). Gewässerschutzbestimmungen in der landwirtschaft. ein internationaler vergleich. Umwelt-wissen 0618, (Bundesamt für Umwelt, Bern. 76 S.).
- Gaston, K. (2000). Global patterns in biodiversity. *Nature*, 405:220–227.
- Gause, G. F. (1934). *The struggle for coexistence*. Williams and Wilkins, Baltimore.
- Gillespie, D. (1977). Exact stochastic simulation of coupled chemical-reactions. *Journal of Physical Chemistry*, 81:2340–2361.
- Giometto, A., Altermatt, F., Carrara, F., Maritan, A., and Rinaldo, A. (2013). Scaling body size fluctuations. *Proceedings of the National Academy of Sciences of the United States of America*, 110:4646–4650.
- Glücksman, E., Bell, T., Griffiths, R., and Bass, D. (2010). Closely related protist strains have different grazing impacts on natural bacterial communities. *Environmental Microbiology*, 12:3105–3113.
- Gonzalez, A., Lawton, J., Gilbert, F., Blackburn, T., and Evans-Freke, I. (1998). Metapopulation dynamics, abundance, and distribution in a microecosystem. *Science*, 281:2045–2047.
- Gonzalez, A., Rayfield, B., and Lindo, Z. (2011). The disentangled bank: how loss of habitat fragments and disassembles ecological networks. *American Journal of Botany*, 98:503–516.
- Grant, E., Lowe, W., and Fagan, W. (2007). Living in the branches: Population dynamics and ecological processes in dendritic networks. *Ecology Letters*, 10:165–175.
- Grant, E., Lynch, H., Muneeppeerakul, R., Arunachalam, M., Rodriguez-Iturbe, I., and Fagan, W. (2012). Interbasin Water Transfer, Riverine Connectivity, and Spatial Controls on Fish Biodiversity. *Plos One*, 7: e34170.
- Gross, K. (2008). Positive interactions among competitors can produce species-rich communities. *Ecology Letters*, 11:929–936.
- Gross, T., Rudolf, L., Levin, S., and Dieckmann, U. (2009). Generalized models reveal stabilizing factors in food webs. *Science*, 325:747–750.

Bibliography

- Haddad, N., Crutsinger, G., Gross, K., Haarstad, J., and Tilman, D. (2011). Plant diversity and the stability of foodwebs. *Ecology Letters*, 14:42–46.
- Haddad, N., Holyoak, M., Mata, T., Davies, K., Melbourne, B., and Preston, K. (2008). Species' traits predict the effects of disturbance and productivity on diversity. *Ecology Letters*, 11:348–356.
- Hanski, I. (1998). Metapopulation dynamics. *Nature*, 396:41–49.
- Hanski, I. (2013). Extinction debt at different spatial scales. *Animal Conservation*, 16:12–13.
- Hanski, I. and Ovaskainen, O. (2000). The metapopulation capacity of a fragmented landscape. *Nature*, 404:755–758.
- Hardin, G. (1960). Competitive exclusion principle. *Science*, 131:1292–1297.
- Harte, J., Kinzig, A., and Green, J. (1999). Self-similarity in the distribution and abundance of species. *Science*, 284:334–336.
- Hastings, A. and Higgins, K. (1994). Persistence of transients in spatially structured ecological models. *Science*, 263:1133–1136.
- Heino, J. (2013). Environmental heterogeneity, dispersal mode, and co-occurrence in stream macroinvertebrates. *Ecology and Evolution*, 3:344–355.
- Hillebrand, H., Bennett, D., and Cadotte, M. (2008). Consequences of dominance: A review of evenness effects on local and regional ecosystem processes. *Ecology*, 89:1510–1520.
- Holyoak, M. and Lawler, S. (2005). The contribution of laboratory experiments on protists to understanding population and metapopulation dynamics. *Advances in Ecological Research*, 37:245–271.
- Holyoak, M., Lawler, S., and Crowley, P. (2000). Predicting extinction: progress with an individual-based model of protozoan predators and prey. *Ecology*, 81:3312–3329.
- Holyoak, M., Leibold, M., and Holt, R. (2005). *Metacommunities. Spatial dynamics and ecological communities*. The University of Chicago Press, Chicago.
- Hooper, D., Adair, E., Cardinale, B. J., Byrnes, J., Hungate, B., Matulich, K. *et al.* (2012). A global synthesis reveals biodiversity loss as a major driver of ecosystem change. *Nature*, 486:105–109.
- Houchmandzadeh, B. (2008). Neutral clustering in a simple experimental ecological community. *Physical Review Letters*, 101:078103.
- Houchmandzadeh, B. and Vallade, M. (2003). Clustering in neutral ecology. *Physical Review E*, 68:061912.

- Hubbell, S. (2001). *The Unified Theory of Biodiversity and Biogeography*. Princeton University Press, Princeton, NJ.
- IPCC (2007). *Climate Change 2007: The physical Science Basis. Summary for Policymakers*. WMO and UNEF, Geneva.
- Ives, A., Cardinale, B., and Snyder, W. (2005). A synthesis of subdisciplines: predator-prey interactions, and biodiversity and ecosystem functioning. *Ecology Letters*, 8:102–116.
- Ives, A. and Carpenter, S. (2007). Stability and diversity of ecosystems. *Science*, 317:58–62.
- Ives, A., Gross, K., and Klug, J. (1999). Stability and variability in competitive communities. *Science*, 286:542–544.
- Jessup, C., Kassen, R., Forde, S., Kerr, B., Buckling, A., Rainey, P., and Bohannan, B. (2004). Big questions, small worlds: Microbial model systems in ecology. *Trends in Ecology & Evolution*, 19:189–197.
- Jetz, W. and Rahbek, C. (2001). Geometric constraints explain much of the species richness pattern in African birds. *Proceedings of the National Academy of Sciences of the United States of America*, 98:5661–5666.
- Jiang, L., Tan, J., and Pu, Z. (2010). An experimental test of Darwin's naturalization hypothesis. *American Naturalist*, 175:415–423.
- Kier, G., Mutke, J., Dinerstein, E., Ricketts, T., Kuper, W., Kreft, H., and Barthlott, W. (2005). Global patterns of plant diversity and floristic knowledge. *Journal of Biogeography*, 32:1107–1116.
- Kokkoris, G., Jansen, V., Loreau, M., and Troumbis, A. (2002). Variability in interaction strength and implications for biodiversity. *Journal of Animal Ecology*, 71:362–371.
- Kraft, N., Comita, L., Chase, J., Sanders, N., Swenson, N., Crist, T. *et al.* (2011). Disentangling the drivers of beta diversity along latitudinal and elevational gradients. *Science*, 333:1755–1758.
- Lake, P. S., Bond, N., and Reich, P. (2007). Linking ecological theory with stream restoration. *Freshwater Biology*, 52:597–615.
- Laska, M. and Wootton, J. (1998). Theoretical concepts and empirical approaches to measuring interaction strength. *Ecology*, 79:461–476.
- Lenoir, J., Gegout, J. C., Marquet, P. A., de Ruffray, P., and Brisse, H. (2008). A significant upward shift in plant species optimum elevation during the 20th century. *Science*, 320:1768–1771.
- Leopold, L., Wolman, M., and Miller, J. (1964). *Fluvial processes in geomorphology*. Freeman.

Bibliography

- Levine, J. and HilleRisLambers, J. (2009). The importance of niches for the maintenance of species diversity. *Nature*, 461:254–257.
- Livingston, G., Matias, M., Calcagno, V., Barbera, C., Combe, M., Leibold, M. A., and Mouquet, N. (2012). Competition-colonization dynamics in experimental bacterial metacommunities. *Nature Communications*, 3:1234.
- Loreau, M. (1998). Separating sampling and other effects in biodiversity experiments. *Oikos*, 82:600–602.
- Loreau, M. and de Mazancourt, C. (2013). Biodiversity and ecosystem stability: a synthesis of underlying mechanisms. *Ecology Letters*, 16:106–115.
- Loreau, M. and Hector, A. (2001). Partitioning selection and complementarity in biodiversity experiments. *Nature*, 412:72–76.
- Loreau, M., Naeem, S., Inchausti, P., Bengtsson, J., Grime, J., Hector, A. *et al.* (2001). Ecology - biodiversity and ecosystem functioning: Current knowledge and future challenges. *Science*, 294:804–808.
- Lowe, W. and Likens, G. (2005). Moving headwater streams to the head of the class. *Bioscience*, 55:196–197.
- Lowe, W., Likens, G., and Power, M. (2006). Linking scales in stream ecology. *Bioscience*, 56:591–597.
- MacArthur, R. and Levins, R. (1967). Limiting similarity convergence and divergence of coexisting species. *American Naturalist*, 101:377–384.
- MacArthur, R. and Wilson, E. (1963). Equilibrium-theory of insular zoogeography. *Evolution*, 17:373–387.
- MacArthur, R. H. (1972). *Geographical Ecology*. Harper and Rowe Publishers, New York.
- Madin, J. and Connolly, S. (2006). Ecological consequences of major hydrodynamic disturbances on coral reefs. *Nature*, 444:477–480.
- Mari, L., Bertuzzo, E., Casagrandi, R., Gatto, M., Levin, S. A., Rodriguez-Iturbe, I., and Rinaldo, A. (2011). Hydrologic controls and anthropogenic drivers of the zebra mussel invasion of the Mississippi-Missouri river system. *Water Resources Research*, 47:W03523.
- Matthiessen, B. and Hillebrand, H. (2006). Dispersal frequency affects local biomass production by controlling local diversity. *Ecology Letters*, 9:652–662.
- May, R. (1972). Will a large complex system be stable? *Nature*, 238:413–415.
- Mayfield, M. and Levine, J. (2010). Opposing effects of competitive exclusion on the phylogenetic structure of communities. *Ecology Letters*, 13:1085–1093.

- McCain, C. (2009). Global analysis of bird elevational diversity. *Global Ecology and Biogeography*, 18:346–360.
- McCann, K. (2000). The diversity-stability debate. *Nature*, 405:228–233.
- McGradySteed, J., Harris, P., and Morin, P. (1997). Biodiversity regulates ecosystem predictability. *Nature*, 390:162–165.
- McKane, A., Alonso, D., and Solé, R. (2000). Mean-field stochastic theory for species-rich assembled communities. *Physical Review E*, 62:8466–8484.
- McKane, A. and Newman, T. (2005). Predator-prey cycles from resonant amplification of demographic stochasticity. *Physical Review Letters*, 94:218102.
- McKane, A. J. and Newman, T. J. (2004). Stochastic models in population biology and their deterministic analogs. *Physical Review E*, 70:041902.
- Melbourne, B. and Hastings, A. (2008). Extinction risk depends strongly on factors contributing to stochasticity. *Nature*, 454:100–103.
- Morrissey, M. and de Kerckhove, D. (2009). The maintenance of genetic variation due to asymmetric gene flow in dendritic metapopulations. *American Naturalist*, 174:875–889.
- Mouquet, N., Leadley, P., Meriguet, J., and Loreau, M. (2004). Immigration and local competition in herbaceous plant communities: a three-year seed-sowing experiment. *Oikos*, 104:77–90.
- Mouquet, N. and Loreau, M. (2003). Community patterns in source-sink metacommunities. *American Naturalist*, 162:544–557.
- Muneepeerakul, R., Bertuzzo, E., Lynch, H., Fagan, W., Rinaldo, A., and Rodriguez-Iturbe, I. (2008a). Neutral metacommunity models predict fish diversity patterns in mississippi-missouri basin. *Nature*, 453:220–222.
- Muneepeerakul, R., Bertuzzo, E., Rinaldo, A., and Rodriguez-Iturbe, I. (2008b). Patterns of vegetation biodiversity: The roles of dispersal directionality and river network structure. *Journal of Theoretical Biology*, 252:221–229.
- Muneepeerakul, R., Weitz, J., Levin, S., Rinaldo, A., and Rodriguez-Iturbe, I. (2007). A neutral metapopulation model of biodiversity in river networks. *Journal of Theoretical Biology*, 245:351–363.
- Newman, M. (2010). *Networks*. Oxford Univeristy Press, Oxford.
- Nogues-Bravo, D., Araujo, M., Romdal, T., and Rahbek, C. (2008). Scale effects and human impact on the elevational species richness gradients. *Nature*, 453:216–219.
- Paine, R. (1992). Food-web analysis through field measurement of per-capita interaction strength. *Nature*, 355:73–75.

Bibliography

- Parmesan, C. (2006). Ecological and evolutionary responses to recent climate change. *Annual Review of Ecology Evolution and Systematics*, 37:637–669.
- Peay, K., Belisle, M., and Fukami, T. (2012). Phylogenetic relatedness predicts priority effects in nectar yeast communities. *Proceedings of the Royal Society B-Biological Sciences*, 279:749–758.
- Perkin, J. S. and Gido, K. B. (2012). Fragmentation alters stream fish community structure in dendritic ecological networks. *Ecological Applications*, 22:2176–2187.
- Petchey, O. and Gaston, K. (2002). Functional diversity (fd), species richness and community composition. *Ecology Letters*, 5:402–411.
- Pigolotti, S., Flammini, A., Marsili, M., and Maritan, A. (2005). Species lifetime distribution for simple models of ecologies. *Proceedings of the National Academy of Sciences USA*, 102:15747.
- Pillai, P., Gonzalez, A., and Loreau, M. (2011). Metacommunity theory explains the emergence of food web complexity. *Proceedings of the National Academy of Sciences of the United States of America*, 108:19293–19298.
- Poff, N. L., Olden, J. D., Merritt, D. M., and Pepin, D. M. (2007). Homogenization of regional river dynamics by dams and global biodiversity implications. *Proceedings of the National Academy of Sciences of the United States of America*, 104:5732–5737.
- Quince, C., Curtis, T. P., and Sloan, W. T. (2008). The rational exploration of microbial diversity. *Isme Journal*, 2:997–1006.
- Rahbek, C. (1995). The elevational gradient of species richness - a uniform pattern. *Ecography*, 18:200–205.
- Rahbek, C. (2005). The role of spatial scale and the perception of large-scale species-richness patterns. *Ecology Letters*, 8:224–239.
- Rahbek, C. and Graves, G. (2001). Multiscale assessment of patterns of avian species richness. *Proceedings of the National Academy of Sciences of the United States of America*, 98:4534–4539.
- Reche, I., Pulido-Villena, E., Morales-Baquero, R., and Casamayor, E. (2005). Does ecosystem size determine aquatic bacterial richness? *Ecology*, 86:1715–1722.
- Ricklefs, R. E. (2004). A comprehensive framework for global patterns in biodiversity. *Ecology Letters*, 7:1–15.
- Rinaldo, A., Banavar, J., and Maritan, A. (2006). Trees, networks and hydrology. *Water Resources Research*, 42:W06D07.

- Rinaldo, A., Rigon, R., and Rodriguez-Iturbe, I. (1999). Channel networks. *Annual Review of Earth and Planetary Sciences*, 26:289–306.
- Rinaldo, A., Rodriguez-Iturbe, I., Rigon, R., Bras, R., Ijjasz-Vasquez, E., and Marani, A. (1992). Minimum energy and fractal structures of drainage networks. *Water Resources Research*, 28:2183–2191.
- Rodriguez-Iturbe, I., Muneeppeerakul, R., Bertuzzo, E., Levin, S., and Rinaldo, A. (2009). River networks as ecological corridors: A complex systems perspective for integrating hydrologic, geomorphologic, and ecologic dynamics. *Water Resources Research*, 45:W01413.
- Rodriguez-Iturbe, I. and Rinaldo, A. (1997). *Fractal River Basins: Chance and Self-Organization*. Cambridge University Press, New York.
- Rodriguez-Iturbe, I., Rinaldo, A., Rigon, R., Bras, R., and Ijjasz-Vasquez, E. (1992). Fractal structures as least energy patterns: The case of river networks. *Geophysical Research Letters*, 19:889–893.
- Rosindell, J., Hubbell, S., and Etienne, R. (2011). The Unified Neutral Theory of Biodiversity and Biogeography at Age Ten. *Trends in Ecology & Evolution*, 26:340–348.
- Roxburgh, S. and Wilson, J. (2000). Stability and coexistence in a lawn community: mathematical prediction of stability using a community matrix with parameters derived from competition experiments. *Oikos*, 88:395–408.
- Saleem, M., Fetzer, I., Dormann, C., Harms, H., and Chatzinotas, A. (2012). Predator richness increases the effect of prey diversity on prey yield. *Nature Communications*, 3:1305.
- Salomon, Y., Connolly, S., and Bode, L. (2010). Effects of asymmetric dispersal on the coexistence of competing species. *Ecology Letters*, 13:432–441.
- Sheldon, A. (1968). Species diversity and longitudinal succession in stream fishes. *Ecology*, 49:193–198.
- Sole, R. and Montoya, J. (2001). Complexity and fragility in ecological networks. *Proceedings of the Royal Society B-Biological Sciences*, 268:2039–2045.
- Staddon, P., Lindo, Z., Crittenden, P., Gilbert, F., and Gonzalez, A. (2010). Connectivity, non-random extinction and ecosystem function in experimental metacommunities. *Ecology Letters*, 13:543–552.
- Stouffer, D. and Bascompte, J. (2011). Compartmentalization increases food-web persistence. *Proceedings of the National Academy of Sciences of the United States of America*, 108:3648–3652.
- Taberlet, P., Zimmermann, N., Englisch, T., Tribsch, A., Holderegger, R., Alvarez, N. *et al.* (2012). Genetic diversity in widespread species is not congruent with species richness in alpine plant communities. *Ecology Letters*, 15:1439–1448.

Bibliography

- Tan, J., Pu, Z., and Wade, A. R. Jiang, L. (2012). Species phylogenetic relatedness, priority effects, and ecosystem functioning. *Ecology*, 93:1164–1172.
- Thuiller, W., Albert, C., Araujo, M., Berry, P., Cabeza, M., Guisan, A., Hickler, T. *et al.* (2008). Predicting global change impacts on plant species' distributions: Future challenges. *Perspectives in Plant Ecology Evolution and Systematics*, 9:137–152.
- Tilman, D. (1980). Resources - a graphical-mechanistic approach to competition and predation. *American Naturalist*, 116:362–393.
- Tilman, D., Lehman, C., and Bristow, C. (1998). Diversity-stability relationships: Statistical inevitability or ecological consequence? *American Naturalist*, 151:277–282.
- Tilman, D., Reich, P., Knops, J., Wedin, D., Mielke, T., and Lehman, C. (2001). Diversity and productivity in a long-term grassland experiment. *Science*, 294:843–845.
- Turnbull, L., Levine, J., Loreau, M., and Hector, A. (2013). Coexistence, niches and biodiversity effects on ecosystem functioning. *Ecology Letters*, 16:116–127.
- Uhlenbeck, G. E. and Ornstein, L. S. (1930). On the theory of the brownian motion. *Physical Review*, 36:823–841.
- Urban, D. and Keitt, T. (2001). Landscape connectivity: A graph-theoretic perspective. *Ecology*, 82:1205–1218.
- Urban, M., Skelly, D., Burchsted, D., Price, W., and Lowry, S. (2006). Stream communities across a rural-urban landscape gradient. *Diversity and Distributions*, 12:337–350.
- Vallade, M. and Houchmandzadeh, B. (2003). Analytical solution of a neutral model of biodiversity. *Physical Review E*, 68:061902.
- Vallade, M. and Houchmandzadeh, B. (2006). Species abundance distribution and population dynamics in a two-community model of neutral ecology. *Physical Review E*, 74:051914.
- van Kampen, N. (2007). *Stochastic Processes in Physics and Chemistry*. Elsevier.
- Vandermeer, J. (1969). Competitive structure of communities - an experimental approach with protozoa. *Ecology*, 50:362–372.
- Vannote, R., Minshall, G., Cummins, K., Sedell, J., and Cushing, C. E. (1980). River continuum concept. *Canadian Journal of Fisheries and Aquatic Sciences*, 37:130–137.
- Vellend, M. (2010). Conceptual synthesis in community ecology. *Quarterly Review of Biology*, 85:183–206.
- Violle, C., Nemergut, D., Pu, Z., and Jiang, L. (2011). Phylogenetic limiting similarity and competitive exclusion. *Ecology Letters*, 14:782–787.

- Volkov, I., Banavar, J., He, F., Hubbell, S., and Maritan, A. (2005). Density dependence explains tree species abundance and diversity in tropical forests. *Nature*, 438:658–661.
- Volkov, I., Banavar, J., Hubbell, S., and Maritan, A. (2003). Neutral theory and relative species abundance in ecology. *Nature*, 424:1035–1037.
- Volkov, I., Banavar, J., Hubbell, S., and Maritan, A. (2009). Inferring species interactions in tropical forests. *Proceedings of the National Academy of Sciences of the United States of America*, 106:13854–13859.
- Volterra, V. (1926). Fluctuations in the abundance of a species considered mathematically. *Nature*, 118:558–560.
- Vörösmarty, C., McIntyre, P., Gessner, M., Dudgeon, D., Prusevich, A., and Green, P. *et al.* (2010). Global threats to human water security and river biodiversity. *Nature*, 467:555–561.
- Walker, B., Kinzig, A., and Langridge, J. (1999). Plant attribute diversity, resilience, and ecosystem function: The nature and significance of dominant and minor species. *Ecosystems*, 2:95–113.
- Warren, P. (1996). Dispersal and destruction in a multiple habitat system: An experimental approach using protist communities. *Oikos*, 77:317–325.
- White, E., Ernest, S., Kerkhoff, A., and Enquist, B. (2007). Relationships between body size and abundance in ecology. *Trends in Ecology & Evolution*, 22:323–330.
- Williams, R. and Martinez, N. (2000). Simple rules yield complex food webs. *Nature*, 404:180–183.
- Willig, M., Kaufman, D., and Stevens, R. (2003). Latitudinal gradients of biodiversity: Pattern, process, scale, and synthesis. *Annual Review of Ecology Evolution and Systematics*, 34:273–309.
- Ziv, G., Baran, E., Nam, S., Rodriguez-Iturbe, I., and Levin, S. A. (2012). Trading-off fish biodiversity, food security, and hydropower in the mekong river basin. *Proceedings of the National Academy of Sciences of the United States of America*, 109:5609–5614.

Curriculum Vitae of Francesco Carrara

Personal Information

Name: Francesco

Surname: Carrara

Date of birth: March 16th 1984

Nationality: Italian

University address: EPFL, GR C1 522, Station 2, Route Cantonale, CH-1015 Lausanne

Office phone: +41 21 693 63 71

Private address: Via Cernaia 50, 35141 Padova (PD), Italy

Mobile phone number: +39 333 913 95 59; +41 (0)78 936 20 38

E-mail: francesco.carrara@epfl.ch; fararrac@gmail.com

Homepage: <http://people.epfl.ch/francesco.carrara>

Research Interest

Stochastic modeling of ecosystems dynamics, complex systems, ecohydrology, riverine ecosystems, food web interactions, microbial communities.

Education

2010-2013: PhD (September), École Polytechnique Fédérale de Lausanne (EPFL), Lausanne, Switzerland (supervisor: Prof. Andrea Rinaldo; co-supervisor: Dr. Florian Altermatt)

2007-2009: MSc., Physics (110/110 cum laude), Università degli Studi di Padova, Padova, Italy (supervisor: Prof. Amos Maritan)

2003-2007: BSc., Physics (103/110), Università degli Studi di Padova, Padova, Italy (supervisor: Prof. Piero Martin)

1998-2006: Piano Diploma, Conservatorio di Musica “Cesare Pollini”, Padova, Italy

Publications

Peer-reviewed journal articles

- F. Altermatt, A. Bieger, F. Carrara, A. Rinaldo, and M. Holyoak (2011) Effect of connectivity and recurrent local disturbance on community structure and population density in experimental metacommunities. *Plos One*, 6: e19525. 10.1371/journal.pone.0019525;
- F. Carrara, F. Altermatt, I. Rodriguez-Iturbe and A. Rinaldo (2012) Dendritic connectivity controls biodiversity patterns in experimental metacommunities, *Proceedings of the US National Academy of Sciences*, 109: 5761–5766;
- A. Giometto, F. Altermatt, F. Carrara, A. Maritan, A. Rinaldo (2013) Scaling body-size fluctuations *Proceedings of the US National Academy of Sciences*, 110: 4646–4650;
- F. Carrara, A. Giometto, A. Rinaldo and F. Altermatt (2013) Complex interaction of dendritic connectivity and hierarchical patch-size on biodiversity in river-like landscapes, *The American Naturalist*, in press;

Conference Abstracts

- F. Carrara, F. Altermatt, I. Rodriguez-Iturbe, A. Rinaldo, Dendritic connectivity control biodiversity patterns in dendritic metacommunities, (Poster) EGU General Assembly 2011, Vienna, Austria
- F. Carrara, A. Giometto, A. Rinaldo, F. Altermatt, Complex interaction of hierarchical patch-size and dendritic connectivity, ESA Annual Meeting 2012, (Oral Presentation) Portland, Oregon, USA

Professional Experiences/Internships

- **2011-2012:** Teaching Assistant for the course Analysis IV (Prof. Philippe Metzener) for Civil and Environmental Engineering bachelor students at EPFL, Lausanne, Switzerland
- **2012-2013:** Teaching Assistant for the course Analysis I (Prof. Boris Buffoni) for Civil and Environmental Engineering bachelor students at EPFL, Lausanne, Switzerland
- **2012-2013:** Teaching Assistant for the graduate course “Limnoecology” at ETH, Zurich, Switzerland

International Experiences

- **June 2010:** Participation at the “BESS Summer School on Biological and Climate Processes: Coupled Dynamics and Scales of Interactions” held by the Istituto Veneto di Scienze, Lettere ed Arti, Venice, Italy

- **September 2010:** Visiting research collaboration with Dr. Florian Altermatt at University of California, Davis, CA
- **February 2013:** Participation at the Winter School on “Ecological Theory” held at Istituto Frascini, Monte Verità, Ascona, Switzerland

Workshop Participation

- **February 2011:** Participation (Oral Presentation) at the “1st Protist Workshop” at Eawag, Switzerland
- **October 2011:** Participation (Oral Presentation) at the “Metacommunity Workshop” at Oldenburg University, Germany
- **March 2012:** Participation (Oral Presentation) at the “2nd Protist Workshop” at Eawag, Switzerland

Other services

- Reviewer for *Ecology Letters*
- Member of American Geophysical Union (AGU), European Geosciences Union (EGU), Ecological Society of America (ESA)

Personal Skills

Languages:

- Italian: mother tongue
- English: proficient user (CEF level¹: listening C1, speaking C1, writing C1)
- French: independent user (CEF level: listening B1, speaking B1, writing B1)

Computer Skills:

Matlab, Mathematica, Office, Adobe Illustrator, LaTeX

¹Common European Framework of Reference

References

To get additional information about me please contact:

- Prof. Andrea Rinaldo (andrea.rinaldo@epfl.ch), Laboratory of Ecohydrology (ECHO), Environmental Engineering Institute (IIE), School of Architecture, Civil and Environmental Engineering (ENAC), École Polytechnique Fédérale de Lausanne (EPFL), Lausanne, Switzerland;
- Dr. Florian Altermatt (florian.altermatt@eawag.ch), Department of Aquatic Ecology, Eawag, Dübendorf, Switzerland;
- Prof. Amos Maritan (amos.maritan@pd.infn.it), Dipartimento di Fisica, Università di Padova, Padova, Italy;